Fermions in Electroweak Baryogenesis

Zong-Gang Mou



Thesis submitted to the University of Nottingham
for the degree of Doctor of Philosophy

August 2015

Supervisors:	Dr. Paul Saffin	
	Prof. Ed Copeland	
Examiners:	Prof. Arttu Rajantie	(Imperial College London)
	Dr. Clare Burrage	(University of Nottingham)

Submitted: 26 August 2015

Examined: 9 October 2015

Final version: 22 October 2015

Abstract

We study the chiral anomaly by solving the Dirac equation for fermions in parallel electric and magnetic fields. In such case, only the lowest-energy Landau levels are relevant to the anomaly. Specifically, for massless fermions, the chiral anomaly is a result of the production of particles of one chirality, and no creation of particles of the other chirality. For massive fermions, we find that the chiral anomaly equation can be simply obtained via a proper regularization of the range of the momentum. We extend the method to anomaly cancellation, and conclude that the conservation of the baryon number plus lepton number must be violated as a quantum anomaly in the context of the Standard Model. Accordingly, such baryon number non-conservation can play a vital role during the electroweak transition to achieve the baryon asymmetry of the Universe.

Through real-time lattice simulations, we refine the implementation of ensemble fermions for a cold electroweak transition, involving the $SU(2)$ gauge field, Higgs field and one generation of fermions. We find that the dynamics and most observables converge quickly with a reasonable number of fermion realizations, and the method of ensemble fermions for the entire electroweak sector becomes numerically tractable. We apply the method to the computation of the effective preheating temperature during a fast electroweak transition, relevant for Cold Electroweak Baryogenesis. We find that the fermion temperature is never below 20 GeV, and this can indirectly rule out Standard Model CP-violation as the origin of the baryon asymmetry of the Universe, as Standard Model cold baryogenesis requires a temperature of at most of order of 1 GeV. For this reason, new CP-violation source from physics beyond the Standard Model is required in order to explain the baryon asymmetry.

We further present a first-principles numerical computation of the baryon asymmetry in electroweak-scale baryogenesis, where the CP-violation is obtained as a consequence of including another Higgs doublet. For one particularly favourable

scalar potential that could provide a high sphaleron transition rate, we calculate the asymmetry through large-scale computer simulations. The numerical signal is at the boundary of what is numerically discernible with the available computer resources, but we tentatively find an asymmetry of $|\eta| \leq 3.5 \times 10^{-7}$.

We also find it is attainable to include the complete electroweak $SU(2) \times U(1)$ gauge fields in the reduced Standard Model that we are using in practical simulations, so that in further studies we can measure the cosmic magnetic field generated during the electroweak phase transition.

Acknowledgements

In proper sequence along the real time, numbers thrived.
In memory, all were ephemeral, lived and lost.
But few were saved, remembered to be valuable.

I am extremely grateful to my PhD supervisor, Paul Saffin. My view on the present physics frontier has been largely shaped through the discussions with him. I also owe many thanks to Anders Tranberg. It is Paul and Anders who brought me into the world of numerical simulations, and without the collaboration with them, this thesis would not exist. I also would like to thank Ed Copeland, Paul Tognarelli and Shuang-Yong Zhou, for inspiring discussions. I owe my deepest gratitude to Lefan Liu for her support and love for years.

My PhD research was supported by the University of Nottingham-China Scholarship Council scholarship. The thesis consists of numerical simulations, which were performed in part at Dirac facility COSMOS (UK) and the Notur facility Abel (Norway).

Contents

Abstract **iii**

Acknowledgements **v**

Published Work **viii**

Notation **ix**

1 Introduction **1**

1.1 Cold Electroweak Baryogenesis 6

1.2 Fermions in real-time simulations 10

1.3 Overview 14

2 Solving the Dirac Equation **17**

2.1 Fermions in an electric field 19

2.1.1 Schwinger mechanism 30

2.2 Fermions in a magnetic field 31

2.2.1 Landau levels 33

2.3 Fermions and the chiral anomaly 35

2.3.1 Chiral anomaly for massless fermions 40

2.3.2 Chiral anomaly for massive fermions 42

2.3.3 B+L anomaly 45

2.4 Fermions on a lattice 50

2.4.1 Spatial Wilson terms 52

2.4.2 Temporal doublers 54

2.4.3 Chiral anomaly on the lattice 55

3 Fermions in the Electroweak Dynamics **58**

3.1 The reduced Standard Model 59

3.1.1 Continuum action 59

3.1.2 The Chern-Simons number 62

3.1.3 Fermion mode functions and correlation functions 65

3.2 Ensemble fermions 68

3.3 Lattice implementation 71

3.3.1 Action and equation of motion 72

3.3.2 Initial conditions 76

3.3.3 Counterterms 78

3.3.4 Quantum field perturbation in real-time simulations 80

3.4 Simulations and results 84

3.4.1 Convergence of observables 85

3.4.2 Fermion occupation number 85

3.4.3 Fermion temperature 89

3.5 Conclusion 92

4 Baryogenesis in the Two-Higgs Doublet Model **94**

4.1 Continuum action 94

4.1.1 Higgs potential and Yukawa interaction 96

4.1.2 CP-symmetric initial conditions 103

4.2 Lattice implementation 105

4.2.1 Counterterms and renormalization 108

4.3 Simulations and results 112

4.3.1 Events and averages 115

4.3.2 Asymmetry 118

4.4 Conclusion 119

5 Summary and Outlook **121**

A Anomaly free $SU(2) \times U(1)$ **124**

Published Work

The vast majority of the work contained in the thesis has already been presented in several published works: Chapter 3 (Paper III), Chapter 4 (Paper I).

I **Z. G. Mou**, P. M. Saffin and A. Tranberg, "Cold Baryogenesis from first principles in the Two-Higgs Doublet model with Fermions," JHEP 1506 (2015) 163 [arXiv:1505.02692 [hep-ph]].

II J. H. Gao and **Z. G. Mou**, "Structure functions in deep inelastic scattering from gauge/string duality beyond single-hadron final states," Phys. Rev. D 90 (2014) 075018 [arXiv:1406.7576 [hep-ph]].

III **Z. G. Mou**, P. M. Saffin and A. Tranberg, "Ensemble fermions for electroweak dynamics and the fermion preheating temperature," JHEP 1311 (2013) 097 [arXiv:1307.7924 [hep-ph]].

IV S. Y. Zhou, E. J. Copeland, R. Easther, H. Finkel, **Z. G. Mou** and P. M. Saffin, "Gravitational Waves from Oscillon Preheating," JHEP 1310 (2013) 026 [arXiv:1304.6094 [astro-ph.CO]].

The work presented in the thesis was performed by the author, with advice from the paper coauthors listed above.

Notation

For 3+1 dimensional Minkowski space, the signature of the spacetime metric $\eta^{\mu\nu}$ is $(-,+,+,+)$.

The antisymmetric Levi-Civita tensor $\epsilon^{\mu\nu\rho\sigma}$ is chosen in such a way that $\epsilon^{0123} = +1$.

The gauge covariant derivative is denoted by $D_\mu = \partial_\mu - iA_\mu$. The field strength tensor is define as $F_{\mu\nu} = i[D_\mu,\ D_\nu]$, and accordingly the electric and magnetic parts are separately $E_i = F_{i0}$ and $B_i = \frac{1}{2}\epsilon_{ijk}F^{jk}$.

For the Dirac algebra, the Weyl representation is employed,

$$\{\gamma^\mu, \gamma^\nu\} = 2\eta^{\mu\nu}, \quad \bar{\psi} = \psi^\dagger i\gamma^0, \quad \gamma^5 = -i\gamma^0\gamma^1\gamma^2\gamma^3.$$

with explicitly

$$\gamma^0 = \begin{pmatrix} 0 & i\mathbb{I} \\ i\mathbb{I} & 0 \end{pmatrix}, \quad \gamma^j = \begin{pmatrix} 0 & i\sigma^j \\ -i\sigma^j & 0 \end{pmatrix}, \quad \gamma^5 = \begin{pmatrix} \mathbb{I} & 0 \\ 0 & -\mathbb{I} \end{pmatrix},$$

where Pauli matrices are,

$$\sigma^1 = \begin{pmatrix} 0 & 1 \\ 1 & 0 \end{pmatrix}, \quad \sigma^2 = \begin{pmatrix} 0 & -i \\ i & 0 \end{pmatrix}, \quad \sigma^3 = \begin{pmatrix} 1 & 0 \\ 0 & -1 \end{pmatrix}.$$

The left-handed projector is define as $\frac{1+\gamma^5}{2}$, so that a left-handed spinor satisfies $\psi_L = \gamma^5\psi_L$; the right-handed projector is $\frac{1-\gamma^5}{2}$, and a right-handed spinor satisfies $\psi_R = -\gamma^5\psi_R$.

Charge conjugation in this convention can be determined respectively,

for the scalar field,

$$\phi^{\mathcal{C}}(t,x) = \phi^{\star}(t,x),$$

for Dirac fermion field,

$$\psi^{\mathcal{C}}(t,x) = -\gamma^2\psi^{\star}(t,x),$$

for the gauge field,

$$A_{\mu}^{\mathcal{C}}(t,x) = -A_{\mu}^{T}(t,x).$$

Parity transformation is performed,
for the scalar field,

$$\phi^{\mathcal{P}}(t,x) = \phi(t,-x),$$

for Dirac fermion field,

$$\psi^{\mathcal{P}}(t,x) = i\gamma^0\psi(t,-x),$$

for the gauge field,

$$A_0^{\mathcal{P}}(t,x) = A_0(t,-x), \qquad A_i^{\mathcal{P}}(t,x) = -A_i(t,-x).$$

CP transformation can be implemented as
for the scalar field,

$$\phi^{\mathcal{C}P}(t,x) = \phi^{\star}(t,-x),$$

for Dirac fermion field,

$$\psi^{\mathcal{C}P}(t,x) = i\gamma^0\gamma^2\psi^{\star}(t,-x),$$

for the gauge field,

$$A_0^{\mathcal{C}P}(t,x) = -A_0^T(t,-x), \qquad A_i^{\mathcal{C}P}(t,x) = A_i^T(t,-x).$$

Chapter 1

Introduction

A great part of this work, which is also the crucial part, is to solve the Dirac equation for quantum fermions. It is striking that almost all properties of fermions, which are rich from an experimental point of view, can be derived merely from solving the Dirac equation, which is itself simple in form. The solutions of the Dirac equation for free fermions can already explain the outstanding features of fermions, like their half-integer spin [1] and the existence of anti-fermions [2], which was first proposed by Dirac himself. Strictly speaking, the Dirac equation can be solved analytically only for fermions in a few circumstances, and for our concern, besides free fermions, these circumstances include a constant magnetic field, constant electric field, and parallel electric and magnetic fields (for other solvable cases, see [29, 66]). Properties of fermions, such as the Landau levels, pair production, and the quantum anomaly, can be provided by these exact solutions. But ultimately, we have to rely on numerical calculations, when exploring more general situations, specifically, as we will consider, the interaction between fermions and bosons. Before we move on to numerical simulations, it is worth examining those circumstances of exact solutions, as they will improve our understanding of fermions in the gauge field.

The Dirac equation for fermions within a constant magnetic field can be transformed into an equation that describes harmonic oscillators, and therefore the fermions in this situation share with harmonic oscillators the same properties, such as quantization and degeneracy of energy levels. For fermions in a constant magnetic field, such levels are known as Landau levels [19, 29], of which the lowest-energy levels are most special, for the spin direction of an electron in these levels must be opposite to the direction of the magnetic field. As a result, the physics for fermions

in the lowest-energy Landau levels is simple and the effective theory would be 1+1 dimensional QED.

For fermions in a constant electric field, the equation was first solved by Sauter [3], who wrote the solution in the form of contour integrals. The solution can also be simply represented by parabolic cylinder functions, which will be the way we adopt in Chapter 2. As a consequence of the existence of the electric field, the system could tunnel from the vacuum state to a state with a pair of electron and positron, with the rate

$$e^{-\frac{m^2+p_\perp^2}{e|E|}\pi}. \tag{1.1}$$

where m is the mass of electron, $p_\perp$ the transverse momentum and E the strength of the electric field. This result is apparently non-perturbative in the gauge field.

Based on Sauter's work, Heisenberg and Euler [4] had considered fermions in parallel electric and magnetic fields, and obtained the energy density in the form of E and B. Through a Legendre transform, they eventually wrote down the famous Heisenberg-Euler lagrangian,

$$\begin{aligned}\mathcal{L}_{HE} =& \frac{1}{2e^2}(\vec{E}^2-\vec{B}^2)+\frac{1}{hc}\int_0^\infty e^{-\eta}\frac{d\eta}{\eta^3}\left[i\eta^2\vec{E}\cdot\vec{B}\frac{\cos\left(\frac{\eta}{|E_k|}\sqrt{\vec{E}^2-\vec{B}^2+2i\vec{E}\cdot\vec{B}}\right)+\text{conj.}}{\cos\left(\frac{\eta}{|E_k|}\sqrt{\vec{E}^2-\vec{B}^2+2i\vec{E}\cdot\vec{B}}\right)-\text{conj.}}\right.\\ &\left.+|E_k|^2+\frac{\eta^2}{3}(\vec{B}^2-\vec{E}^2)\right],\end{aligned} \tag{1.2}$$

where the critical field strength is $|E_k| = m^2c^3/\hbar$, and electric and magnetic fields are supposed to be constant or slow varying. Because of these non-linear terms, the theory predicts the light-light scattering in high energy regime. Also notice that the last term will be closely related to the field strength renormalization. For a review of Heisenberg-Euler lagrangian, see [57, 74].

Instead of solving the Dirac equation directly, the Heisenberg-Euler lagrangian can also be achieved by integrating out fermions in the path integral,

$$e^{i\int d^4x\mathcal{L}_{HE}} = \int[D\bar{\psi}][D\psi]e^{iS_G+iS_F}, \tag{1.3}$$

where

$$S_G = -\int d^4x \frac{1}{4e^2} F_{\mu\nu}F^{\mu\nu}, \qquad S_F = -\int d^4x \left[\bar{\psi}\gamma^\mu(\partial_\mu - iA_\mu)\psi + m\bar{\psi}\psi\right].$$

or equivalently,

$$\int d^4x \mathcal{L}_{HE} = S_G - i \ln \mathrm{Det}\left[\gamma^\mu D_\mu + m\right]. \tag{1.4}$$

Schwinger [5] solved (1.4) using the method of proper-time quantization, and as one of results, the Heisenberg-Euler lagrangian (1.2) was rediscovered. In [5], Schwinger also obtained the vacuum persistence probability for a system of spatial volume V over time T that the vacuum state remains to be the vacuum state with the existence of the electric field,

$$P = e^{-wVT}, \qquad \text{with} \quad w = \frac{2(eE)^2}{(2\pi)^3}\sum_{n=1}^{+\infty}\frac{1}{n^2}e^{-\frac{n\pi m^2}{eE}}. \tag{1.5}$$

As we will see in Chapter 2, such probability can also be derived from the pair-production rate (1.1).

The chiral anomaly is another extraordinary feature of fermions, satisfying the equation,

$$\partial_\mu\langle \mathrm{T}\bar{\psi}(t,x)i\gamma^\mu\gamma^5\psi(t,x)\rangle = 2im\langle \mathrm{T}\bar{\psi}(t,x)\gamma^5\psi(t,x)\rangle + \frac{e^2}{16\pi^2}\epsilon^{\mu\nu\rho\sigma}F_{\mu\nu}F_{\rho\sigma}. \tag{1.6}$$

In comparison with other properties of fermions, the chiral anomaly was discovered later [10, 11] and hence was not included in the early works that we mentioned above. But as we will demonstrate in Chapter 2, the discussed setup of parallel electric and magnetic fields is sufficient to illustrate the existence of the anomaly, which is in practice caused only by the lowest-energy Landau levels. For this reason, the chiral anomaly can be fully interpreted by 1+1 dimensional calculations [23, 35].

The chiral anomaly reveals a general fact that any "classical" symmetries could be violated by quantization [1] and symmetries working in the quantum level are the symmetries that have the anomaly cancelled through all fermion triangle diagrams. The cancellation essentially depends on the fermion content. As a matter of fact,

[1] More precisely, it is the regularization that breaks the chiral anomaly.

the Standard Model fermions suffice to support the symmetry $SU(3)\times SU(2)\times U(1)$ being anomaly free. Moreover, the same fermion content also preserves the $B-L$ symmetry, which stands for the conservation of the baryon number B minus the lepton number L. In comparison, in the context of the Standard Model, the $B+L$ symmetry (referring to the conservation of the baryon number plus the lepton number) must be violated as a quantum anomaly, in the form of,

$$\partial_\mu j_b^\mu = \partial_\mu j_l^\mu = \frac{n_f}{64\pi^2}\epsilon^{\mu\nu\rho\sigma}F^a_{\mu\nu}F^a_{\rho\sigma} - \frac{n_f}{64\pi^2}\epsilon^{\mu\nu\rho\sigma}B_{\mu\nu}B_{\rho\sigma}, \tag{1.7}$$

where $F^a_{\mu\nu}$ and $B_{\mu\nu}$ are separately the field strength tensor for $SU(2)$ and $U(1)$ gauge fields. Each quark is assigned with baryon number $B=+\frac{1}{3}$, and each anti-quark $B=-\frac{1}{3}$. Similarly, for a lepton $L=1$ and for an anti-lepton $L=-1$. The factor $n_f=3$ is the number of fermion generations. The integral expression of (1.7) leads to [17]

$$\begin{aligned} N_B(t)-N_B(0) &= \int_0^t d\tau\int d^3x\partial_\mu j_b^\mu(x) \\ =N_{CS}(t)-N_{CS}(0) &= \int_0^t d\tau\int d^3x\frac{n_f}{64\pi^2}\epsilon^{\mu\nu\rho\sigma}F^a_{\mu\nu}F^a_{\rho\sigma}, \end{aligned} \tag{1.8}$$

and the integral of the $U(1)$ part vanishes. This connects the baryon number to the topological number of the $SU(2)$ gauge field, the Chern-Simons number, and the change of the Chern-Simons number corresponds to the change of the baryon number.

Theoretically, the $B+L$ anomaly during the evolution of the early universe could lead to the observed baryon asymmetry, which is represented in the present baryon-to-photon ratio of the value [73, 81]

$$\eta = \frac{n_B}{n_\gamma} = 6.0\times 10^{-10}, \tag{1.9}$$

where n_r is the number density of photons and n_B the number density of baryons minus anti-baryons. The asymmetry could be imposed as an initial condition, but it is unnatural to explain its value. Moreover, if the inflation theory is correct, any such initial value will be diluted by the inflation. To have baryogenesis, by which we refer to the mechanism that can produce the observed value of η in (1.9), three necessary conditions have been proposed by Sakharov [9],

1. baryon number non-conservation;

2. C- and CP-violation;

3. out-of-thermal-equilibrium.

The non-conservation of baryon number is obviously necessary, for baryogenesis is essentially a mechanism during which more baryons are produced than anti-baryons. The C-symmetry, if it is not broken, can account for the production of the same amount of baryons and anti-baryons that have the same momentum and spin. Similarly, the CP-symmetry corresponds to the symmetry between baryons and anti-baryons that have the opposite momentum but the same spin. If either symmetry exists, there will be no opportunity to achieve an excess of baryons over anti-baryons. In thermal equilibrium, if a process increases the baryon number, then the baryon number will be decreased at the same rate by its reverse process. Therefore the out-of-equilibrium is also necessary.

The Standard Model has sources for all Sakharov's three conditions. The baryon number non-conservation can be accomplished directly as a consequence of the $B+L$ anomaly. Furthermore, the C-symmetry is maximally broken in the electroweak theory. Also, the CP-violation is contained in the Standard Model, in the form of a complex phase included in the CKM matrix [12], the three-generation quark mixing matrix. In addition, there could also exist similar CP-violation in the lepton (neutrino) mixing matrix, known as PMNS matrix [6, 7]. The out-of-equilibrium can commonly be caused during the phase transition of Higgs field, [2] for instance, by the spinodal (tachyonic) instability in Higgs IR modes that we will consider later.

The main goal of the thesis is to study electroweak baryogenesis through real-time simulations, with quantum fermions fully included. The only approximation that we need to do is the mean field approximation for bosonic fields. But as we will see in the following section, such approximation is well justified, that the bosonic fields in the electroweak transition can be accurately described by classical physics, because of their large occupation numbers. We will first implement the simulations based on the Standard Model, as close as possible and the mechanism we follow is Cold Electroweak Baryogenesis [56].

[2] While as a matter of fact, the Standard Model Higgs field does not suffice to produce the first-order phase transition [38, 39].

1.1 Cold Electroweak Baryogenesis

Cold electroweak baryogenesis proposes that baryogenesis happened during the electroweak symmetry breaking, triggered by the Higgs field going through a rapid and cold quench transition, with the potential that can be written as,

$$V(\phi) = \mu_{\rm eff}^2 \phi^\dagger \phi + \lambda (\phi^\dagger \phi)^2 + \frac{\mu^2}{4\lambda}. \tag{1.10}$$

where the effective mass parameter $\mu_{\rm eff}^2$ changed from positive value to the present negative value, $-\mu^2 = -(125\ \ {\rm GeV})^2/2$. The reason for the quench might be that the Higgs field coupled to gravity or the inflaton via the effective mass term and these fields changed during the (p)reheating [3] [46, 47, 53, 56]. But here, we will not pursue the dynamics for the quench. Instead, we in practice introduce the quench time τ_Q and parameterize the effective mass parameter as

$$\begin{aligned} \mu_{\rm eff}^2(t) =& \mu^2 \left(1 - \frac{2t}{\tau_Q}\right), \qquad t < \tau_Q, \\ =& -\mu^2, \qquad t > \tau_Q, \end{aligned} \tag{1.11}$$

or more frequently, in the form of the instantaneous quench,

$$\begin{aligned} \mu_{\rm eff}^2(t) =& +\mu^2, \qquad t < 0, \\ =& -\mu^2, \qquad t > 0. \end{aligned} \tag{1.12}$$

In the framework of Cold Electroweak Baryogenesis, the baryon number non-conservation is achieved through the $B + L$ anomaly. With regard to the CP-violation source, the CKM matrix has been considered for baryogenesis in [56], where a cold electroweak transition was originally proposed. The temperature during the electroweak transition should be low, as the CP-violation due to CKM matrix is highly suppressed by the temperature. The study in [68] further suggested that the electroweak transition temperature should be at most of order 1 GeV, in order to have a viable Standard Model baryogenesis. However, the results in lattice simulations [60, 76] (see also Chapter 3) indicate the temperature is never below 20 GeV

[3] The energy is assumed to be transferred from the inflaton to Higgs field and then to other Standard Model particles to reheat the Universe. The process can happen quickly through the parametric resonance, for bosonic fields [34, 42], as well as for fermionic fields [43, 48]

during cold electroweak transition. Thus, the Standard Model CP-violation as the origin of the baryon asymmetry can be ruled out. Therefore to achieve a realistic baryogenesis, it is necessary to recruit a new CP-violation source from physics beyond the Standard Model. For this reason, we consider the minimal extension, that is, including another Higgs doublet, so that the CP-symmetry is broken as a result of the extra C-violating terms contained in the two-Higgs potential [13, 30, 31]. In Chapter 4, we are going to simulate such a Cold Electroweak Baryogenesis and estimate the baryon asymmetry.

In the scenario of cold electroweak transition, the out-of-equilibrium is generated by the spinodal (tachyonic) instability developed in IR modes during the Higgs field rolling down from the center of the potential. Immediately after the departure, a long-wave mode of momentum k can grow exponentially,

$$\phi_k(t) \to e^{t\sqrt{\mu^2-k^2}}, \qquad \text{if} \qquad k^2 < \mu^2, \tag{1.13}$$

as the solution of the equation of motion,

$$\ddot{\phi}_k + k^2\phi_k - \mu^2\phi_k = 0,$$

and eventually the exponential growth will be stopped when the quartic term in the potential becomes no longer negligible. As a consequence, the Higgs occupation numbers for those unstable modes can become very large, and in addition, through interactions, low-momentum modes of the gauge field can also be highly occupied [56].

One advantage of Cold Electroweak Baryogenesis is that the evolution of quantum Higgs and gauge fields in the process can be accurately described by the classical physics, owing to the large occupation numbers [49, 50, 52]. Large particle number can indeed lead to some simplification. For instance, for creation operator $b_k^\dagger$, annihilation operator b_k, and n-particle state $|n\rangle$, the following approximation,

$$\langle n|b_k^\dagger b_k|n\rangle = n \simeq n+1 = \langle n|b_k b_k^\dagger|n\rangle, \tag{1.14}$$

would be valid when the particle number $n \gg 1$. Actually, for most physical observables, which would be in the form of the time-ordered product, such that

$\langle n|\mathrm{T}\phi(x)\phi(y)|n\rangle \sim \langle n|b_k b_k^\dagger + b_k^\dagger b_k|n\rangle$, the error caused by the approximation will be the same order of $1/n$. To some extent, equation (1.14) corresponds to ignoring the commutation relation for bosons, $\langle n|[b_k,\ b_k^\dagger]|n\rangle$ which is tiny compared to $\langle n|b_k b_k^\dagger|n\rangle$ and $\langle n|b_k^\dagger b_k|n\rangle$.

In Fig 1.1, we show the typical energy partition during the cold electroweak transition. The Higgs field is initialized in the false vacuum ($\langle\phi\rangle = 0$), and the main

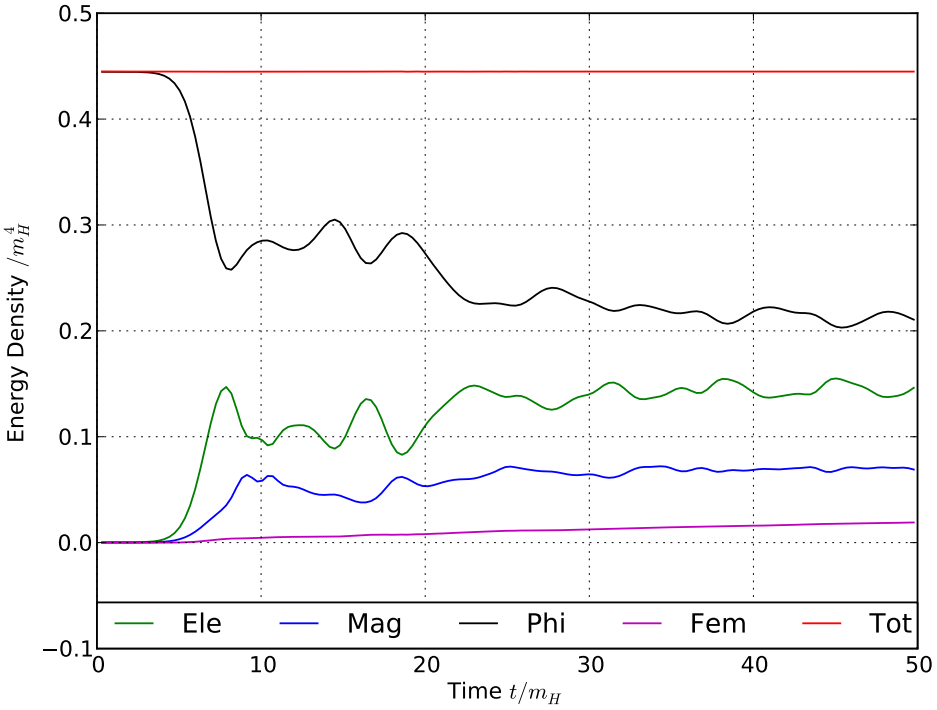


Figure 1.1. The energy densities of the electric part of the gauge field (Ele), magnetic part (Mag), the Higgs field (Phi) and fermions (Fem) in the cold electroweak transition. The time and energy densities are rescaled with $m_H = 125$ GeV. The physical volume is $V = \left(\frac{48\times 0.63}{m_H}\right)^3$. For more details, see Chapter 3.

energy in the beginning is in the form of Higgs potential energy. The evolution is triggered by the Higgs field rolling down from the center of the potential and the spinodal instability in IR modes is developed accordingly. The energy is quickly dispensed to the Higgs kinetic part as well as to the gauge field, and the Higgs field will eventually undergo damped oscillations around the minimum of the potential. The energy transfer during the first Higgs oscillation ($t < 7/m_H$) is quick and massive, and the production of bosons mainly occurs during this period. In practical simulations, large occupation numbers are indeed achieved. By assuming that only low-momentum Higgs bosons are produced and moreover their momenta can be

ignored in comparison with the mass, as for unstable modes $k^2 < \mu^2$, we arrive at

$$\frac{N m_H}{V m_H^4} \simeq 0.2, \qquad \rightarrow \qquad N \simeq 5 \times 10^3, \tag{1.15}$$

with N the total Higgs particle number. For each IR mode, the occupation number is of the order of 100, given the total number of such unstable modes being 56. Similarly, occupation numbers of the gauge boson would be of the same order.

In reality, fermions are usually excluded in numerical simulations of Cold Electroweak Baryogenesis. [4] This is not because fermions are not important; on the contrary, fermions are crucial in the $B + L$ anomaly as well as C-, P- and CP-violation. The reason for the exclusion is that a large number of variables is always required to represent fermions in real-time simulations. The approximation condition (1.14) does not apply to fermionic fields, as fermion occupation numbers, restricted by the Pauli exclusion principle, can never be larger than one. Fermionic fields should be always treated as quantum fields.

While the gauge and Higgs fields are classical, fermion dynamics can accordingly become simpler. One attempt that we can imagine is to integrate out fermions, as a Gauss integral of Grassmann numbers. At least, integration can be carried out in form,

$$\mathrm{Det}\left[\gamma^\mu D_\mu + y_{\mathrm{uk}}\phi\right] = \int [D\bar{\psi}][D\psi] e^{iS_F + iS_Y}. \tag{1.16}$$

where fermions interact with the gauge field through the covariant term in S_F and coupling to the Higgs field via the Yukawa interaction S_Y, with Yukawa parameter y_{uk}. Only for some simple background fields, the left-handed side can be sorted out explicitly. [5] One example is the Heisenberg-Euler lagrangian (1.2), which is obtained with the assumption of constant electric and magnetic fields. Except for those special background fields, the practical calculation of (1.16) will strongly depend on the perturbation of background fields, (for instance, by the heat kernel expansion [55]). On the other hand, the gauge and Higgs fields, after experiencing the exponential growth during the electroweak transition, may not be treated as small. For this

[4] Notice, Fig 1.1 comes from the simulation with fermions. From the perspective of the energy, fermionic fields are less dominant in the time evolution of the system, in comparison with bosonic fields.

[5] Quite possibly, if one can do so, one can also solve analytically the Dirac equation for fermions in such background.

reason, it does not look promising to integrate out fermions during the electroweak transition.

Our primary goal of the thesis is to establish real-time simulations to embrace Standard Model fermions, including interactions between quantum fermions and classical bosons. The classical gauge and Higgs fields can indeed simplify the calculations of quantum fermions. In the Feynman diagram, the bosonic fields appear merely as external lines, and therefore the fermion one-loop is the only possible inner loop. In the language of the correlation function, what we know about fermions can all come from their two-point functions. In fact, the essence of the numerical method that we will introduce in the following section is that the method can represent precisely the fermion two-point functions.

1.2 Fermions in real-time simulations

The first real-time simulation with fermions was given by [44], in a 1+1 dimensional lattice, with the method known as mode function method, which is to evolve all quantum mode functions according to the Dirac equation. When extending the method to 3+1 dimension, one would encounter the difficulty to accommodate a large number of variables for fermions on a lattice of reasonable size. For example, to a cubic lattice with N sites along each direction, the number of variables is of order N^6, which is accounted for by the rapidly increasing number and size of mode functions.

The proper way to show what the large number of variable corresponds to is to consider the matrix constructed with all mode functions. For the sake of simplicity, we will illustrate the analysis in 1+1 dimension and extend the result directly to 3+1 dimension. The 1+1 dimensional Dirac equation reads

$$\left(\gamma^0 \frac{d}{dt} + \gamma^1 \frac{d}{dx} + m\right) \psi(t,x) = 0, \tag{1.17}$$

which can be written as a Schrodinger equation,

$$i\frac{d}{dt}\psi(t,x) = \hat{H}\psi(t,x), \tag{1.18}$$

with the Hamilton operator,

$$\hat{H} = i\gamma^0\gamma^1\frac{d}{dx} + im\gamma^0. \tag{1.19}$$

For a lattice of N sites along x direction, the Hamilton operator acts on the wave function as, [6]

$$\hat{H}\psi(x) = -\frac{i\gamma^0\gamma^1}{2dx}\psi(x-dx) + im\gamma^0\psi(x) + \frac{i\gamma^0\gamma^1}{2dx}\psi(x+dx). \tag{1.20}$$

In the continuum theory, the operator could be represented as a infinite-dimensional matrix; while on the lattice, the size of the matrix is only $2N \times 2N$. In order to display it, we write the wave function into a $2N$ dimensional vector, and therefore the super-vector and Hamilton can be written as

$$\psi(x)=\begin{pmatrix} \psi(0dx) \\ \psi(1dx) \\ \psi(2dx) \\ \psi(3dx) \\ \psi(4dx) \\ \psi(5dx) \end{pmatrix}, \quad \hat{H}=\begin{pmatrix} im\gamma^0 & \frac{i\gamma^0\gamma^1}{2dx} & . & . & . & \frac{i\gamma^0\gamma^1}{2dx} \\ -\frac{i\gamma^0\gamma^1}{2dx} & im\gamma^0 & \frac{i\gamma^0\gamma^1}{2dx} & . & . & . \\ . & -\frac{i\gamma^0\gamma^1}{2dx} & im\gamma^0 & \frac{i\gamma^0\gamma^1}{2dx} & . & . \\ . & . & -\frac{i\gamma^0\gamma^1}{2dx} & im\gamma^0 & \frac{i\gamma^0\gamma^1}{2dx} & . \\ . & . & . & -\frac{i\gamma^0\gamma^1}{2dx} & im\gamma^0 & \frac{i\gamma^0\gamma^1}{2dx} \\ -\frac{i\gamma^0\gamma^1}{2dx} & . & . & . & -\frac{i\gamma^0\gamma^1}{2dx} & im\gamma^0 \end{pmatrix}, \tag{1.21}$$

where $N = 6$ is chosen for the purpose of demonstration. It is easy to show that super-matrix $\hat{H}$ in (1.21) is Hermitian matrix, and therefore can be factorized as

$$\hat{H}M = M\Lambda, \tag{1.22}$$

where the diagonal matrix Λ is a collection of eigenvalues and the unitary matrix M is a collection of eigenfunctions (mode functions). Similar analysis in 3+1 dimension will lead to the super-matrix M as a $4N^3 \times 4N^3$ unitary matrix, with N the number of site on each direction.

Moreover, the super-matrix M can be constructed specifically. In canonical

[6] The derivative is transformed into the difference in the form of,

$$\frac{d}{dx}\psi(x) \to \frac{\psi(x+dx) - \psi(x-dx)}{2dx}.$$

quantization, the fermion field operator can be written as

$$\hat{\psi}(t,x) = \frac{1}{\sqrt{V}} \sum_{q,s} \left[\hat{b}_{q,s} U_{q,s}(t,x) + \hat{d}^{\dagger}_{-q,-s} V_{-q,-s}(t,x) \right], \tag{1.23}$$

with the physical volume V, mode functions $U_{q,s}(t,x)$, $V_{-q,-s}(t,x)$, and the anti-commutation relation of creation and annihilation operators,

$$\{\hat{b}^{\dagger}_{p,r}, \hat{b}_{p',s}\} = \delta_{rs}\delta^{3}_{pp'}, \qquad \{\hat{d}^{\dagger}_{-p,-r}, \hat{d}_{-p',-s}\} = \delta_{rs}\delta^{3}_{pp'}, \tag{1.24}$$

where we have already adopted the discretized version of the expressions (for more details, see Chapter 3). The evolution of the field operator is described by Heisenberg equation,

$$i\frac{d}{dt}\hat{\psi} = -[H,\ \hat{\psi}] = \hat{H}\hat{\psi}. \tag{1.25}$$

We simply write the spatial variable as a subscript and also manifest the spinor component by the subscript α,

$$\hat{\psi}_{x,\alpha}(t) = \frac{1}{\sqrt{V}} \sum_{q,s} \left[\hat{b}_{q,s} U_{x,\alpha;q,s}(t) + \hat{d}^{\dagger}_{-q,-s} V_{x,\alpha;-q,-s}(t) \right]. \tag{1.26}$$

Then the unitary matrix M can be constructed, with components,

$$M_{x,\alpha;q,s,0}(t) = U_{x,\alpha;q,s}(t), \qquad M_{x,\alpha;q,s,1}(t) = V_{x,\alpha;-q,-s}(t). \tag{1.27}$$

Notice that the spinor index α ranges from 0 to 3, and spin index $s = 0$, 1, so that M is indeed a $4N^3 \times 4N^3$ matrix. As a result, the field operator can be written as

$$\hat{\psi} = M\hat{c}, \tag{1.28}$$

where similarly we write the creation/annihilation operator into a super-vector, in the form of, $\hat{c} = (\hat{b}_{p_0,s_0},\ \hat{d}^{\dagger}_{-p_0,-s_0},\ \hat{b}_{p_0,s_1}, ...)^T$. Therefore from Heisenberg equation (1.25), we can deduce the evolution equation for the unitary matrix M,

$$i\frac{d}{dt}M = \hat{H}M. \tag{1.29}$$

Such super-matrix convention is also useful to simplify the equal-time two-point function of fermion fields,

$$D(x,y) = \langle \mathrm{T}\psi(x)\psi^\dagger(y)\rangle, \tag{1.30}$$

from which the fermion backreaction to gauge field and Higgs field, as well as other interesting fermion observables can be extracted. By writing $D(x,y)$ in the form of the super-matrix, we can get the simple expression,

$$D = \frac{1}{2V} MSM^\dagger, \tag{1.31}$$

where the $4N^3 \times 4N^3$ matrix $S = \mathrm{diag}(+1,-1,+1,...)$ comes in as a result of the time-ordered product $\langle \mathrm{T}\ \hat{c}\otimes\hat{c}^\dagger\rangle = \frac{1}{2}S$, for the time-ordered product at equal-time is simply written as $\langle \mathrm{T}\ \hat{a}\hat{b}\rangle = \langle \hat{a}\hat{b} - \hat{b}\hat{a}\rangle/2$. For these reasons, we can finally conclude that representing the super-matrix M would be identical to representing quantum fermions in a classical bosonic background.

In reality, to depict the $4N^3 \times 4N^3$ unitary matrix, at least $8N^6$ independent real variables are required, which is the number of generators of the unitary group $U(4N^3)$. As it shows, the N^6-dependence will become a big challenge to numerical simulations. For instance when $N = 32$, it requires 256 GB of computer memory space to represent a single fermionic field in $3 + 1$ real-time simulations; while when $N = 48$, the number becomes a desperate 2.916 TB.

To alleviate the problem, a Monte Carlo method has been proposed in [61]. The method, also known as low-cost fermions or ensemble fermions, could reduce the N^6-dependence to N^3N_q-dependence, with N_q a number to be determined in practical simulations. The validity of the method can be easily demonstrated in the language of super-matrix. For this purpose, we define two matrices as

$$M_M = \frac{1}{\sqrt{2N_q}} MQ, \qquad M_F = \frac{1}{\sqrt{2N_q}} MSQ, \tag{1.32}$$

where the constant Q is a $4N^3 \times N_q$ matrix, so are M_M and M_F. Then the evolution is described by

$$i\frac{d}{dt}M_M = \hat{H}M_M, \qquad i\frac{d}{dt}M_F = \hat{H}M_F, \tag{1.33}$$

and the two-point function can be calculated as,

$$D = \frac{1}{V} M_M M_F^\dagger = \frac{1}{2VN_q} MQQ^\dagger SM^\dagger. \tag{1.34}$$

In comparison with (1.31), the method would be identical to the exact mode function method, if the equation

$$\frac{1}{N_q} QQ^\dagger = I, \tag{1.35}$$

can be satisfied. Strictly speaking, the exact equation (1.35) would require N_q never smaller than $4N^3$. But we are more interested in the case that $N_q < 4N^3$, especially $N_q \ll 4N^3$.

The equation (1.35) can be achieved, approximately, when each component q_{ij} of matrix Q is assigned with a random complex number, according to a specific distribution (say Gaussian distribution), such that statistic expectation $\mathrm{E}[q_{ij} q^\star_{mn}] = \delta_{im}\delta_{jn}$. Accordingly, the equation (1.35) can be illustrated as,

$$\frac{1}{N_q} \begin{pmatrix} q_{00} & q_{01} & q_{02} \\ q_{10} & q_{11} & q_{12} \\ q_{20} & q_{21} & q_{22} \\ q_{30} & q_{31} & q_{32} \\ q_{40} & q_{41} & q_{42} \end{pmatrix} \begin{pmatrix} q^\star_{00} & q^\star_{10} & q^\star_{20} & q^\star_{30} & q^\star_{40} \\ q^\star_{01} & q^\star_{11} & q^\star_{21} & q^\star_{31} & q^\star_{41} \\ q^\star_{02} & q^\star_{12} & q^\star_{22} & q^\star_{32} & q^\star_{42} \end{pmatrix} = \begin{pmatrix} 1 & . & . & . & . \\ . & 1 & . & . & . \\ . & . & 1 & . & . \\ . & . & . & 1 & . \\ . & . & . & . & 1 \end{pmatrix}, \tag{1.36}$$

and as a result the method reduces the number of variables from $(4N^3)^2$ to $(8N^3 N_q)$.

According to the law of large numbers, the ensemble-fermion method in the limit $N_q \to \infty$ would match exactly the mode function method, and on the way of increasing N_q, one would observe that the physics converge to the final limit. In practice, in comparison with N^3, a reasonable N_q, would guarantee that the evolution of the system and most observables converge accurately [61, 76, 77, 78, 79].

1.3 Overview

The main topic of the thesis is to establish real-time simulations for cold baryogenesis from first principles, with one generation of fermions explicitly included. As a

consequence, a baryon asymmetry can be measured through practical simulations.

In Chapter 2, we focus on the quantum anomaly. By solving the Dirac equation for fermions in parallel electric and magnetic fields, we find the chiral anomaly related only to the lowest-energy Landau levels. For massless fermions, the anomaly can be seen as a result of the production of particles of one chirality, and no production of particles of the other chirality. For massive fermions, the chiral anomaly equation can be achieved as a consequence of the regularization. Then we extend the method to calculate other quantum anomalies and this leads to the anomaly cancellation. To our concern, we find the fermion content of the Standard Model can yield the $B - L$ symmetry being anomaly free, but the $B + L$ symmetry must be violated as a quantum anomaly. We also show in the chapter that the quantum anomaly on a lattice can be replicated by Wilson fermions [16], which were originally proposed to deal with the fermion doubling problem, the problem that more unwanted species appear when fermions are represented on the lattice in a naive way. We further demonstrate only spatial Wilson terms are necessary in real-time simulations, and the temporal doubling problem can be solved by choosing properly fermion initialization.

In Chapter 3, we implement ensemble fermions for a reduced electroweak sector of the Standard Model and calculate the effective preheating temperature during a fast electroweak transition, relevant for Cold Electroweak Baryogenesis. We find that with ensemble fermions, the dynamics and most observables can converge with a viable number of fermion realizations. Via measuring the occupation number, we discover that in the later time of the evolution, an equilibrium can emerge in the IR modes of fermions. According to the Fermi-Dirac distribution, we extract the temperature and find the temperature never below 20 GeV, which, in combination with the results in [68], can indirectly rule out the Standard Model CP-violation as the origin of the baryon asymmetry of the Universe. The chapter is based on [76].

In Chapter 4, we further investigate the baryon asymmetry with new CP-violation mechanism in a minimal extension of the Standard Model, by recruiting another Higgs doublet, and therefore involving extra C-violating terms in the two-Higgs potential. As a result, all Sakharov's three conditions are represented in our first-principles numerical simulations. We also in practice choose possibly large CP violation by scrutinizing the two-Higgs potential and Yukawa interaction. Through

large-scale computer simulations, we calculate the baryon number for one particularly favourable scalar potential, and find an asymmetry of $|\eta| \leq 3.5 \times 10^7$. The chapter is based on [83].

Finally, we give the summary and outlook. In particular, we consider how to realize the complete electroweak $SU(2) \times U(1)$ theory, with fermions explicitly included.

Chapter 2

Solving the Dirac Equation

The chapter is dedicated to solving the Dirac equation for fermions in different situations, specifically, in an electric field, in a magnetic field, in parallel electric and magnetic fields and on a lattice. A detailed study of related solutions will also be carried out to reveal their Physical implications, including, pair production, Landau levels and the chiral anomaly. The Dirac equation for fermions in a homogeneous electric field has been first solved by Sauter in 1931 [3]. When the electric field is on, virtual pairs of electron and positron could become real pairs and the system tunnels from the vacuum state to a state of particles. The vacuum persistence probability has been originally obtained by Schwinger in 1951 [5], where the proper-time method has been implemented to calculate and regularize the fermion determinant. The result can also be achieved in the canonical quantization, and one of our goals is to demonstrate that the same expression can also be reached by solving the Dirac equation and calculating the Bogoliubov coefficients. Our other concern is Landau levels of fermions in a homogeneous magnetic field, whose discretization and degeneracy can be easily reckoned in the solution of the Dirac equation. Having established an understanding of pair production and Landau levels, one can discover the chiral anomaly of massless fermions in parallel electric and magnetic fields. For massive fermions, we make manifest the role of regularization, which, if established properly, can easily lead to the chiral anomaly. Such way of calculation on massive fermions, to the best of our knowledge, is still absent in the literature. We also want to convince ourselves that there must be a similar anomaly to the $B + L$ symmetry with the Standard Model baryons and leptons. Our last, but not least, concern is the realization of fermions on a lattice, particularly the doubling problem and

accomplishment of chiral anomaly.

The mode function expansion will be adopted throughout the work. Each mode function can be seen as a solution of the Dirac equation which, in our convention, reads

$$\gamma^\mu D_\mu \psi(t,x) + m\psi(t,x) = 0. \tag{2.1}$$

For free fermions in canonical quantization, the field operator can have a mode function expansion

$$\psi(t,x) = \sum_s \int \frac{d^3p}{(2\pi)^3} \frac{e^{ip.x}}{\sqrt{2\omega}} \left[e^{-i\omega t} b_s(p) U_s(p) + e^{i\omega t} d^\dagger_{-s}(-p) V_{-s}(-p) \right], \tag{2.2}$$

where the creation and annihilation operators satisfy non-zero anti-commutation relations

$$\begin{aligned} \{b_r(p), b^\dagger_s(p')\} &= (2\pi)^3 \delta_{rs} \delta^3(p-p'), \\ \{d_{-r}(-p), d^\dagger_{-s}(-p')\} &= (2\pi)^3 \delta_{rs} \delta^3(p-p'), \end{aligned} \tag{2.3}$$

and any other anti-commutation relations will be zero. When fermions interact with other fields, either by coupling to gauge fields or gravity through the covariant derivative, or by coupling to scalar fields via Yukawa interaction, the expansion (2.2) should be replace by a more general form:

$$\psi(t,x) = \sum_s \int \frac{d^3p}{(2\pi)^3} \left[b_s(p) U_s(p;t,x) + d^\dagger_{-s}(-p) V_{-s}(-p;t,x) \right]. \tag{2.4}$$

All mode functions $\psi_s(p;t,x)$, ($U_s(p;t,x)$ and $V_{-s}(-p;t,x)$), of any p and s should satisfy the Dirac equation,

$$\gamma^\mu D_\mu \psi_s(p;t,x) + m\psi_s(p;t,x) = 0., \tag{2.5}$$

and they are orthonormal in the following way,

$$\sum_s \int \frac{d^3p}{(2\pi)^3} \left[U_s(p;t,x)U_s^\dagger(p;t,y) + V_{-s}(-p;t,x)V_{-s}^\dagger(-p;t,y)\right] = \delta^3(x-y)\mathbb{I}_{4\times 4}, \tag{2.6}$$

$$\int d^3x U_s^\dagger(p;t,x)U_{s'}(q;t,x) = \int d^3x V_{-s}^\dagger(-p;t,x)V_{-s'}(-q;t,x) = (2\pi)^3\delta^3(p-q)\delta_{ss'}, \tag{2.7}$$

and any similar product of U and V will be zero. With the mode functions, the equal-time two-point correlation functions can be expanded as

$$\begin{aligned}\langle \mathrm{T}\psi(t,x)\psi^\dagger(t,y)\rangle = -\sum_s \int \frac{d^3p}{(2\pi)^3} \Big[&U_s(p;t,x)U_s^\dagger(p;t,y)(n_s^u(p)-\frac{1}{2}) \\ &-V_{-s}(-p;t,x)V_{-s}^\dagger(-p;t,y)(n_{-s}^v(-p)-\frac{1}{2})\Big],\end{aligned} \tag{2.8}$$

where $n_s^u(p)$ is the initial occupation number of the particle of momentum p and spin $s/2$ and $n_{-s}^v(-p)$ the initial occupation number of the anti-particle of momentum $-p$ and spin $-s/2$. The symbol T denotes the product of operators is time-ordered, i.e.

$$\mathrm{T}a(t_1)b(t_2) = \theta(t_1-t_2)a(t_1)b(t_2) - \theta(t_2-t_1)b(t_2)a(t_1), \tag{2.9}$$

where the step function is defined unambiguously as

$$\theta(x-y) = \begin{cases} 1 & \text{if} \quad x > y, \\ 0.5 & \text{if} \quad x = y, \\ 0 & \text{if} \quad x < y. \end{cases} \tag{2.10}$$

2.1 Fermions in an electric field

Without loss of generality, we assume the electric field is applied along the third direction. We also assume the electric field is turned on instantly at $t = 0$, and could be turned off instantly thereafter. To generate it, the gauge field can be chosen as $(0, 0, 0, A_3(t))$ with $A_3(t) = -Et$, under the convention $\vec{E} = -\dot{\vec{A}}$. Since the gauge field is a function of time only, spatial plane waves are still valid to serve as eigenfunctions. Given a single mode function of the form $\psi_s(p;t,x) =$

$\exp(ip_1x_1 + ip_2x_2 + ip_3x_3)\psi_s(t,p)$ with p_1, p_2 and p_3 constant, the Dirac equation (2.5) becomes

$$\left(\gamma^0\frac{\partial}{\partial t} + i\gamma^3[p_3 - eA_3(t)] + i\gamma^1 p_1 + i\gamma^2 p_2 + m\right)\psi_s(t,p) = 0. \tag{2.11}$$

A further separation of variables can be implemented in a way that

$$\psi_s(t,p) = \sqrt{2}\left[A(t,p_3)\frac{1+\gamma^0\gamma^3}{2} + C(t,p_3)\frac{1-\gamma^0\gamma^3}{2}\right]\psi_{p_1,p_2,s}, \tag{2.12}$$

where the spinor product $\psi^\dagger_{p_1,p_2,s}\psi_{p_1,p_2,s} = 1$ and $|A(t,p_3)|^2 + |C(t,p_3)|^2 = 1$ to meet the requirement that the mode functions are orthonormal as in (2.6). The Dirac equation then leads to

$$\left(i\gamma^1 p_1 + i\gamma^2 p_2 + m\right)\psi_{p_1,p_2,s} = -i\gamma^0\epsilon\psi_{p_1,p_2,s}, \tag{2.13}$$

$$\left(\gamma^0\frac{\partial}{\partial t} + i\gamma^3[p_3 - eA_3(t)]\right)[AP_{b+} + CP_{b-}] = [AP_{b+} + CP_{b-}]\, i\gamma^0\epsilon, \tag{2.14}$$

where P_{b+} and P_{b-} are the abbreviation for the projector $\frac{1+\gamma^0\gamma^3}{2}$ and $\frac{1-\gamma^0\gamma^3}{2}$ respectively.

The equation (2.13) indicates $\psi_{p_1,p_2,s}$ and ϵ are the eigenspinor and eigenvalue of the matrix $H = -i\gamma^0\left(i\gamma^1 p_1 + i\gamma^2 p_2 + m\right)$. As a consequence, they can be chosen as:

$$\psi_{p_1,p_2,s} = \frac{1}{\sqrt{2\omega_3}}\begin{pmatrix} -\sqrt{\omega_3 - \sigma^1 p_1 - \sigma^2 p_2}\;\eta_s \\ \\ \sqrt{\omega_3 + \sigma^1 p_1 + \sigma^2 p_2}\;\eta_s \end{pmatrix}, \quad \epsilon = -\omega_3 < 0; \tag{2.15}$$

$$\psi_{p_1,p_2,s} = \frac{1}{\sqrt{2\omega_3}}\begin{pmatrix} \sqrt{\omega_3 + \sigma^1 p_1 + \sigma^2 p_2}\;\eta_s \\ \\ \sqrt{\omega_3 - \sigma^1 p_1 - \sigma^2 p_2}\;\eta_s \end{pmatrix}, \quad \epsilon = \omega_3 > 0, \tag{2.16}$$

where $\omega_3 = \sqrt{m^2 + p_1^2 + p_2^2}$ and η_s= $\begin{pmatrix} 1 \\ 0 \end{pmatrix}, \begin{pmatrix} 0 \\ 1 \end{pmatrix}$ for s=+1, -1.

As the two projectors P_{b+} and P_{b-} are orthogonal to each other, their coefficients

in (2.14) become two independent equations,

$$\frac{\partial}{\partial t}A(t,p_3) = i[p_3 - eA_3(t)]A(t,p_3) + i\epsilon C(t,p_3), \tag{2.17}$$

$$\frac{\partial}{\partial t}C(t,p_3) = i\epsilon A(t,p_3) - i[p_3 - eA_3(t)]C(t,p_3), \tag{2.18}$$

or in a concise way,

$$\frac{\partial}{\partial t}\begin{pmatrix} A \\ C \end{pmatrix} = i\left(p_3'\sigma^3 + \epsilon\sigma^1\right)\begin{pmatrix} A \\ C \end{pmatrix}, \tag{2.19}$$

with $p_3' = p_3 - eA_3(t)$.

Before the electric field turned on and after it is turned off, the vacuum states are well-defined and they are actually identical, up to a gauge transformation. For A_3 will be a constant after the turn-off, the gauge field can be shifted to $A_\mu' = 0$ by a gauge transformation of the form $e^{-ieA_3x_3}$. At the same time, the fermion mode number must be changed from p_3 to $p_3' = p_3 - eA_3$, and the physical momentum that can be observed is p_3'. For these vacuum states, we solve the equation (2.19), and select the convention

$$\begin{pmatrix} A^F \\ C^F \end{pmatrix}_U = \frac{e^{-i\omega t}}{\sqrt{2\omega}}\begin{pmatrix} \sqrt{\omega - p_3'} \\ \\ \sqrt{\omega + p_3'} \end{pmatrix} = \frac{e^{-i\omega t}}{\sqrt{2\cosh\theta}}\begin{pmatrix} \cosh\frac{\theta}{2} - \sinh\frac{\theta}{2} \\ \\ \cosh\frac{\theta}{2} + \sinh\frac{\theta}{2} \end{pmatrix}, \tag{2.20}$$

$$\begin{pmatrix} A^F \\ C^F \end{pmatrix}_V = \frac{e^{i\omega t}}{\sqrt{2\omega}}\begin{pmatrix} \sqrt{\omega + p_3'} \\ \\ \sqrt{\omega - p_3'} \end{pmatrix} = \frac{e^{i\omega t}}{\sqrt{2\cosh\theta}}\begin{pmatrix} \cosh\frac{\theta}{2} + \sinh\frac{\theta}{2} \\ \\ \cosh\frac{\theta}{2} - \sinh\frac{\theta}{2} \end{pmatrix}, \tag{2.21}$$

where the total energy $\omega = \sqrt{\omega_3^3 + p_3'^2} = \omega_3\cosh\theta$ and the third momentum component $p_3' = \omega_3\sinh\theta$. Notice

$$\begin{pmatrix} A \\ C \end{pmatrix}_V = \sigma^1\begin{pmatrix} A \\ C \end{pmatrix}_U^\star, \tag{2.22}$$

which is true for the free fermions and which will also be conserved during the

evolution by equation (2.19). Therefore we can use A_U and C_U only to compose mode functions, and we further omit their subscript U for simplicity. Finally, free fermions have explicit mode functions

$$U_s^F(p_1,p_2,p_3';t,x) = \frac{e^{ip_1x_1+ip_2x_2+ip_3'x_3}}{\sqrt{\omega_3}}\left[A^F(t,p_3)P_{b+}+C^F(t,p_3)P_{b-}\right] \begin{pmatrix} -\sqrt{\omega_3-\sigma^1p_1-\sigma^2p_2}\ \eta_s \\ \\ \sqrt{\omega_3+\sigma^1p_1+\sigma^2p_2}\ \eta_s \end{pmatrix}, \tag{2.23}$$

$$V_{-s}^F(-p_1,-p_2,-p_3';t,x) = \frac{e^{ip_1x_1+ip_2x_2+ip_3'x_3}}{\sqrt{\omega_3}}\left[C^{F\star}(t,p_3)P_{b+}+A^{F\star}(t,p_3)P_{b-}\right] \begin{pmatrix} \sqrt{\omega_3+\sigma^1p_1+\sigma^2p_2}\ \eta_s \\ \\ \sqrt{\omega_3-\sigma^1p_1-\sigma^2p_2}\ \eta_s \end{pmatrix}. \tag{2.24}$$

In this convention, the variables of the mode functions will indicate directly the physical quantities. For example, $U_s(p;t,x)$ represents a particle of momentum p and spin $s/2$, and $V_{-s}(-p;t,x)$ stands for an antiparticle of momentum $-p$ and spin $-s/2$. Such convention can also make straightforward the interpretation of the charge conjugation, which when acting on spinors, is denoted as $\psi^C = -\gamma^2\psi^\star$. As a consequence, the expression $U_s^C(p;t,x) = sV_s(p;t,x)$ manifests the truth that the charge conjugation does not affect the momentum and spin.

When $A_3(t) = -Et$, the only equation one needs to solve is

$$\frac{\partial}{\partial t}\begin{pmatrix} A \\ C \end{pmatrix} = i\left([p_3+eEt]\sigma^3-\omega_3\sigma^1\right)\begin{pmatrix} A \\ C \end{pmatrix}. \tag{2.25}$$

With redefined parameters

$$S = \frac{p_3+eEt}{\sqrt{eE}}, \quad a = \frac{\omega_3^2}{eE}, \tag{2.26}$$

the equation (2.25) becomes

$$\frac{d}{dS}\begin{pmatrix} A \\ C \end{pmatrix} = i\left(S\sigma^3-\sqrt{a}\sigma^1\right)\begin{pmatrix} A \\ C \end{pmatrix}. \tag{2.27}$$

or into second-order differential equation

$$\left[\frac{d^2}{dS^2} + S^2 + a + i\right] C = 0, \quad A = \frac{1}{\sqrt{a}}\left(i\frac{d}{dS} - S\right) C. \tag{2.28}$$

Two independent solutions can be written down with the parabolic cylinder function $D_s(x)$,

$$\begin{aligned} A_1 &= \frac{1+i}{2}\sqrt{a}e^{-\frac{a\pi}{8}} D_{-1-i\frac{a}{2}}([1+i]S), & A_2 &= e^{-\frac{a\pi}{8}} D_{i\frac{a}{2}}([-1+i]S), \\ C_1 &= e^{-\frac{a\pi}{8}} D_{-i\frac{a}{2}}([1+i]S), & C_2 &= \frac{1-i}{2}\sqrt{a}e^{-\frac{a\pi}{8}} D_{-1+i\frac{a}{2}}([-1+i]S), \end{aligned} \tag{2.29}$$

with properties

$$\begin{aligned} A_1(S) = C_2^\star(-S), \quad C_1(S) = A_2^\star(-S), \\ |A_1(S)|^2 + |C_1(S)|^2 = 1, \quad |A_2(S)|^2 + |C_2(S)|^2 = 1, \end{aligned} \tag{2.30}$$

and asymptotic values

$$\begin{aligned} |A_1(-\infty)| &= \sqrt{1 - e^{-\frac{a\pi}{2}}}, & |C_1(-\infty)| &= e^{-\frac{a\pi}{2}}, \\ |A_1(+\infty)| &= 0, & |C_1(+\infty)| &= 1. \end{aligned} \tag{2.31}$$

Also notice the combination $c_{ab} = A_1(S)C_2(S) - C_1(S)A_2(S)$ is a constant and therefore one can determine $|c_{ab}| = e^{-\frac{a\pi}{2}}$ by its asymptotic value.

The general solution will be the superposition of the two special solutions above, in the following way,

$$\begin{pmatrix} A(t,p_3) \\ C(t,p_3) \end{pmatrix} = \frac{1}{c_{ab}} \begin{pmatrix} A_1(S) & A_2(S) \\ C_1(S) & C_2(S) \end{pmatrix} \begin{pmatrix} C_2(S_0) & -A_2(S_0) \\ -C_1(S_0) & A_1(S_0) \end{pmatrix} \begin{pmatrix} A^F(0,p_3) \\ C^F(0,p_3) \end{pmatrix}, \tag{2.32}$$

where $S_0 = \frac{p_3}{\sqrt{eE}}$. So mode functions of initial momentum (p_1, p_2, p_3) are

$$U_s(p_1,p_2,p_3;t,x) = \frac{e^{ip\cdot x}}{\sqrt{\omega_3}}\left[A(t,p_3)P_{b+} + C(t,p_3)P_{b-}\right]\begin{pmatrix} -\sqrt{\omega_3 - \sigma^1 p_1 - \sigma^2 p_2}\,\eta_s \\ \\ \sqrt{\omega_3 + \sigma^1 p_1 + \sigma^2 p_2}\,\eta_s \end{pmatrix},$$

$$V_{-s}(-p_1,-p_2,-p_3;t,x) = \frac{e^{ip\cdot x}}{\sqrt{\omega_3}}\left[C^\star(t,p_3)P_{b+} + A^\star(t,p_3)P_{b-}\right]\begin{pmatrix} \sqrt{\omega_3 + \sigma^1 p_1 + \sigma^2 p_2}\,\eta_s \\ \\ \sqrt{\omega_3 - \sigma^1 p_1 - \sigma^2 p_2}\,\eta_s \end{pmatrix}.$$

At the instance τ, if the electric field is removed, the fermions become free ones again and the Bogoliubov transformation can be implemented in the following way,

$$\begin{aligned} e^{ieE\tau x_3}U_s(p_1,p_2,p_3;\tau,x) &= \alpha U_s^F(p_1,p_2,p_3';\tau,x) + \beta V_{-s}^F(-p_1,-p_2,-p_3';\tau,x), \\ e^{ieE\tau x_3}V_{-s}(-p_1,-p_2,-p_3;\tau,x) &= \gamma U_s^F(p_1,p_2,p_3';\tau,x) + \delta V_{-s}^F(-p_1,-p_2,-p_3';\tau,x). \end{aligned} \tag{2.33}$$

As the mode functions are orthonormal, there exist two restrictions on Bogoliubov coefficients,

$$|\alpha|^2 + |\beta|^2 = |\gamma|^2 + |\delta|^2 = 1, \quad \alpha^\star\gamma + \beta^\star\delta = 0. \tag{2.34}$$

Accordingly, there are only four free parameters, and one can choose α, β with $|\alpha|^2 + |\beta|^2 = 1$ and $\gamma = -\beta^\star e^{i\theta}$, $\delta = \alpha^\star e^{i\theta}$. Furthermore, the angle θ can be pinned down when initial values are considered, for instance, $e^{i\theta} = 1$ if initially $\alpha = \delta = 1$. $|\beta|^2 = |\gamma|^2$ is the result of pair productions of particle and anti-particle. The coefficient β can be solved out as,

$$\beta(\tau,p_3) = -s\left[C^F(\tau,p_3')A(t,p_3) - A^F(\tau,p_3')C(\tau,p_3)\right], \tag{2.35}$$

where $p_3' = p_3 + eE\tau$, and therefore the occupation number for the particle of momentum p, as well as for the anti-particle of momentum $-p$, is [1]

$$n(\tau,p_3) = |\beta(\tau,p_3)|^2 = \left|C^F(0,p_3')A(t,p_3) - A^F(0,p_3')C(\tau,p_3)\right|^2, \tag{2.36}$$

[1] One way to show that $|\beta|^2$ is the occupation number is to put the Bogoliubov transformation (2.33) into fermion two-point function (2.9).

where we omit the spin index as the occupation number does not depend on the spin choice, and we also drop the time-dependence of A^F and C^F, because both depend on time in the same way through a phase factor $e^{-i\omega t}$.

A comparison among distributions of occupation numbers with different $a = \frac{\omega_3^2}{eE}$ is displayed in Figure 2.1, and a study of the distribution of different time scales is performed in Figure 2.2. There are two features about the pair creation that we want to highlight:

(I) the distributions of occupation numbers have a reflection symmetry with respect to axis $p_3' = eE\tau/2$;

(II) the stable pair creation rate is $e^{-a\pi}$, given $a = \frac{w_3^2}{eE}$ and $2\omega_3$ being the energy gap between levels above and below the Dirac sea. Specifically, the pair production rate is non-perturbative of the electric strength E.

On the other hand, we can prove theoretically these two conclusions from the definition of the occupation number. For the purpose, we write

$$|\beta(\tau, p_3)|^2 = |\beta(p_3'; p_3)|^2 = \left| \frac{1}{c_{ab}} F^T(p_3') \begin{pmatrix} 0 & -1 \\ 1 & 0 \end{pmatrix} F(p_3) \right|^2 , \tag{2.37}$$

where $p_3' = p_3 + eE\tau$ and the abbreviation stands for

$$F(p_3) = \begin{pmatrix} A_1\left(\frac{p_3}{\sqrt{eE}}\right) & C_1\left(\frac{p_3}{\sqrt{eE}}\right) \\ A_2\left(\frac{p_3}{\sqrt{eE}}\right) & C_2\left(\frac{p_3}{\sqrt{eE}}\right) \end{pmatrix} \begin{pmatrix} C^F(0, p_3) \\ -A^F(0, p_3) \end{pmatrix}, \tag{2.38}$$

Because of the property of A_1 and C_1 in (2.30) and the expression of A^F and C^F in (2.20), one can calculate

$$F(-p_3) = -\begin{pmatrix} 0 & 1 \\ 1 & 0 \end{pmatrix} F^\star(p_3), \tag{2.39}$$

and consequently,

$$|\beta(p_3'; p_3)|^2 = |\beta(-p_3; -p_3')|^2, \tag{2.40}$$

which states the created particle number of the mode of initial momentum p_3 and finial momentum $p_3' = p_3 + eE\tau$ would be the same as the one of momentum changing

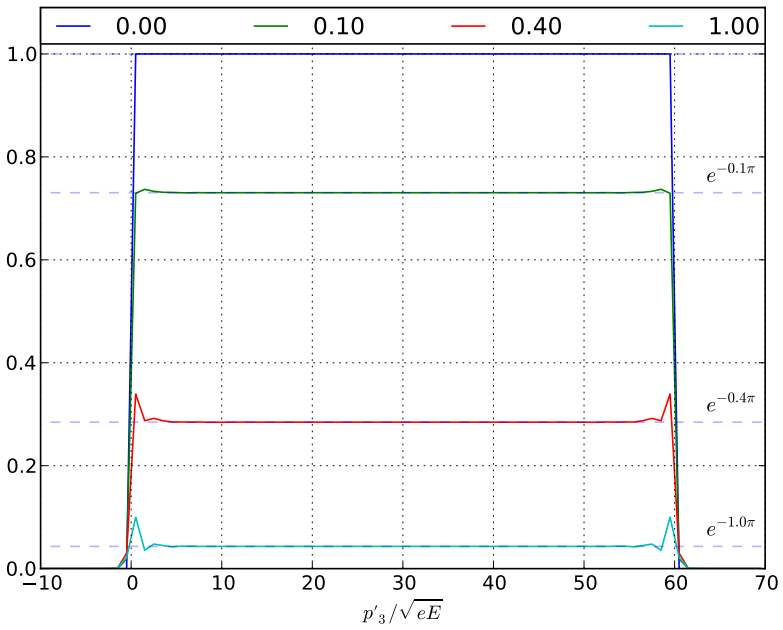


Figure 2.1. Distributions of occupation numbers at $\tau = 60/\sqrt{eE}$ with a=0.0, 0.1, 0.4 and 1.0 separately. The plot is symmetric along $p'_3 = 30\sqrt{eE}$. Values of the central plateau agree precisely with $\exp(-a\pi)$. The structures around $p'_3 = 0$ and $p'_3 = 60\sqrt{eE}$ are caused by the instant turn-on. When $a = 0$, the distribution is depicted exactly by step functions.

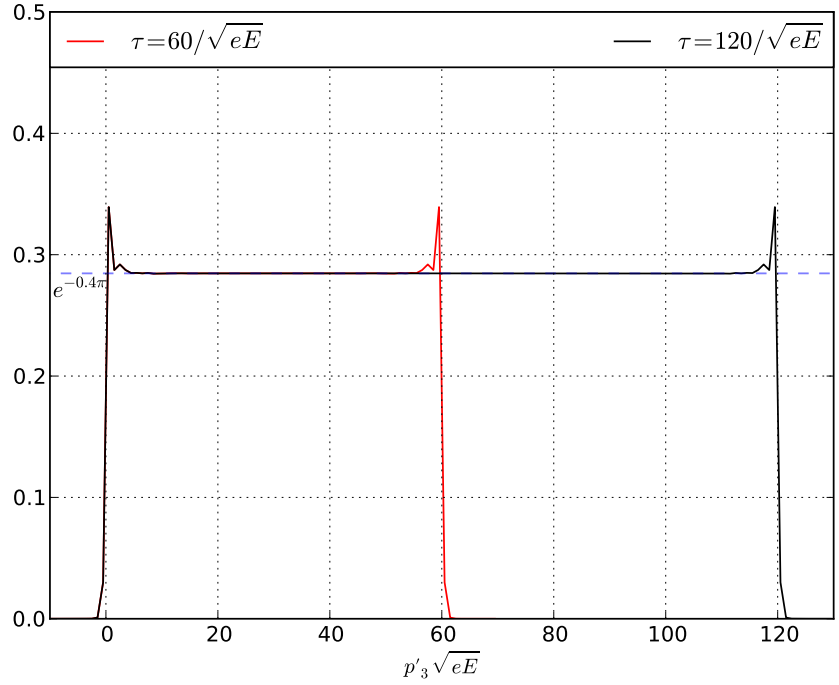


Figure 2.2. Distributions of occupation numbers of a=0.4 at τ=$60/\sqrt{eE}$ (red line) and $120/\sqrt{eE}$ (black line) respectively. Soon after the initial turn-on, the structure caused by the instant turn-on keeps the same and the particle creation rate is properly $\exp(-a\pi)$.

from $-p_3'$ to $-p_3$. Such two modes are located symmetrically on the left and right side of $(p_3' - p_3)/2 = eE\tau/2$.

The stable particle number on the plateau is associated to the modes of initially large negative momentum p_3 and finally large positive p_3'. By utilizing asymptotic values of A_1 and C_1 in (2.31), we eventually obtain

$$|\beta(+\infty; -\infty)|^2 = \left| \frac{C_1^\star(-\infty) C_1(-\infty)}{c_{ab}} \right|^2 = e^{-\alpha\pi}. \tag{2.41}$$

We can also learn from the plots that the asymptotic value is attained quickly and accurately by finite p_3' on the plateau. While the instant turn-on impacts the distribution in the form of the fluctuations on the two ends of the plateau. Apart from this, the particle production can be properly depicted by step functions,

$$n(\tau, p_3) = e^{-a\pi} \theta(p_3') \theta(-p_3). \tag{2.42}$$

Specifically, the above step-function description is precise when $a = 0$ ($\omega_3 = 0$). Given the fact $\omega = |p_3'|$ when $\omega_3 = 0$, one could deduce from (2.20) that $A^F = 0$ when $p_3' > 0$ and $C^F = 0$ when $p_3' < 0$. Thus, the free mode functions can be written

simply as [2]

$$p_3' < 0 : \tag{2.43}$$

$$U_+^F(p_3';t,x) = e^{-i|p_3'|t+ip_3'x_3}\begin{pmatrix}1\\0\\0\\0\end{pmatrix}, \quad U_-^F(p_3';t,x) = e^{-i|p_3'|t+ip_3'x_3}\begin{pmatrix}0\\0\\0\\1\end{pmatrix},$$

$$V_-^F(-p_3';t,x) = e^{i|p_3'|t+ip_3'x_3}\begin{pmatrix}0\\0\\1\\0\end{pmatrix}, \quad V_+^F(-p_3';t,x) = e^{i|p_3'|t+ip_3'x_3}\begin{pmatrix}0\\1\\0\\0\end{pmatrix},$$

$$p_3' > 0 :$$

$$U_+^F(p_3';t,x) = e^{-i|p_3'|t+ip_3'x_3}\begin{pmatrix}0\\0\\1\\0\end{pmatrix}, \quad U_-^F(p_3';t,x) = e^{-i|p_3'|t+ip_3'x_3}\begin{pmatrix}0\\1\\0\\0\end{pmatrix},$$

$$V_-^F(-p_3';t,x) = e^{i|p_3'|t+ip_3'x_3}\begin{pmatrix}1\\0\\0\\0\end{pmatrix}, \quad V_+^F(-p_3';t,x) = e^{i|p_3'|t+ip_3'x_3}\begin{pmatrix}0\\0\\0\\1\end{pmatrix}.$$

Similarly, one could take the limit $a \to 0$ on the parabolic cylinder functions in equation (2.1). Or one can revise the equation (2.25) in light of $\epsilon = 0$, and consequently arrives at

$$\frac{\partial}{\partial t}A(t,p_3) = i[p_3 - eA_3(t)]A(t,p_3), \qquad \frac{\partial}{\partial t}C(t,p_3) = -i[p_3 - eA_3(t)]C(t,p_3), \tag{2.44}$$

to which the solutions are

$$A(t,p_3) = e^{i\int_0^t (p_3 - eA_3(t_0))dt_0}A_0, \qquad C(t,p_3) = e^{-i\int_0^t (p_3 - eA_3(t_0))dt_0}C_0. \tag{2.45}$$

[2] Since $\omega_3 = 0$ also suggests $p_1 = p_2 = 0$, we omit p_1 and p_2 in expressions.

Therefore,

$$
\begin{aligned}
&p_3 < 0 : \qquad\qquad (2.46)\\
&U_+(p_3;t,x) \;= e^{ip_3x_3}A\begin{pmatrix}1\\0\\0\\0\end{pmatrix}, \quad U_-(p_3;t,x) \;= e^{ip_3x_3}A\begin{pmatrix}0\\0\\0\\1\end{pmatrix},\\
&V_-(-p_3;t,x) = e^{ip_3x_3}C\begin{pmatrix}0\\0\\1\\0\end{pmatrix}, \quad V_+(-p_3;t,x) = e^{ip_3x_3}C\begin{pmatrix}0\\1\\0\\0\end{pmatrix},\\
&p_3 > 0 :\\
&U_+(p_3;t,x) \;= e^{ip_3x_3}C\begin{pmatrix}0\\0\\1\\0\end{pmatrix}, \quad U_-(p_3;t,x) \;= e^{ip_3x_3}C\begin{pmatrix}0\\1\\0\\0\end{pmatrix},\\
&V_-(-p_3;t,x) = e^{ip_3x_3}A\begin{pmatrix}1\\0\\0\\0\end{pmatrix}, \quad V_+(-p_3;t,x) = e^{ip_3x_3}A\begin{pmatrix}0\\0\\0\\1\end{pmatrix}.
\end{aligned}
$$

When $p_3 < 0$ and $p_3' = p_3 - eA_3(\tau) > 0$, the Bogoliubov transformation can be performed in the following way,

$$
\begin{aligned}
e^{ieA_3(\tau)x_3}U_\pm(p_3;\tau,x) &= \;\beta V_\mp^F(-p_3';\tau,x), \qquad (2.47)\\
e^{ieA_3(\tau)x_3}V_\mp(-p_3;\tau,x) &= -\beta^\star U_\pm^F(p_3';\tau,x),
\end{aligned}
$$

and in all $|\beta|^2 = 1$. Otherwise, $|\beta|^2 = 0$. In such a way, the precise particle number is

$$
n(\tau,p_3) = \theta(p_3')\theta(-p_3). \qquad (2.48)
$$

Notice the mode functions above are also eigenstates of the chirality operator

γ^5, and the chiral symmetry holds in the evolution in the following aspects:

(1) a left-handed spinor will remain left-handed, and a right-handed will remain being right-handed;

(2) the same amount of left- and right-handed (anti-)particle will be created.

We will see the second statement can be violated when there is also a magnetic field applied along the same direction as the electric field.

The pair production can also be interpreted as a result of the level-shift due to the electric field. As an example, Figure 2.3 illustrates such an explanation to anti-particle productions in the Dirac sea.

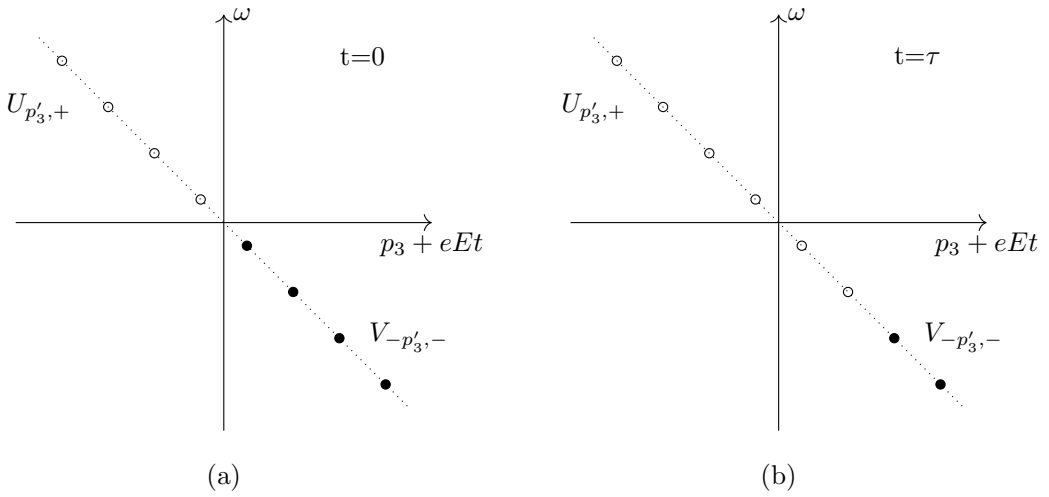


Figure 2.3. The particle creation interpreted as level-shift in the Dirac sea. The black dots denote the occupied states, while the empty dots referring the unoccupied ones. (a): before the electric field is on, all sea states with negative energy have been fully occupied. (b): after the electric field is off, two sea states become unoccupied, and this can be interpreted as two anti-particles have been created. See reference [23] for more detailed description.

2.1.1 Schwinger mechanism

When the electric field is on, pair productions could happen, and if so, the system would tunnel from the vacuum state to a state of particles and anti-particles. The probability of the system staying in the vacuum over time T was first calculated by Schwinger [5], in so called vacuum persistence probability, which can be defined of the form [62, 63]

$$P \equiv |\langle vac|U(t)|vac\rangle|^2 = e^{-wVT}, \tag{2.49}$$

with the spatial volume $V = L_1 L_2 L_3$ where L_i of $i = 1, 2, 3$ are the length of i-th direction. In other words, the probability stands for the chance that there is no single pair produced over the period,

$$P = \prod_{p_1,p_2,p_3,s} (1 - f_{p,s}), \tag{2.50}$$

where $f_{p,s}$ denotes the probability of creating a particle-anti-particle pair with the particle of momentum (p_1, p_2, p_3) and spin $s/2$. From the calculation in the last section, we can determine $f_{p,s}$ properly, that $f_{p,s} = e^{-a\pi}\theta(p_3')\theta(-p_3)$, and bearing in mind $a = \omega_3^2/(eE)$ and $\omega_3^2 = m^2 + p_1^2 + p_2^2$. Taking the logarithm of the both sides of equations, we arrive at a result,

$$\begin{aligned} -wVT &= \ln \prod_{p_1,p_2} \left(1 - e^{-\frac{m^2+p_1^2+p_2^2}{eE}\pi}\right)^{\frac{2eETL_3}{2\pi}} = \frac{2eETL_3}{2\pi} \sum_{p_1,p_2} \ln\left(1 - e^{-\frac{m^2+p_1^2+p_2^2}{eE}\pi}\right) \\ &= -\frac{2eETL_3}{2\pi}\frac{L_1L_2}{(2\pi)^2}\int dp_1 dp_2 \sum_{n=1}^{+\infty}\frac{1}{n} e^{-\frac{m^2+p_1^2+p_2^2}{eE}n\pi} \\ &= -\frac{2(eE)^2VT}{(2\pi)^3}\sum_{n=1}^{+\infty}\frac{1}{n^2}e^{-\frac{n\pi m^2}{eE}}, \end{aligned} \tag{2.51}$$

where on the first line, the exponent $2ETL_3/(2\pi)$ is the number of modes whose $\theta(p_3')\theta(-p_3) = 1$, including the two spin choices, and the relation $dp_i = 2\pi/L_i$ is also utilized to reach the result.

In the end, we obtain

$$w = \frac{2(eE)^2}{(2\pi)^3}\sum_{n=1}^{+\infty}\frac{1}{n^2}e^{-\frac{n\pi m^2}{eE}}, \tag{2.52}$$

as initially given by Schwinger in [5].

2.2 Fermions in a magnetic field

Assume a magnetic field of strength B is produced along the third direction, by the gauge field $A_\mu = (0, -Bx_2, 0, 0)$, for $\vec{B} = \nabla \times \vec{A}$. So the Dirac equation can be written as

$$\left(\gamma^0\partial_0 + \gamma^3\partial_3 + \gamma^1[\partial_1 + ieBx_2] + \gamma^2\frac{\partial}{\partial x_2} + m\right)\psi(t, x) = 0. \tag{2.53}$$

As in the equation, t, x_1 and x_3 appear only through derivatives, plane wave functions could still be eigenfunctions for these variables. By considering a single mode $\psi_s(p;t,x) = \exp(\mp i\omega t + ip_1x_1 + ip_3x_3)\psi_s(x_2,p)$, we can implement the separation of variables in the following way

$$\psi_s(x_2,p) = \left[M(x_2,p_1)\frac{1+i\gamma^1\gamma^2}{2} + N(x_2,p_1)\frac{1-i\gamma^1\gamma^2}{2}\right]\psi_{p_3,s}, \tag{2.54}$$

and put constraints $\psi^\dagger_{p_3,s}\psi_{p_3,s} = 1$ and $\int dx_2|M|^2 = \int dx_2|N|^2 = 1$ to meet the requirement that the mode functions are orthonormal as in (2.6). In the Dirac equation, by replacing the wave function of the expansion above, we obtain

$$\left[\mp i\gamma^0\omega + i\gamma^3p_3 + m\right]\psi_{p_3,s} = -i\gamma^1\epsilon\psi_{p_3,s}, \tag{2.55}$$

$$\left[i\gamma^1(p_1+eBx_2) + \gamma^2\frac{\partial}{\partial x_2}\right][MP_{r+} + NP_{r-}] = [MP_{r+} + NP_{r-}]i\gamma^1\epsilon, \tag{2.56}$$

where abbreviations P_{r+} and P_{r-} represent projector $\frac{1+i\gamma^1\gamma^2}{2}$ and $\frac{1-i\gamma^1\gamma^2}{2}$ individually. A further simplification on the second equation can lead to,

$$\left(p_1 + eBx_2 - \frac{\partial}{\partial x_2}\right)M = \epsilon N, \quad \left(p_1 + eBx_2 + \frac{\partial}{\partial x_2}\right)N = \epsilon M, \tag{2.57}$$

or with second-order derivatives

$$\left(\frac{d^2}{dy^2} + \frac{\epsilon^2}{eB} - 1 - y^2\right)M = 0, \quad \left(\frac{d^2}{dy^2} + \frac{\epsilon^2}{eB} + 1 - y^2\right)N = 0, \tag{2.58}$$

where $y = \sqrt{eB}x_2 + \frac{p_1}{\sqrt{eB}}$ with fixed p_1. The equations have similar form as the one for quantum harmonic oscillators and accordingly we can write their solutions in the following way, [3]

$$\epsilon = \sqrt{2neB}, \quad M = U_{n-1}\left(\sqrt{eB}x_2 + \frac{p_1}{\sqrt{eB}}\right), \quad N = U_n\left(\sqrt{eB}x_2 + \frac{p_1}{\sqrt{eB}}\right), \tag{2.59}$$

[3] There exist two solutions, which can be normalized in the form of ($\epsilon = \sqrt{2neB},\ M = U_{n-1},\ N = U_n$) and ($\epsilon = -\sqrt{2neB},\ M = -U_{n-1},\ N = U_n$). But they are not independent, and we chose the one of $\epsilon = \sqrt{2neB}$.

where Hermite functions $U_n(y)$ are related to the Hermite polynomials $H_n(y)$ through the relation

$$U_n(y) = \frac{1}{\sqrt{2^n n! \sqrt{\pi}}} e^{-\frac{y^2}{2}} H_n(y), \quad H_n(y) = (-1)^n e^{y^2} \frac{d^n}{dy^n} e^{-y^2}, \tag{2.60}$$

and Hermite functions are orthonormal,

$$\int_{-\infty}^{+\infty} U_m(y) U_n(y) dy = \delta_{m,n}, \quad \sum_{n=0}^{+\infty} U_n(y_1) U_n(y_2) = \delta(y_1 - y_2). \tag{2.61}$$

In addition, $\frac{\epsilon^2}{2eB} = n$ is forced to be a non-negative integer, otherwise M or N will behave asymptotically like $\exp(y^2/2)$ and mode functions cannot be normalized. As a result, $\omega = \sqrt{p_3^2 + m^2 + 2neB}$, thus the energy is discretized. Such quantization of the energy is known as Landau quantization, and the energy levels are called Landau levels.

2.2.1 Landau levels

Figure 2.4 displays the $n = 0$ and 1 Landau levels of massless fermions. The $n = 1$ energy levels have a energy gap of width $2\sqrt{2eB}$. For massless fermions, the lowest-energy Landau levels are gap-less. Such energy gaps will determine the pair production rate as $e^{-\frac{2neB}{eE}}$, if there is an electric field applied along the third direction.

When $n = 0$, the mode functions can be written as

$$U_{0,+}(p;t,x) = \frac{e^{-i\omega t + ip_1 x_1 + ip_3 x_3}}{\sqrt{2\omega_3}} U_0(x_2, p_1) P_{r-} \begin{pmatrix} -\sqrt{\omega_3 - \sigma^3 p_3}\ \eta_+ \\ \\ \sqrt{\omega_3 + \sigma^3 p_3}\ \eta_+ \end{pmatrix},$$

$$V_{0,-}(-p;t,x) = \frac{e^{i\omega t + ip_1 x_1 + ip_3 x_3}}{\sqrt{2\omega_3}} U_0(x_2, p_1) P_{r-} \begin{pmatrix} \sqrt{\omega_3 + \sigma^3 p_3}\ \eta_+ \\ \\ \sqrt{\omega_3 - \sigma^3 p_3}\ \eta_+ \end{pmatrix}.$$

Only $\eta_+ = (1, 0)$ is allowed, because the following constraint should be satisfied to

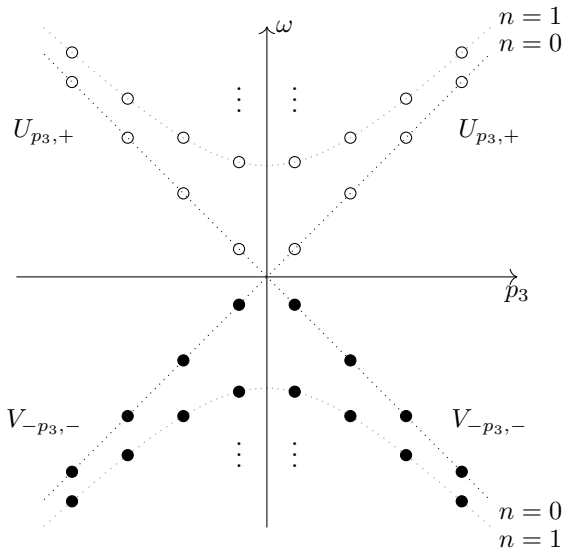


Figure 2.4. Landau levels of massless fermions. The states in the lowest-energy Landau level $n = 0$ are connected. Comparatively, there exist gaps of width $2\sqrt{2neB}$ for higher energy levels.

avoid $M = U_{-1}(y)$ to appearing in the expression,

$$P_{r+}\begin{pmatrix} -\sqrt{\omega_3 - \sigma^3 p_3}\ \eta_s \\ \\ \sqrt{\omega_3 + \sigma^3 p_3}\ \eta_s \end{pmatrix} = 0, \quad \text{where} \quad P_{r+} = \begin{pmatrix} 0 & & & \\ & 1 & & \\ & & 0 & \\ & & & 1 \end{pmatrix}.$$

This indicates the fact that the spin direction in the lowest-energy Landau levels is locked.

Another feature of Landau levels is that they are degenerate, which is a result of the fact that the dispersion relation $\omega = \sqrt{p_3^2 + m^2 + 2neB}$ does not depend on the variable p_1. On the other hand, $\frac{p_1}{eB} < L_2$, as any shift $\frac{p_1}{eB}$ along x_2 in $U_n\left(\sqrt{eB}x_2 + \frac{p_1}{\sqrt{eB}}\right)$ should be dismissed if it is larger than the length L_2. By counting $dp_1 = 2\pi/L_1$, the total possible number of p_1 can be found to be $\frac{L_1 L_2 eB}{2\pi}$, which is the right number of degeneracy of Landau levels [29].

2.3 Fermions and the chiral anomaly

Given the equation of motion for fermions, $\gamma^\mu \partial_\mu \psi(t,x) + m\psi(t,x) = 0$, the following relation is expected to be correct,

$$\partial_\mu \langle \mathrm{T}\bar{\psi}(t,x) i\gamma^\mu \gamma^5 \psi(t,x)\rangle = 2im\langle \mathrm{T}\bar{\psi}(t,x)\gamma^5\psi(t,x)\rangle. \tag{2.62}$$

But in practice, when the fermions are treated in quantum field theory, the precise expression comes to be

$$\partial_\mu \langle \mathrm{T}\bar{\psi}(t,x) i\gamma^\mu \gamma^5 \psi(t,x)\rangle = 2im\langle \mathrm{T}\bar{\psi}(t,x)\gamma^5\psi(t,x)\rangle + \frac{e^2}{16\pi^2}\epsilon^{\mu\nu\rho\sigma}F_{\mu\nu}F_{\rho\sigma}, \tag{2.63}$$

or in an integral equation form

$$\frac{d}{dt}Q_5(t) = 2im\int d^3x \langle \mathrm{T}\bar{\psi}(t,x)\gamma^5\psi(t,x)\rangle - \frac{e^2}{2\pi^2}\int d^3x E\cdot B, \tag{2.64}$$

where the chiral charge is defined as $Q_5(t) = \int d^3x \langle T\bar{\psi}(t,x) i\gamma^0\gamma^5\psi(t,x)\rangle$ and we have also utilized the relation $\epsilon^{\mu\nu\rho\sigma}F_{\mu\nu}F_{\rho\sigma} = -8E\cdot B$.

The effect of the appearance of the extra term is more dramatic for massless fermions. When $m = 0$, the fermion action is invariant under the chiral transformation of constant phase ϕ performed in a manner $\psi' = \exp(i\gamma^5\phi)\psi$, and according to the Noether's theorem, the chiral current should be conserved, $\partial_\mu J_5^\mu = 0$, where $J_5^\mu = \langle \mathrm{T}\bar{\psi} i\gamma^\mu\gamma^5\psi\rangle$. Moreover, the chiral charge is exactly the sum

$$\begin{aligned}\Delta Q_5(\tau) = L_1 L_3 \sum_{n,s}\int \frac{dp_1}{2\pi}\frac{dp_3'}{2\pi}\Big(& n_{n,s}^{L,U}(\tau,p_3) - n_{n,-s}^{L,V}(\tau,-p_3) \\ & - n_{n,s}^{R,U}(\tau,p_3) + n_{n,-s}^{R,V}(\tau,-p_3)\Big),\end{aligned} \tag{2.65}$$

where $n_{n,s}^{L,U}(\tau,p_3)$ is the occupation number of left-handed particle with Landau level index n, momentum p_3 and spin $s/2$, and similar interpretations are applied to $n_{n,-s}^{L,V}(\tau,-p_3)$, $n_{n,s}^{R,U}(\tau,p_3)$ and $n_{n,-s}^{R,V}(\tau,-p_3)$. So the existence of the extra term indicates that the chiral symmetry is violated in quantum field theory, and production rates of left- and right-handed (anti-)particle will be different.

To obtain the chiral anomaly equation (2.64), we can solve analytically the Dirac equation for fermions in parallel electric and magnetic fields. The solution will simply

be a combination of the results of fermions in an electric field and in a magnetic field. This is due to the fact that the gamma matrix $\gamma^0\gamma^3$ commutates with $\gamma^1\gamma^2$, so that the parameter separations in both cases are still valid, without affecting each other. [4]

To generate the parallel electric and magnetic fields, the gauge field A_μ can be chosen as,

$$A_\mu = (0, -Bx_2, 0, -Et). \tag{2.66}$$

The Dirac equation then becomes

$$\left[\gamma^0\partial_0 + \gamma^1(\partial_1 + ieBx_2) + \gamma^2\partial_2 + \gamma^3(\partial_3 + eEt) + m\right]\psi = 0, \tag{2.67}$$

to which, the mode function for particle and anti-particle can be written separately as

$$\begin{aligned} U_{n,s}(p_1,p_3;t,x) =& e^{ip_1x_1+ip_3x_3}\sqrt{\frac{1}{\omega_3}}\left[A(t,p_3)P_{b+} + C(t,p_3)P_{b-}\right] \\ & \left[M(x_2,p_1)P_{r+} + N(x_2,p_1)P_{r-}\right]\begin{pmatrix} -\sqrt{\omega_3 - \sigma^1\sqrt{2neB}}\,\eta_s \\ \sqrt{\omega_3 + \sigma^1\sqrt{2neB}}\,\eta_s \end{pmatrix}, \end{aligned} \tag{2.68}$$

$$\begin{aligned} V_{n,-s}(-p_1,-p_3;t,x) =& e^{ip_1x_1+ip_3x_3}\sqrt{\frac{1}{\omega_3}}\left[C^\star(t,p_3)P_{b+} + A^\star(t,p_3)P_{b-}\right] \\ & \left[M(x_2,p_1)P_{r+} + N(x_2,p_1)P_{r-}\right]\begin{pmatrix} \sqrt{\omega_3 + \sigma^1\sqrt{2neB}}\,\eta_s \\ \sqrt{\omega_3 - \sigma^1\sqrt{2neB}}\,\eta_s \end{pmatrix}. \end{aligned} \tag{2.69}$$

[4] And it shares the same reason with the fact that the boost and rotation along the third direction will not disturb each other, as gamma matrices $\gamma^0\gamma^3$ and $\gamma^1\gamma^2$ are infinitesimal generators of these two operations in the spinor representation of Lorentz group [36, 37].

One can check they are the right solutions by implementing the following relations

$$\left(\frac{\partial}{\partial t} + i[p_3 + eEt]\right) C(t, p_3) = -i\omega_3 A(t, p_3), \tag{2.70}$$

$$\left(\frac{\partial}{\partial t} - i[p_3 + eEt]\right) A(t, p_3) = -i\omega_3 C(t, p_3), \tag{2.71}$$

$$\left([p_1 + eBx_2] + \frac{\partial}{\partial x_2}\right) N(x_2, p_1) = \sqrt{2neB} M(x_2, p_1), \tag{2.72}$$

$$\left([p_1 + eBx_2] - \frac{\partial}{\partial x_2}\right) M(x_2, p_1) = \sqrt{2neB} N(x_2, p_1), \tag{2.73}$$

$$\left(-i\gamma^0\omega_3 + i\gamma^1\sqrt{2neB} + m\right) \begin{pmatrix} -\sqrt{\omega_3 - \sigma^1\sqrt{2neB}}\ \eta_s \\ \sqrt{\omega_3 + \sigma^1\sqrt{2neB}}\ \eta_s \end{pmatrix} = 0, \tag{2.74}$$

$$\left(i\gamma^0\omega_3 + i\gamma^1\sqrt{2neB} + m\right) \begin{pmatrix} \sqrt{\omega_3 + \sigma^1\sqrt{2neB}}\ \eta_s \\ \sqrt{\omega_3 - \sigma^1\sqrt{2neB}}\ \eta_s \end{pmatrix} = 0, \tag{2.75}$$

where the explicit forms of $A(t, p_3)$, $C(t, p_3)$, $M(x_2, p_1)$ and $N(x_2, p_1)$ can be found in equation (2.32) and (2.59). For the sake of simplicity, we will shorten the projectors appearing above and define P_U and P_V as,

$$P_U \equiv [A(t, p_3)P_{b+} + C(t, p_3)P_{b-}]\,[M(x_2, p_1)P_{r+} + N(x_2, p_1)P_{r-}]\,, \tag{2.76}$$

$$P_V \equiv [C^\star(t, p_3)P_{b+} + A^\star(t, p_3)P_{b-}]\,[M(x_2, p_1)P_{r+} + N(x_2, p_1)P_{r-}]\,. \tag{2.77}$$

By recalling the expression of projectors

$$P_{b+} = \begin{pmatrix} 1 & & & \\ & 0 & & \\ & & 0 & \\ & & & 1 \end{pmatrix}, \quad P_{b-} = \begin{pmatrix} 0 & & & \\ & 1 & & \\ & & 1 & \\ & & & 0 \end{pmatrix},$$

$$P_{r+} = \begin{pmatrix} 0 & & & \\ & 1 & & \\ & & 0 & \\ & & & 1 \end{pmatrix}, \quad P_{r-} = \begin{pmatrix} 1 & & & \\ & 0 & & \\ & & 1 & \\ & & & 0 \end{pmatrix},$$

one can find P_U and P_V are actually

$$P_U = \begin{pmatrix} AN & & & \\ & CM & & \\ & & CN & \\ & & & AM \end{pmatrix}, \tag{2.78}$$

$$P_V = \begin{pmatrix} C^\star N & & & \\ & A^\star M & & \\ & & A^\star N & \\ & & & C^\star M \end{pmatrix}. \tag{2.79}$$

With the abbreviations, the solutions simply become

$$U_{n,s}(p_1,p_3;t,x) = e^{ip_1x_1+ip_3x_3}\sqrt{\frac{1}{\omega_3}}P_U \begin{pmatrix} -\sqrt{\omega_3-\sigma^1\sqrt{2neB}}\ \eta_s \\ \sqrt{\omega_3+\sigma^1\sqrt{2neB}}\ \eta_s \end{pmatrix} \tag{2.80}$$

$$V_{n,-s}(-p_1,-p_3;t,x) = e^{ip_1x_1+ip_3x_3}\sqrt{\frac{1}{\omega_3}}P_V \begin{pmatrix} \sqrt{\omega_3+\sigma^1\sqrt{2neB}}\ \eta_s \\ \sqrt{\omega_3-\sigma^1\sqrt{2neB}}\ \eta_s \end{pmatrix}. \tag{2.81}$$

Furthermore, mode functions are orthonormal in the following way

$$\sqrt{eB}\sum_{n,s}\int \frac{dp_1}{2\pi}\frac{dp_3'}{2\pi}\Big[U_{n,s}(p_1,p_3;t,x)U^\dagger_{n,s}(p_1,p_3;t,y) + V_{n,-s}(-p_1,-p_3;t,x)V^\dagger_{n,-s}(-p_1,-p_3;t,y)\Big] = \delta^3(x-y)\mathbb{I}_{4\times4}, \tag{2.82}$$

with $\mathbb{I}_{4\times4}$ a 4 by 4 identity matrix, and

$$\int d^3x U^\dagger_{n,s}(p_1,p_3;t,x)U_{n',s'}(q_1,q_2;t,x) = (2\pi)^2\delta(p_1-q_1)\delta(p_3'-q_3')\frac{\delta_{nn'}}{\sqrt{eB}}\delta_{ss'}, \tag{2.83}$$

$$\int d^3x V^\dagger_{n,-s}(-p_1,-p_3;t,x)V_{n',-s'}(-q_1,-q_2;t,x) = (2\pi)^2\delta(p_1-q_1)\delta(p_3'-q_3')\frac{\delta_{nn'}}{\sqrt{eB}}\delta_{ss'},$$

where any other product of U and V is zero. The expressions above can be seen as a result of the substitution, because of the existence of the magnetic field,

$$\int \frac{dp_2}{2\pi} \to \sqrt{eB}\sum_n, \quad 2\pi\delta(p_2-p_2') \to \frac{\delta_{nn'}}{\sqrt{eB}}. \tag{2.84}$$

At the end, the field operator in configuration space can be expanded as

$$\begin{aligned}\psi(t,x) =&\sqrt{eB}\sum_{n,s}\int\frac{dp_1}{2\pi}\frac{dp_3'}{2\pi}\left[b_{n,s}(p_1,p_3)U_{n,s}(p_1,p_3;t,x)\right.\\ &\left.+d^\dagger_{n,-s}(-p_1,-p_3)V_{n,-s}(-p_1,-p_3;t,x)\right],\end{aligned}\tag{2.85}$$

where the creation and annihilation operators satisfy anti-commutation relations,

$$\begin{aligned}\{b_{n,r}(p_1,p_3),b^\dagger_{n',s}(q_1,q_3)\} &= (2\pi)^2\delta(p_1-q_1)\delta(p_3-q_3)\frac{\delta_{nn'}}{\sqrt{eB}}\delta_{rs},\\ \{d_{n,-r}(-p_1,-p_3),d^\dagger_{n',-s}(-q_1,-q_3)\} &= (2\pi)^2\delta(p_1-q_1)\delta(p_3-q_3)\frac{\delta_{nn'}}{\sqrt{eB}}\delta_{rs}.\end{aligned}\tag{2.86}$$

If the fermions are initially in the vacuum state, with all initial particle numbers zero, $\langle b^\dagger b\rangle = \langle d^\dagger d\rangle = 0$, the equal-time two-point function comes to be

$$\begin{aligned}\langle \mathrm{T}\psi(t,x)\psi^\dagger(t,y)\rangle = \frac{1}{2}\sqrt{eB}\sum_{n,s}\int\frac{dp_1}{2\pi}\frac{dp_3'}{2\pi}&\left[U_{n,s}(p_1,p_3;t,x)U^\dagger_{n,s}(p_1,p_3;t,y)\right.\\ &\left.-V_{n,-s}(-p_1,-p_3;t,x)V^\dagger_{n,-s}(-p_1,-p_3;t,y)\right].\end{aligned}\tag{2.87}$$

There is one thing we need to emphasize. The variable in the integral should be the physical momentum $p_3' = p_3 + eEt$ at time t, instead of p_3. It is important to discriminate between them, because some integrals will not be invariant under the shift of the integration variable.

The Bogoliubov transformation can be implemented in the same way as it is in (2.33), for a single mode

$$\begin{aligned}e^{ieE\tau x_3}U_{n,s}(p_1,p_3;\tau,x) &= \alpha U^F_{n,s}(p_1,p_3';\tau,x)+\beta V^F_{n,-s}(-p_1,-p_3';\tau,x),\\ e^{ieE\tau x_3}V_{n,-s}(-p_1,-p_3;\tau,x) &= -\beta^\star U^F_{n,s}(p_1,p_3';\tau,x)+\alpha^\star V^F_{n,-s}(-p_1,-p_3';\tau,x),\end{aligned}\tag{2.88}$$

which should also obey the chiral symmetry in a sense that a left-handed U can only be expanded by left-handed U^F and V^F. Furthermore, if U and V are eigenstates of γ^5, then

$$\left[U^\dagger\gamma^5U - V^\dagger\gamma^5V\right] = (1-2|\beta|^2)\left[U^{F\dagger}\gamma^5U^F - V^{F\dagger}\gamma^5V^F\right],\tag{2.89}$$

where there will not appear any crossing terms like $V^{F\dagger}U$ or $U^{F\dagger}V$, because they

are really zero. Therefore, the chiral charge of massless fermions can be interpreted as,

$$\begin{aligned} Q_5(\tau) &= \int d^3x \langle T\psi^\dagger(\tau,x)\gamma^5\psi(\tau,x)\rangle \\ &= -\frac{L_1L_3}{2}\sum_{n,s}\int \frac{dp_1}{2\pi}\frac{dp_3'}{2\pi}\Big((1-2n_{n,s}^{L,U}(\tau,p_3)) - (1-2n_{n,-s}^{L,V}(\tau,-p_3)) \\ &\qquad -(1-2n_{n,s}^{R,U}(\tau,p_3)) + (1-2n_{n,-s}^{R,V}(\tau,-p_3))\Big), \end{aligned} \tag{2.90}$$

or

$$\Delta Q_5(\tau) = \sum_{p_1,p_3',n,s}\Big[(n_{n,s}^{L,U}(\tau,p_3)) + n_{n,-s}^{L,V}(\tau,-p_3) + n_{n,s}^{R,U}(\tau,p_3) + n_{n,-s}^{R,V}(\tau,-p_3)\Big], \tag{2.91}$$

given $dp_1 = 2\pi/L_1$ and $dp_3' = 2\pi/L_3$ for finite spatial lengths L_1 and L_3.

2.3.1 Chiral anomaly for massless fermions

Massless fermions have simple expressions of mode functions. When $n = 0$, they can be written as

$$\begin{aligned} p_3' < 0: \quad & U_{0,+}(p_1,p_3;t,x) = fe^{-i|p_3'|t}\begin{pmatrix}1\\0\\0\\0\end{pmatrix}, \quad V_{0,-}(-p_1,-p_3;t,x) = fe^{i|p_3'|t}\begin{pmatrix}0\\0\\1\\0\end{pmatrix}, \\ p_3' > 0: \quad & U_{0,+}(p_1,p_3;t,x) = fe^{-i|p_3'|t}\begin{pmatrix}0\\0\\1\\0\end{pmatrix}, \quad V_{0,-}(-p_1,-p_3;t,x) = fe^{i|p_3'|t}\begin{pmatrix}1\\0\\0\\0\end{pmatrix}, \end{aligned} \tag{2.92}$$

where $f = (\pi)^{-1/4}e^{ip_1x_1+ip_3x_3}e^{-y^2/2}$ and $y = \sqrt{eB}x_2 + \frac{p_1}{\sqrt{eB}}$. If one draws the pair productions within the lowest-energy Landau levels, as in Figure 2.5, one would conclude that only right-handed particles and left-handed anti-particles can be created in the process. Thus, the chiral charge is not conserved. Therefore, in this sense, the chiral symmetry is violated, but still, a left(right)-handed spinor will continue

to be left(right)-handed.

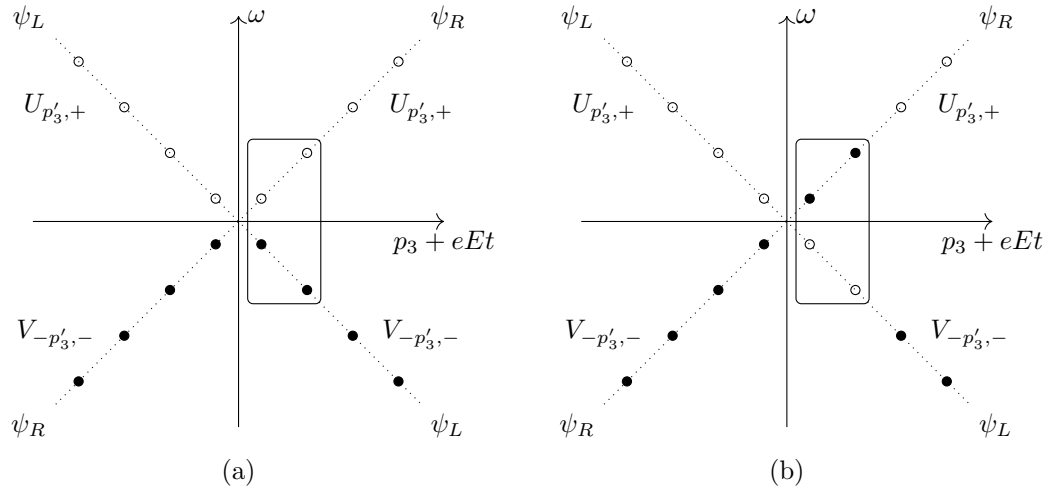


Figure 2.5. Pair productions in lowest-energy Landau levels, (a) before the electric field is on; (b) after the electric field is off. The parity transform can be seen as a mirror reflection along ω axis, and (a) is symmetric under the reflection; while (b) not. This can be understood as the parity is also violated in the process.

To the lowest-energy Landau levels of $n = 0$, one can count the chiral charge by its definition (2.91), and the final number comes to be:

$$\Delta Q_5(T) = -2\frac{eETL_3}{2\pi}\frac{L_1L_2eB}{2\pi} = -\frac{e^2}{2\pi^2}E\cdot BVT = \frac{e^2VT}{16\pi^2}\epsilon^{\mu\nu\rho\sigma}F_{\mu\nu}F_{\rho\sigma}. \qquad (2.93)$$

In the expression, the factor -2 is because of only right-handed particles and left-handed anti-particles which contribute and both have minus sign in front. During time T, there are $\frac{eETL_3}{2\pi}$ states whose momentums have crossed zero, therefore having particle number changed from 0 to 1. $\frac{L_1L_2eB}{2\pi}$ is the degeneracy of the lowest-energy Landau levels.

On the other hand, Landau levels of $n > 0$ do not contribute to ΔQ_5. When $n > 0$, $\omega_3 = \sqrt{2neB}$ and $\sqrt{\omega_3 \pm \sigma^1\sqrt{2neB}}\,\eta_s = \sqrt{\omega_3}\sqrt{1 \pm \sigma^1}\,\eta_s$. If η_s is chosen as an eigenvector of σ^1, that is, $(1/\sqrt{2}, 1/\sqrt{2})$ or $(1/\sqrt{2}, -1/\sqrt{2})$, the left- or right-handed

spinors comes out naturally,

$$U_{n,L}(p_1,p_3;t,x)=\begin{pmatrix}-AN\\ CM\\ 0\\ 0\end{pmatrix},\quad V_{n,L}(-p_1,-p_3;t,x)=\begin{pmatrix}C^\star N\\ A^\star M\\ 0\\ 0\end{pmatrix},\tag{2.94}$$

$$U_{n,R}(p_1,p_3;t,x)=\begin{pmatrix}0\\ 0\\ CN\\ AM\end{pmatrix},\quad V_{n,R}(-p_1,-p_3;t,x)=\begin{pmatrix}0\\ 0\\ A^\star N\\ -C^\star M\end{pmatrix},$$

where an overall factor $\exp(ip_1x_1+ip_3x_3)$ has been omitted. As a left(right)-handed spinor through the evolution will keep to be left(right)-handed, one can write down separate Bogoliubov transformations for left- and right-handed spinors,

$$\begin{aligned}U_L&=\alpha_L U_L^F+\beta_L V_L^F,\quad V_L=-\beta_L^\star U_L^F+\alpha_L^\star V_L^F,\\ U_L&=\alpha_R U_L^F+\beta_R V_L^F,\quad V_L=-\beta_R^\star U_L^F+\alpha_R^\star V_L^F,\end{aligned}\tag{2.95}$$

which yield same expression of particle numbers

$$|\beta_L|^2=|\beta_R|^2=|C^FA-A^FC|^2.\tag{2.96}$$

Therefore the same amount of left- and right-handed (anti-)particle have been produced. We come to the conclusion that Landau levels of $n>0$ do not contribute to the ΔQ_5.

2.3.2 Chiral anomaly for massive fermions

The chiral anomaly could also happen to massive fermions. To show this, we start by defining a term

$$\begin{aligned}K_{n,s}(t,p_3)=\int dx_2\quad &U_{n,s}(p_1,p_3;t,x)U_{n,s}^\dagger(p_1,p_3;t,x)\\ &-V_{n,-s}(-p_1,-p_3;t,x)V_{n,-s}^\dagger(-p_1,-p_3;t,x),\end{aligned}\tag{2.97}$$

with which, Q_5 could be simplified as

$$\begin{aligned} Q_5(t) =& -\frac{1}{2}\int dx_1 dx_3 \sum_{n,s}\int \frac{dp_1}{2\pi}\frac{dp_3'}{2\pi}\mathrm{Tr}\left[K_{n,s}(t,p_3)\gamma^5\right] \\ =& -\frac{1}{2}L_1L_3\sum_{n,s}\int \frac{dp_1}{2\pi}\frac{dp_3'}{2\pi}\mathrm{Tr}\left[K_{n,s}(t,p_3)\gamma^5\right] \\ =& -\frac{VeB}{4\pi}\sum_{n,s}\int \frac{dp_3'}{2\pi}\mathrm{Tr}\left[K_{n,s}(t,p_3)\gamma^5\right], \end{aligned} \tag{2.98}$$

where $V = L_1L_2L_3$ is the spatial volume and on the third line, we have utilized the relation

$$L_1\int\frac{dp_1}{2\pi} = \sum_{p_1} = \frac{L_1L_2eB}{2\pi}, \tag{2.99}$$

to count the number of the degeneracy of Landau levels. Similarly,

$$2im\int d^3x\langle \mathrm{T}\bar{\psi}(t,x)\gamma^5\psi(t,x)\rangle = 2m\frac{VeB}{4\pi}\sum_{n,s}\int\frac{dp_3'}{2\pi}\mathrm{Tr}\left[K_{n,s}(t,p_3)\gamma^0\gamma^5\right]. \tag{2.100}$$

When the spin can be summed up, that is, when $n > 0$, one can calculate

$$\begin{aligned} \sum_s K_{n,s}(t,p_3) = \int dx_2 \Big[& P_U i\gamma^0(i\gamma^0\omega + i\gamma^1\sqrt{2neB} + m)P_U^\dagger \\ & - P_V i\gamma^0(i\gamma^0\omega - i\gamma^1\sqrt{2neB} - m)P_V^\dagger\Big], \end{aligned} \tag{2.101}$$

and with the explicit expression of P_U and P_V as in equation (2.78), one can also show that,

$$\sum_s \mathrm{Tr}\left[K_{n,s}(t,p_3)\gamma^5\right] = \sum_s \mathrm{Tr}\left[K_{n,s}(t,p_3)\gamma^0\gamma^5\right] = 0, \tag{2.102}$$

which means Landau levels of $n > 0$ do not contribute to either Q_5 or the chiral mass term (2.100).

For $n = 0$, there is only one spin choice, and mode functions can be written

explicitly as

$$U_{0,+}(p_1,p_3;t,x) = f\begin{pmatrix} -A \\ 0 \\ C \\ 0 \end{pmatrix}, \quad V_{0,-}(-p_1,-p_3;t,x) = f\begin{pmatrix} C^\star \\ 0 \\ A^\star \\ 0 \end{pmatrix}, \tag{2.103}$$

where $f = (\pi)^{-1/4} e^{ip_1x_1 + ip_3x_3} e^{-y^2/2}$ and $y = \sqrt{eB}x_2 + \frac{p_1}{\sqrt{eB}}$. This leads to

$$K_{0,+}(t,p_3) = \begin{pmatrix} |A|^2 - |C^2| & 0 & -2AC^\star & 0 \\ 0 & 0 & 0 & 0 \\ -2CA^\star & 0 & |C|^2 - |A|^2 & 0 \\ 0 & 0 & 0 & 0 \end{pmatrix}. \tag{2.104}$$

We denote

$$\begin{aligned} T^3(t,p_3) \equiv& \frac{1}{2}\mathrm{Tr}\left[K_{0,+}(t,p_3)\gamma^5\right] = (|A(t,p_3)|^2 - |C(t,p_3)|^2), \\ T^2(t,p_3) \equiv& -\frac{1}{2}\mathrm{Tr}\left[K_{0,+}(t,p_3)\gamma^0\gamma^5\right] = i(A(t,p_3)C^\star(t,p_3) - C(t,p_3)A^\star(t,p_3)). \end{aligned}$$

The evolution of $A(t,p_3)$ and $C(t,p_3)$ of constant p_3 is provided by revising the equation (2.19),

$$\frac{\partial}{\partial t}\begin{pmatrix} A(t,p_3) \\ C(t,p_3) \end{pmatrix} = i\left(p_3'\sigma^3 - m\sigma^1\right)\begin{pmatrix} A(t,p_3) \\ C(t,p_3) \end{pmatrix}, \tag{2.105}$$

where $p_3' = p_3 + eEt$ and the partial derivative is employed in the expression to emphasize that the equation is valid for constant p_3. As a result of the evolution equation (2.105), we obtain the following relation,

$$\frac{\partial}{\partial t}T^3(t,p_3) = 2mT^2(t,p_3). \tag{2.106}$$

At the end, we arrive at

$$Q_5(t) = -\frac{VeB}{2\pi}\int \frac{dp_3'}{2\pi}T^3(t,p_3' - eEt), \tag{2.107}$$

and the exact chiral anomaly

$$\begin{aligned}\frac{d}{dt}Q_5(t) =& -\frac{VeB}{2\pi}\int\frac{dp_3'}{2\pi}\left[\frac{\partial}{\partial t}T^3(t,p_3) - eE\frac{\partial}{\partial p_3'}T^3(t,p_3'-eEt)\right]\\ =& -\frac{VeB}{2\pi}\int\frac{dp_3'}{2\pi}2mT^2(t,p_3) + \frac{Ve^2EB}{4\pi^2}T^3(t,p_3'-eEt)\Big|_{p_3'=-\infty}^{p_3'=+\infty}\\ =& 2im\langle \mathrm{T}\bar{\psi}(t,x)\gamma^5\psi(t,x)\rangle - \frac{Ve^2EB}{2\pi^2},\end{aligned} \tag{2.108}$$

of same form as in (2.64). The asymptotic values are determined by the fact that in equation (2.105) when $|p_3'|$ is large, and the evolution eventually becomes

$$\frac{\partial}{\partial t}\begin{pmatrix} A \\ C \end{pmatrix} = ip_3'\sigma^3\begin{pmatrix} A \\ C \end{pmatrix},$$

under which T^3 is a constant. In addition, initial values provide $T^3(0,-\infty)=1$ and $T^3(0,+\infty)=-1$.

2.3.3 B+L anomaly

The quantization of fermions could violate a symmetry but the symmetry survives if the anomaly arising from individual fermion cancels out when all fermions are considered. Such anomaly cancellation depends on the whole fermion content of the Standard Model. To demonstrate the effect, we follow the trick in Weinberg's book [41], so that the general quantum anomaly can be obtained in a similar way to the chiral anomaly. To this end, we transform all fermions into left-handed spinors, for instance, a field ψ now being written as

$$\Psi = \begin{pmatrix} \frac{1}{2}(1+\gamma^5)\psi \\ \\ \left[\frac{1}{2}(1-\gamma^5)\psi\right]^{\mathcal{C}} \end{pmatrix}. \tag{2.109}$$

Ψ is actually left-handed due to the fact that the charge conjugation, acting on fermion as $\psi^{\mathcal{C}} = -\gamma^2\psi^\star$, will change a right-handed spinor into a left-handed one. Any gauge or global transformation performed on ψ of the form

$$\delta\psi = i\delta\theta\left[\frac{t_L}{2}(1+\gamma^5)\psi + \frac{t_R}{2}(1-\gamma^5)\psi\right], \tag{2.110}$$

now becomes

$$\delta\Psi = i\delta\theta \begin{pmatrix} t_L & 0 \\ 0 & -t_R^\star \end{pmatrix} \begin{pmatrix} \frac{1}{2}(1+\gamma^5)\psi \\ \frac{1}{2}(1+\gamma^5)(-\gamma^2)\psi^\star \end{pmatrix}. \tag{2.111}$$

The Lagrangian can be simply written as:

$$L = -\frac{1}{4}F_{\mu\nu}F^{\mu\nu} - \bar{\Psi}_L\gamma^\mu D_\mu \Psi_L, \tag{2.112}$$

which yields the chiral current,

$$J_5^\mu = i\bar{\Psi}_L\gamma^\mu\gamma^5\Psi_L,, \tag{2.113}$$

and the total chiral charge

$$Q_5 = \int d^3x \langle T\Psi_L^\dagger\gamma^5\Psi_L\rangle = \sum_{n,s}\int \frac{dp_1}{2\pi}\frac{dp_3'}{2\pi}\left(n_{n,s}^{L,U}(\tau,p_3) - n_{n,-s}^{L,V}(\tau,-p_3)\right). \tag{2.114}$$

The Landau levels are displayed in Figure 2.6. Again the levels of $n > 0$ do not contribute to Q_5 as there will be same amount of particles and anti-particles. In the lowest-energy Landau levels, no particles are produced and the Q_5 depends only on created anti-particles, with a value

$$Q_5 = -\frac{eETL_3}{2\pi}\frac{L_1L_2eB}{2\pi} = -\frac{e^2}{4\pi^2}E\cdot BVT \tag{2.115}$$

Similarly, the anomaly is of the form

$$\partial_\mu J_5^\mu = \frac{e^2}{32\pi^2}\epsilon^{\mu\nu\rho\sigma}F_{\mu\nu}F_{\rho\sigma}. \tag{2.116}$$

For general abelian and non-abelian gauge fields, the quantum anomalies should be written as,

$$\partial_\mu J_t^\mu = \frac{e^2}{32\pi^2}\epsilon^{\mu\nu\rho\sigma}F_{\mu\nu}^\alpha F_{\rho\sigma}^\beta\frac{1}{2}\mathrm{Tr}\left[\{t_\alpha,t_\beta\}t\right]. \tag{2.117}$$

which is the result of the calculation of the triangle diagrams shown in Fig 2.7. For example, the chiral anomaly in the electromagnetic theory can be recovered by

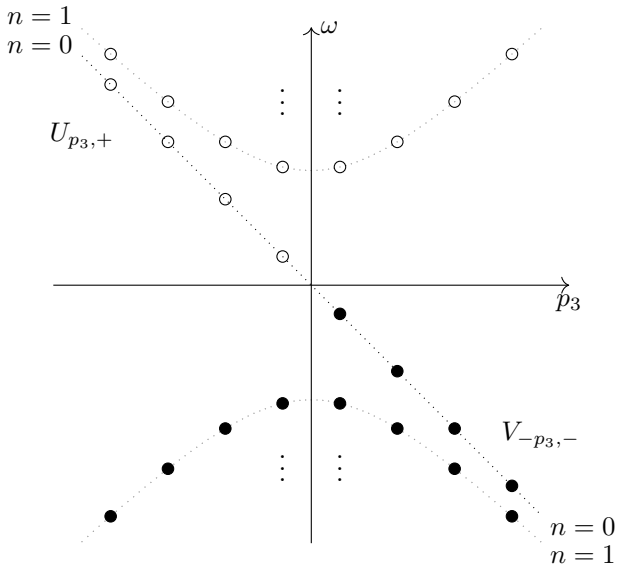


Figure 2.6. Landau levels for left-handed and massless fermions only.

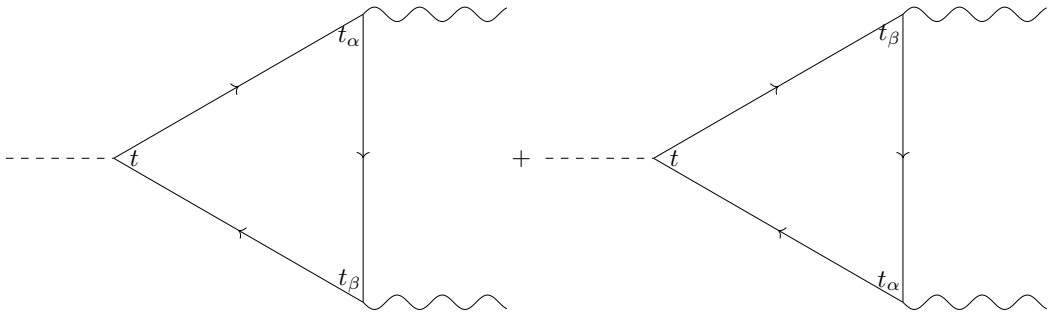


Figure 2.7. Triangle diagrams for anomalies.

noticing

$$t_\alpha = t_\beta = \begin{pmatrix} 1 & 0 \\ 0 & -1 \end{pmatrix}, \quad t = \begin{pmatrix} 1 & 0 \\ 0 & 1 \end{pmatrix}, \tag{2.118}$$

therefore,

$$\partial_\mu J_5^\mu = \frac{e^2}{16\pi^2} \epsilon^{\mu\nu\rho\sigma} F_{\mu\nu} F_{\rho\sigma}, \tag{2.119}$$

the right expression of chiral anomaly in QED.

A symmetry is free of anomaly, if $\mathrm{Tr}\,[\{t_\alpha, t_\beta\}t]$ vanish. This indeed happens to the $SU(3) \times SU(2) \times U(1)$ gauge theory, when one generation of the Standard Model fermions is considered [41]. With the same fermion content, we now study if there

is any other $U(1)$ symmetry that could be adopted by the Standard Model. To this end, we denote the extra symmetry as $U(1)'$ to distinguish the one in the Standard Model. As in (2.109), instead of choosing the $SU_L(2)$ singlets u_R, d_R and e_R, we select their charge conjugate, $u_R^{\mathcal{C}}$, $d_R^{\mathcal{C}}$ and $e_R^{\mathcal{C}}$, which would be left-handed spinors. We assume the $U'(1)$ charge of $(u_L,\ d_L)$, $u_R^{\mathcal{C}}$, $d_R^{\mathcal{C}}$, $(\nu_L,\ e_L)$ and $e_R^{\mathcal{C}}$ are a, b, c, d and e respectively.

First of all, in order to have the anomaly cancelled in $SU(3) - SU(3) - U(1)'$ triangle diagrams, the following equation must be satisfied,

$$\sum \mathrm{Tr}\left[\{t_\alpha, t_\beta\}t\right] = 0, \tag{2.120}$$

where the sum is performed to include all fermions. In practice, only quarks can couple to the $SU(3)$ gauge field. Accordingly, the equation could be written as

$$\sum \mathrm{Tr}\left[\{t_\alpha, t_\beta\}t\right] = \mathrm{Tr}\left[\{T_\alpha, T_\beta\}\right](2a + b + c) = 0, \tag{2.121}$$

where T_α, T_β are $SU(3)$ generators and specifically for the $SU(N)$ group, $\mathrm{Tr}\left[T_\alpha T_\beta\right] = \delta_{\alpha\beta}/2$. As a result,
$SU(3) - SU(3) - U(1)'$:

$$2a + b + c = 0, \tag{2.122}$$

and similarly
$SU(2) - SU(2) - U(1)'$:

$$3a + d = 0, \tag{2.123}$$

$U(1) - U(1) - U(1)'$:

$$6\left(-\frac{1}{6}\right)^2 a + 3\left(\frac{2}{3}\right)^2 b + 3\left(-\frac{1}{3}\right)^2 c + 2\left(\frac{1}{2}\right)^2 d + (-1)^2 e = 0, \tag{2.124}$$

with the weak hypercharges that can be found in Table 2.1. There are only two independent solutions, and it is no surprise that the Standard Model $U(1)$ will be one of them, which is presented by $(a, b, c, d, e) = (-\frac{1}{6},\ \ \frac{2}{3}, -\frac{1}{3},\ \ \frac{1}{2}, -1)$; to our

	electromagnetic charge $Q = T_3 - Y$	weak isospin T_3	weak hypercharge Y
$\begin{pmatrix} u \\ d \end{pmatrix}_L$	$+2/3$ $-1/3$	$+1/2$ $-1/2$	$-1/6$
$u_R^{\mathcal{C}}$	$-2/3$	0	$+2/3$
$d_R^{\mathcal{C}}$	$+1/3$	0	$-1/3$
$\begin{pmatrix} \nu \\ e \end{pmatrix}_L$	0 -1	$+1/2$ $-1/2$	$+1/2$
$e_R^{\mathcal{C}}$	$+1$	0	-1

Table 2.1. The electromagnetic charge Q, weak isospin T_3 and weak hypercharge Y of the first-generation fermions, with a relation $Q = T_3 - Y$.

concern, the other solution is $(a, b, c, d, e) = (\frac{1}{3}, -\frac{1}{3}, -\frac{1}{3}, -1, \ \ 1)$, which is $B - L$. [5]

Therefore, with Standard Model fermion content, we expect the symmetry $B+L$ should be violated as quantum anomaly, while $B-L$ is still a good symmetry in the Standard Model. Particularly, the $B+L$ anomaly happens only in $SU(2)-SU(2)-U(1)'$ and $U(1)-U(1)-U(1)'$. If the fermionic lagrangian is in a shape of

$$\begin{aligned} \mathcal{L}_f \ &= \ \bar{q}_L \gamma^\mu D_\mu q_L \ + \ \bar{u}_R \gamma^\mu \partial_\mu u_R \ + \ \bar{d}_R \gamma^\mu \partial_\mu d_R \\ &+ \ \bar{l}_L \gamma^\mu D_\mu l_L \ + \ \bar{\nu}_R \gamma^\mu \partial_\mu \nu_R \ + \ \bar{e}_R \gamma^\mu \partial_\mu e_R \end{aligned} \tag{2.125}$$

[5] If considering the graviton-graviton-$U(1)'$, we can constrain further that there must exist $SU(3) \times SU(2) \times U(1)$ singlet(s) of $U(1)'$ charge f_i, and $\sum_i f_i = -1$.

If the global symmetry is from a gauge theory which should be broken in a high energy as there is no such massless gauge boson being found in the experiment, there will exist two more requirements: $U(1) - U(1)' - U(1)'$:

$$6\left(-\frac{1}{6}\right)a^2 + 3\left(\frac{2}{3}\right)b^2 + 3\left(-\frac{1}{3}\right)c^2 + 2\left(\frac{1}{2}\right)d^2 + (-1)\,e^2 = 0$$

$U(1)' - U(1)' - U(1)'$:

$$6a^3 + 3b^3 + 3c^3 + 2d^3 + e^3 + \sum f^3$$

The first requirement can be satisfied by the solution in the text, and the second one add a further constraint on extra singlet(s), that is, $\sum f^3 = -1$. The simplest solution is the right-handed neutrino.

with the covariant derivative [8, 41],

$$D_\mu = \partial_\mu - iYB_\mu - \frac{i\sigma^a}{2}A^a_\mu, \tag{2.126}$$

which will guarantee the electric charge defined by the relation $Q = T_3 - Y$, the baryon number, summing over the SU(3) color

$$j^\mu_b = \frac{1}{3}\sum \; i\bar{q}_L\gamma^\mu q_L + i\bar{u}_R\gamma^\mu u_R + i\bar{d}_R\gamma^\mu d_R, \tag{2.127}$$

and the lepton number

$$j^\mu_l = i\bar{l}_L\gamma^\mu l_L + i\bar{\nu}_R\gamma^\mu \nu_R + i\bar{e}_R\gamma^\mu e_R, \tag{2.128}$$

would have an anomaly in the form of [6]

$$\partial_\mu j^\mu_b = \partial_\mu j^\mu_l = \frac{1}{64\pi^2}\epsilon^{\mu\nu\rho\sigma}F^a_{\mu\nu}F^a_{\rho\sigma} - \frac{1}{64\pi^2}\epsilon^{\mu\nu\rho\sigma}B_{\mu\nu}B_{\rho\sigma}. \tag{2.129}$$

2.4 Fermions on a lattice

The most notorious problem of fermions on a lattice is the fermion doubling problem, that there are more unwanted species propagating when the fermion field is realized naively on a lattice. To solve, or at least to alleviate the issue, lots of methods have been proposed, such as Wilson fermions [16], staggered fermions [15, 18] and Ginsparg-Wilson fermions [21]. In practice, it is the Wilson fermion that we will adopt in our work to remove the spatial doublers. It also turns out that the temporal doubler in real-time simulations is no longer a practical problem if the initialization is well chosen and time step of the evolution is small enough. We will reveal these two aspects in this section.

First of all, we consider the naive realization of fermions on a lattice with the

[6] In the Euclidean spacetime, any finite integral $\int_E \frac{1}{64\pi}\epsilon^{\mu\nu\rho\sigma}F^a_{\mu\nu}F^a_{\rho\sigma} = n$, will be an integer; comparatively, $\int_E \frac{1}{64\pi}\epsilon^{\mu\nu\rho\sigma}B_{\mu\nu}B_{\rho\sigma} = 0$.

action [54],

$$\begin{aligned} S =& dtd^3x \sum_{t,x} \quad -\bar{\psi}(t,x)\gamma^0 \frac{U_0(t,x)\psi(t+dt,x) - U_0^\dagger(t-dt,x)\psi(t-dt,x)}{2dt} \\ & - \sum_i \bar{\psi}(t,x)\gamma^i \frac{U_i(t,x)\psi(t,x+dx_i) - U_i^\dagger(t,x-dx_i)\psi(t,x-dx_i)}{2dx_i} \\ & - m\bar{\psi}(t,x)\psi(t,x), \end{aligned} \tag{2.130}$$

where the gauge link $U_\mu(x) = e^{-iedx_\mu A_\mu(x)}$ [14] is employed to maintain gauge invariance on the lattice. In real-time simulations, a convenient gauge fixing is the temporal gauge, that any $U_0(t,x) = 1$.

The discretized Dirac equation is obtained through a derivative of the action with respect to $\bar{\psi}(t,x)$, as a result,

$$\begin{aligned} \gamma^0 \frac{\psi(t+dt,x) - \psi(t-dt,x)}{2dt} + \sum_i \gamma^i \frac{U_i(t,x)\psi(t,x+dx_i) - U_i^\dagger(t,x-dx_i)\psi(t,x-dx_i)}{2dx_i} \\ + m\psi(t,x) = 0. \end{aligned} \tag{2.131}$$

For free fermions, the mode functions of U and V parts can be written in the form of plane wave functions,

$$U_{p,s}(t,x) = e^{-iEt+ip.x}U_{q,s}, \quad V_{-p,-s}(t,x) = e^{iEt+ip.x}V_{-q,-s}, \tag{2.132}$$

where the length $x_i = s_i dx_i$, the momentum $p_i = \left(q_i + \frac{1}{2}\right)\frac{2\pi}{N_i dx_i}$ and the integers s_i and q_i could be 0, 1, 2 ... $N_i - 1$, with N_i the total number of site along i-th direction. Then the Dirac equation becomes the equation of spinors,

$$\left[-i\gamma^0 \frac{\sin E}{dt} + \sum_i i\gamma^i \frac{\sin p_i}{dx_i} + m\right] U_{q,s} = 0, \tag{2.133}$$

$$\left[i\gamma^0 \frac{\sin E}{dt} + \sum_i i\gamma^i \frac{\sin p_i}{dx_i} + m\right] V_{-q,-s} = 0, \tag{2.134}$$

for which, the solutions can be chosen as

$$U_{q,s} = \frac{1}{\sqrt{2\omega}} \begin{pmatrix} -\sqrt{\omega - \sigma.\tilde{p}} & \eta_s \\ \sqrt{\omega + \sigma.\tilde{p}} & \eta_s \end{pmatrix}, \quad V_{-q,-s} = \frac{1}{\sqrt{2\omega}} \begin{pmatrix} \sqrt{\omega + \sigma.\tilde{p}} & \eta_s \\ \sqrt{\omega - \sigma.\tilde{p}} & \eta_s \end{pmatrix}, \tag{2.135}$$

where $\tilde{p}_i = \frac{\sin(p_i dx_i)}{dx_i}$ and the energy $\omega = \sqrt{|\tilde{p}|^2 + m^2}$, which is related to E via $e^{-iEdt} = \left(\sqrt{1-\omega^2 dt^2} - i\omega dt\right)$.

Presumably, if the energy operator on the lattice is defined similarly as the one in the continuous theory, $i\frac{\partial}{\partial t}\psi = \omega\psi$, only by replacing the derivative with the difference, one would obtain $\omega = \sqrt{\sum_i \sin^2(p_i dx_i) + m^2}$. It is easy to show when $p_i dx_i = 0$ or π, the energy $\omega = \mathrm{m}$, and there are a total of 2^3 such solutions. This refers to the existence of 2^d species of fermions, with d being the spatial dimension. To remove these spatial doublers, we will introduce the spatial Wilson terms to the action,

$$\sum_i \frac{r_W dx_i}{2}\bar{\psi}(t,x)\frac{U_i(t,x)\psi(t,x+dx_i) - 2\psi(t,x) + U_i^\dagger(t,x-dx_i)\psi(t,x-dx_i)}{dx_i^2},$$

2.4.1 Spatial Wilson terms

Without losing generality, we study the Dirac equation for massless fermion in $1+1$ dimension,

$$\gamma^0\frac{\psi(t+dt,x)-\psi(t-dt,x)}{2dt} + \gamma^1\frac{\psi(t,x+dx)-\psi(t,x-dx)}{2dx} = 0, \tag{2.136}$$

and implement the separation of variables in a manner,

$$\gamma^0\frac{\psi(t+dt,x)-\psi(t-dt,x)}{2dt} = -i\omega\gamma^0\psi(t,x), \tag{2.137}$$

$$\gamma^1\frac{\psi(t,x+dx)-\psi(t,x-dx)}{2dx} = \quad i\omega\gamma^0\psi(t,x). \tag{2.138}$$

The second equation gives the eigenenergies $\omega = |\frac{\sin(pdx)}{dx}|$ and the dispersion relation is shown in Figure (2.8). Two particles can be identified in the plot, with zero modes at 0 and π respectively.

For Wilson fermions, an extra term will be added to the equation, as a result,

$$\begin{aligned} i\omega\gamma^0\psi(t,x) =& \gamma^1\frac{\psi(t,x+dx)-\psi(t,x-dx)}{2dx} \\ &+ \frac{r_w dx}{2}\frac{\psi(t,x+dx) - 2\psi(t,x) + \psi(t,x-dx)}{dx^2}. \end{aligned} \tag{2.139}$$

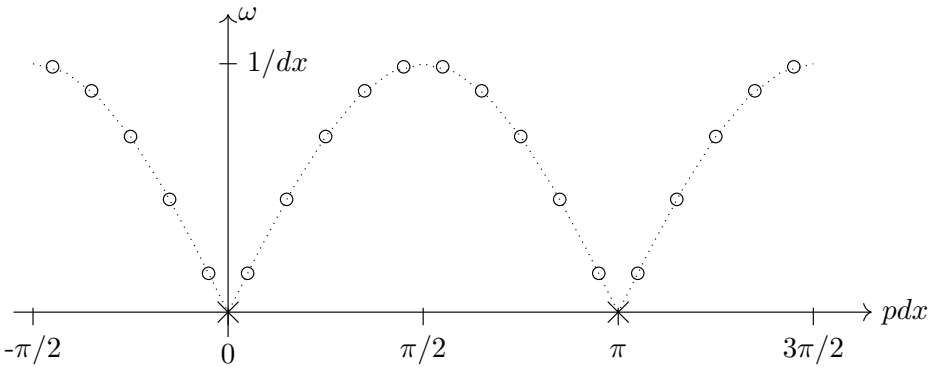


Figure 2.8. The dispersion relation without Wilson term. The plot is periodic with period 2π.

Moreover, the energy will be adjusted to the expression

$$\omega = \sqrt{\left(\frac{\sin(pdx)}{dx}\right)^2 + \left(\frac{r_W dx}{2}\right)^2 \left(\frac{2-2\cos(pdx)}{dx^2}\right)^2}. \tag{2.140}$$

The new dispersion relation of $r_W = 1$ is displayed in Figure (2.9). In this case, the degeneracy is totally removed. The physical modes around 0 are less affected by the Wilson mass, in comparison with the doubler modes close to π (or -π) whose energies have been dramatically raised by the large Wilson mass. Note also, the highest energy in this case is twice the cut-off energy.

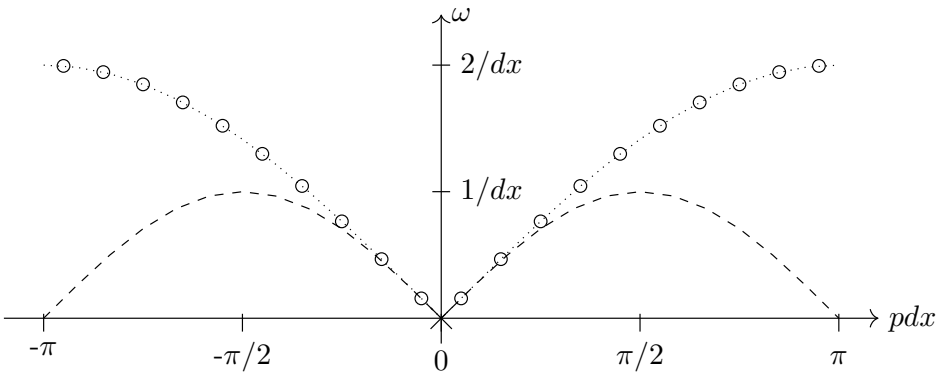


Figure 2.9. The dispersion relation with Wilson mass and $r_W = 1$. In the case, the degeneracy is totally removed.

As a comparison, the dispersion relation of $r_W = 0.5$ is plotted in Figure (2.10). In the case, the doubler becomes a mode of mass $m = 1/dx$, as large as the lattice cut-off.

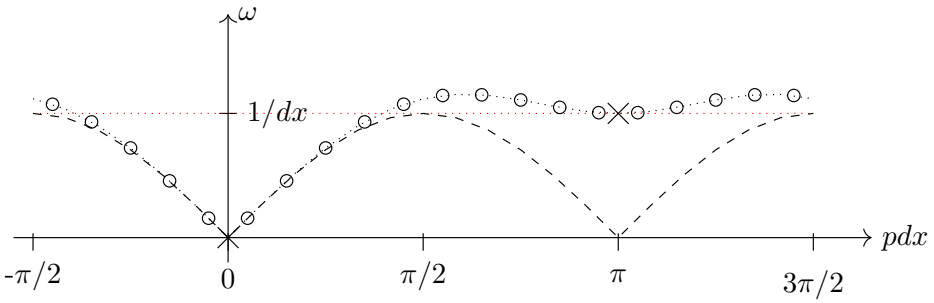


Figure 2.10. The dispersion relation with Wilson parameter $r_W = 0.5$. It can be treated as a massless particle located at 0 and a massive particle of mass $1/dx$ sitting at π.

2.4.2 Temporal doublers

The existence of temporal doublers become obvious if one solves the equation (2.137), which is essentially a recurrence relation and can be written in the form of

$$a_{n+1} + i2\omega dt a_n - a_{n-1} = 0, \tag{2.141}$$

where a_n refers to $\psi(t, x)$ as $t = ndt$. The general solution can be written into the following form,

$$\psi(t) = \frac{e^{-iEt}}{2\cos(Edt)}\left[\psi(dt) + e^{iEdt}\psi(0)\right] + (-1)^{\frac{t}{dt}}\frac{e^{iEt}}{2\cos(Edt)}\left[e^{-iEdt}\psi(0) - \psi(dt)\right], \tag{2.142}$$

where $e^{-iEdt} = \sqrt{1-\omega^2 dt^2} - i\omega dt$. From the above expression, one can find that there are two propagating modes, associated respectively to e^{-iEt} and $(-1)^n e^{iEt}$. The second term is supposed to be a doubler mode, which, comparatively, changes its sign on each step. Therefore, if both physical and doubler modes exist in the simulation, high-frequency oscillations are likely to be detected among measures of observables. To remove the doubler, one can simply set $\psi(dt) = e^{-iEdt}\psi(0)$ during the initialization to any single mode function.

On the other hand, in Minkowski spacetime, one should be cautious to include the temporal Wilson term, as ghost degrees of freedom will exist, because of these extra temporal higher order operators. For instance, the full Wilson fermion will have the action of the form,

$$S = \int dt d^3x \quad \left[\frac{r_W a}{2}\bar{\psi}\partial^\mu\partial_\mu\psi - \bar{\psi}\gamma^\mu\partial_\mu\psi\right], \tag{2.143}$$

where $a = dt = dx$ for simplicity. The propagator in the question can be written as

$$\frac{1}{-\frac{r_W a}{2}\partial^\mu\partial_\mu + \gamma^\mu\partial_\mu} = \frac{1}{\gamma^\mu\partial_\mu} - \frac{1}{\gamma^\mu\partial_\mu - \frac{2}{r_W a}}, \tag{2.144}$$

where on the right-hand side, the first term is a result of a massless fermion and the minus sign in the front of the second term reveals the existence of the ghost, of mass $m = \frac{2}{r_W a}$. Theoretically, this might not be a problem, as the large mass will forbid the ghost degree being excited. Another interesting aspect is that the fermion statistics will be modified due to the existence of the second-order derivative [27, 33].

2.4.3 Chiral anomaly on the lattice

The chiral anomaly can be realized on the lattice by Wilson fermions [20] , with the fermion action

$$S_F = -\int d^4x \left[\bar{\psi}\gamma^\mu D_\mu\psi - \frac{r_W a}{2}\bar{\psi}D^i D_i\psi\right], \tag{2.145}$$

where the fermions interact with the gauge field through the gauge covariant derivative $D_\mu = \partial_\mu - iA_\mu$. The action has been written in continuous form for the sake of simplicity, and in practice the lattice spacing $a = dx$ is small but not infinitesimal. It is apparent that the chiral symmetry of the action is broken due to the existence of the Wilson term (the second term in the action (2.145)). In the limit $a \to 0$, the Wilson term vanishes and therefore the Wilson fermions turn into the Dirac fermions in the continuum theory. But the violation of the chiral symmetry will be reserved and this is the origin of the chiral anomaly. Karsten and Smit [20] have proved that the chiral anomaly can be produced by Wilson fermions on a Euclidean lattice, in the perturbative limit of the gauge field,

$$\partial_\mu\langle\bar{\psi}i\gamma^\mu\gamma^5\psi\rangle = -r_W a\langle\bar{\psi}\gamma^5\psi D^\mu D_\mu\psi\rangle = \frac{e^2}{16\pi^2}\epsilon^{\mu\nu\rho\sigma}F_{\mu\nu}F_{\rho\sigma}. \tag{2.146}$$

Kerler [22] has further shown that the equation can be established independently of the perturbation theory. What is even more interesting is that the validity of the chiral anomaly equation (2.146) does not depend on the value of r_W, as long as it is not zero [20, 69, 70]. In real-time simulations, the chiral anomaly can also be

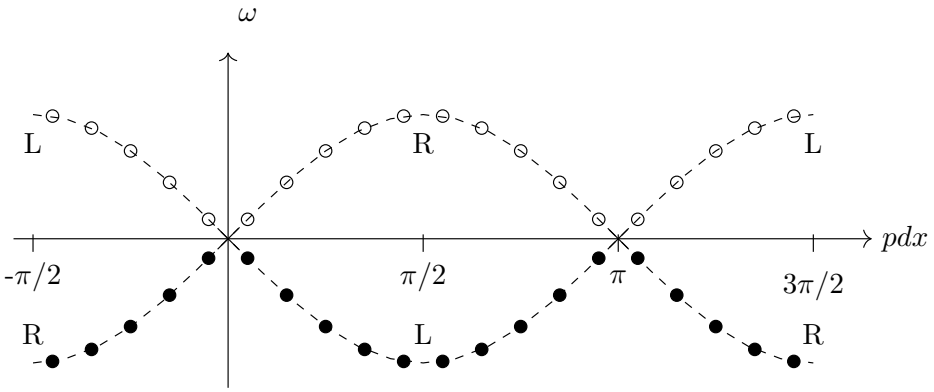
achieved when only the spatial Wilson term is involved [70, 76].

It is complicated to prove that the Wilson fermions can lead to the chiral anomaly, but it is easy to demonstrate that without the Wilson term, the anomaly can not be obtained. Without the Wilson term, the discretized Dirac equation for fermions in parallel electric and magnetic field can be solved analytically. The solution will be a result of the discretization of the continuous solution. However, the doublers will appear in the discretized solution. Actually, the appearance of doublers is avoidable when the fermion action is chiral symmetric, and this is summed up by the Nielsen and Ninomiya theorem, which states that a local, real fermion lattice action, having chiral and translational invariance, must have fermion doubling. It is the existence of the doublers that make the chiral anomaly impossible.

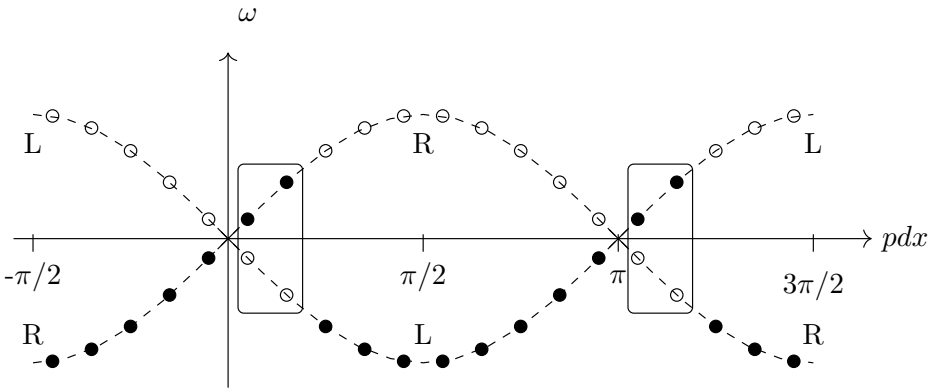
Figure 2.11 illustrates the pair production in the lowest-energy Landau levels. On the lattice, the Landau levels are actually periodic over the momentum and therefore closed, in comparison with the open ones in the continuum theory (for example, see Figure 2.4). This periodicity is due to the lattice regularization, [7] and the 1-momentum space is homeomorphic to the 1-torus. In the plots, there are two zero-points $pdx = 0$ and π, which correspond to the rest states of physical mode and doubler mode. Within the electric field, the same amount of pair productions occur around these two zero-points, but with opposite chirality. As a result, the chiral charge of the physical model is exactly cancelled out by the chiral charge of the doubler mode, and therefore the chiral anomaly can not happen.

Above all, the regularization method that are used to derive the chiral anomaly should be consistent with the range of the momentum. The dimensional regularization and the method that we utilized in this chapter can adopt the infinite range of the momentum. While in comparison, for finite range of the momentum, the possible way to achieve the chiral anomaly is to break the chiral symmetry by some higher-order operator, like the Wilson term. This applies to the lattice regularization and the gauge covariant Pauli-Villars regularization [26].

[7] The range of the momentum is finite on the lattice. Imagine a mode function of initial momentum inside the range, accelerates in an electric field, and eventually reaches the final momentum which is outside of the range. Without the periodicity, this does not make any sense on the lattice.



(a) t=0



(b) t=τ

Figure 2.11. Pair productions in the naive fermion realization. Chiral charges in IR are exactly opposite to ones in UV. The plot is periodic with period 2π. So points of $pdx = -\pi/2$ are the same as points of $pdx = 3\pi/2$.

Chapter 3

Fermions in the Electroweak Dynamics

In this chapter, we are going to implement numerical simulations of electroweak dynamics with fermions involved. On the one hand, fermions are crucial to obtain the $B+L$ anomaly, which is supposed to play an important role in the early universe of spontaneous electroweak symmetry breaking to accomplish the baryogenesis. On the other hand, it requires a large number of degree of freedom to represent fermions in practical simulations. Unlike gauge fields or Higgs fields which can be well approximated by classical field configurations due to their large occupation numbers during the time, fermions should always be treated as quantum fields, as the occupation number of any mode is never large than one, restricted by the Pauli exclusion principle. Nevertheless, nowadays numerical computations gradually become powerful enough to tackle the challenge, as well as some new methods [61] proposed to reduce the memory consumption to represent quantum fermions in real-time simulations. We will take the opportunity to study the fermion behavior in the electroweak phase transition.

The aim of the chapter is to study the cold electroweak transition through numerical simulations, and eventually measure the fermion temperature during the transition. A cold transition is crucial to Cold Electroweak Baryogenesis with the Standard Model CP-violation as the origin of the baryon asymmetry of the Universe, as the CP-violation in the CKM matrix is highly suppressed by the temperature [56]. In fact, the study in [68] suggested that the transition temperature should be at most of order 1 GeV, in order to have a viable Standard Model baryogenesis. We will in practice apply the method of ensemble fermions to measure the fermion occupation number and accordingly check the transition temperature.

3.1 The reduced Standard Model

For the sake of simplicity, we restrict ourselves to consider a reduced electroweak theory, involving $SU(2)$ gauge fields, Higgs fields and one family of quarks and leptons, including a right-handed neutrino, and with $SU(3)$ color index and $U(1)$ charge omitted.

3.1.1 Continuum action

The continuum action takes the form

$$S = S_H + S_G + S_F + S_Y, \tag{3.1}$$

with individual components,

$$S_H = -\int d^4x \left[(D_\mu\phi)^\dagger D^\mu\phi - \mu^2\phi^\dagger\phi + \lambda(\phi^\dagger\phi)^2 + \frac{\mu^4}{4\lambda}\right], \tag{3.2}$$

$$S_G = -\int d^4x \frac{1}{4g^2}F^a_{\mu\nu}F^{a,\mu\nu}, \tag{3.3}$$

$$S_F = -\int d^4x \left[\bar{q}_L\gamma^\mu D_\mu q_L + \bar{u}_R\gamma^\mu\partial_\mu u_R + \bar{d}_R\gamma^\mu\partial_\mu d_R + \bar{l}_L\gamma^\mu D_\mu l_L + \bar{\nu}_R\gamma^\mu\partial_\mu\nu_R + \bar{e}_R\gamma^\mu\partial_\mu e_R\right], \tag{3.4}$$

$$S_Y = -\int d^4x \left[G^u\bar{q}_L\tilde{\phi}u_R + G^d\bar{q}_L\phi d_R + G^\nu\bar{l}_L\tilde{\phi}\nu_R + G^e\bar{l}_L\phi e_R + h.c.\right], \tag{3.5}$$

where the Higgs mass $m_H = \sqrt{2}\mu = 125$ GeV [82] and vacuum expectation value $v = \mu/\sqrt{\lambda} = 246$ GeV.

The covariant derivative acts on doublets, in the form of,

$$D_\mu\phi = \left(\partial_\mu - \frac{i\sigma^a}{2}A^a_\mu\right)\phi, \quad D_\mu q_L = \left(\partial_\mu - \frac{i\sigma^a}{2}A^a_\mu\right)q_L, \quad D_\mu l_L = \left(\partial_\mu - \frac{i\sigma^a}{2}A^a_\mu\right)l_L, \tag{3.6}$$

and the field strength tensor is defined accordingly by,

$$-\frac{i\sigma^a}{2}F^a_{\mu\nu} = [D_\mu, D_\nu], \quad F^a_{\mu\nu} = \partial_\mu A^a_\nu - \partial_\nu A^a_\mu + \epsilon^{abc}A^b_\mu A^c_\nu. \tag{3.7}$$

The $SU(2)$ generators of the representation are chosen as,

$$T^a = \frac{1}{2}\sigma^a, \quad \text{so} \quad \mathrm{Tr}\left[T^a T^b\right] = \frac{1}{2}\delta^{ab}, \quad T^a T^b - T^b T^a = [T^a, T^b] = i\epsilon^{abc}T^c. \tag{3.8}$$

By denoting $A_\mu = T^a A^a_\mu$ and $F_{\mu\nu} = T^a F^a_{\mu\nu}$, one can show that

$$F_{\mu\nu} = \partial_\mu A_\nu - \partial_\nu A_\mu - i[A_\mu, A_\nu]. \tag{3.9}$$

The field $\tilde{\phi}$ in the Yukawa interaction is defined as $\tilde{\phi}(x) = i\sigma^2\phi^\star(x)$, [1] and for any $SU(2)$ gauge transformation $\phi'(x) = U(x)\phi(x)$, it is easy to show $\tilde{\phi}'(x) = U(x)\tilde{\phi}(x)$. We will also commonly use the field $\Phi(x) = \left(\tilde{\phi}(x), \phi(x)\right)$, which behaves like $\Phi'(x) = U(x)\Phi(x)$ under the $SU(2)$ gauge transformation, These different expressions of Higgs field can be written explicitly as

$$\phi(x) = \begin{pmatrix} \phi_1(x) \\ \phi_2(x) \end{pmatrix}, \quad \tilde{\phi}(x) = \begin{pmatrix} \phi_2^\star(x) \\ -\phi_1^\star(x) \end{pmatrix}, \quad \Phi(x) = \begin{pmatrix} \phi_2^\star(x) & \phi_1(x) \\ -\phi_1^\star(x) & \phi_2(x) \end{pmatrix}, \tag{3.10}$$

and the matrix expression can have the expansion

$$\Phi(x) = k^b\Phi^b = \mathbb{I}\Phi^0 + i\sigma^1\Phi^1 + i\sigma^2\Phi^2 + i\sigma^3\Phi^3, \tag{3.11}$$

with $k^b = (\mathbb{I}, i\sigma^1, i\sigma^2, i\sigma^3)$. Especially, one can verify that the normalized matrix $\hat{\Phi} = \Phi/\sqrt{\phi^\dagger\phi}$ is a $SU(2)$ matrix, as long as $|\phi|$ is not zero.

To our concern, the baryon number and lepton number are defined separately by

$$j_b^\mu = i\left[\bar{q}_L\gamma^\mu q_L + \bar{u}_R\gamma^\mu u_R + \bar{d}_R\gamma^\mu d_R\right] = i\bar{q}\gamma^\mu q, \tag{3.12}$$

$$j_l^\mu = i\left[\bar{l}_L\gamma^\mu l_L + \bar{\nu}_R\gamma^\mu \nu_R + \bar{e}_R\gamma^\mu e_R\right] = i\bar{l}\gamma^\mu l,, \tag{3.13}$$

where as the $SU(3)$ color index is omitted, we assign $B = 1$ to each quark and -1 to each anti-quark. Provided the fermion content $(q_L,\ (u_R^{\mathcal{C}},\ d_R^{\mathcal{C}}),\ l_L,\ (\nu_R^{\mathcal{C}},\ e_R^{\mathcal{C}}))^T$ (for the detailed definition, see section 2.3.3), the $B + L$ anomaly will happen in the

[1] This is because any $SU(2)$ representation is self-conjugate and in this case, it is matrix $i\sigma^2$ transforming the $SU(2)$ fundamental representation to its anti-fundamental one.

following way

$$\partial_\mu J^\mu_{b+l} = \frac{1}{32\pi^2}\epsilon^{\mu\nu\rho\sigma}F^a_{\mu\nu}F^b_{\rho\sigma}\frac{1}{2}\mathrm{Tr}\left[\{t_a, t_b\}t\right], \tag{3.14}$$

where now

$$t_a = \begin{pmatrix} \frac{\sigma^a}{2} & & & \\ & 0 & & \\ & & \frac{\sigma^a}{2} & \\ & & & 0 \end{pmatrix}, \quad t = \begin{pmatrix} \mathbb{I} & & & \\ & 0 & & \\ & & \mathbb{I} & \\ & & & 0 \end{pmatrix}, \tag{3.15}$$

therefore, the $B + L$ anomaly in the reduced Standard Model model can be written precisely in the form of

$$\partial_\mu j^\mu_b + \partial_\mu j^\mu_l = \partial_\mu J^\mu_{b+l} = \frac{1}{32\pi^2}\epsilon^{\mu\nu\rho\sigma}F^a_{\mu\nu}F^a_{\rho\sigma}. \tag{3.16}$$

On the other hand, for $B - L$,

$$t = \begin{pmatrix} \mathbb{I} & & & \\ & 0 & & \\ & & -\mathbb{I} & \\ & & & 0 \end{pmatrix}, \tag{3.17}$$

hence there is no $B - L$ anomaly,

$$\partial_\mu j^\mu_b - \partial_\mu j^\mu_l = \partial_\mu J^\mu_{b-l} = 0. \tag{3.18}$$

As a result, the anomaly in the reduced model can be written in the form of

$$\partial_\mu j^\mu_b = \partial_\mu j^\mu_l = \frac{1}{64\pi^2}\epsilon^{\mu\nu\rho\sigma}F^a_{\mu\nu}F^a_{\rho\sigma}, \tag{3.19}$$

which is exactly the same as the $B + L$ anomaly in the Standard Model, with the expression in (2.129).

We write the actions of fermions more concisely by adopting following fields,

$$\Psi_L = q_L, \qquad \Psi_R = -i\sigma^2\gamma^2 l_L^\star, \tag{3.20}$$

$$\chi_L = -\gamma^2 e_R^\star, \qquad \chi_R = u_R, \tag{3.21}$$

$$\xi_L = \gamma^2 \nu_R^\star, \qquad \xi_R = d_R, \tag{3.22}$$

and accordingly we can obtain

$$\bar{l}_L \gamma^\mu \left(\partial_\mu - \frac{i\sigma^a}{2} A_\mu^a\right) l_L = \bar{\Psi}_R \gamma^\mu \left(\partial_\mu - \frac{i\sigma^a}{2} A_\mu^a\right) \Psi_R, \tag{3.23}$$

$$\bar{e}_R \gamma^\mu \partial_\mu e_R = \bar{\chi}_L \gamma^\mu \partial_\mu \chi_L, \qquad \bar{\nu}_R \gamma^\mu \partial_\mu \nu_R = \bar{\xi}_L \gamma^\mu \partial_\mu \xi_L, \tag{3.24}$$

bearing in mind that the fermionic fields, like Grassmann numbers, anti-commutate with each other, and also noticing Pauli's matrix σ^a satisfying, $-i\sigma^2(\sigma^a)^T i\sigma^2 = -\sigma^a$. As a result, the revised actions of fermions turn into

$$S_F = -\int d^4x \, \left[\bar{\Psi}\gamma^\mu D_\mu \Psi + \bar{\chi}\gamma^\mu \partial_\mu \chi + \bar{\xi}\gamma^\mu \partial_\mu \xi\right], \tag{3.25}$$

$$S_Y = -\int d^4x \, \left[G^u \bar{\Psi}\tilde{\phi} P_R \chi + G^d \bar{\Psi}\phi P_R \xi + G^\nu \bar{\Psi}\tilde{\phi} P_L \xi + G^e \bar{\Psi}\phi P_L \chi + h.c.\right], \tag{3.26}$$

with projectors $P_L = \frac{1+\gamma^5}{2}$ and $P_R = \frac{1-\gamma^5}{2}$. One can also check the chiral anomaly in the new action is the $B + L$ anomaly in the original action, in the form of,

$$j_5^\mu = i\left[\bar{\Psi}\gamma^\mu\gamma^5\Psi - \bar{\chi}\gamma^\mu\gamma^5\chi - \bar{\xi}\gamma^\mu\gamma^5\xi\right] = j_b^\mu + j_l^\mu.$$

3.1.2 The Chern-Simons number

The terms appearing on the right-handed side of the anomaly equation can be written in the form of derivatives [58],

$$\frac{1}{32\pi^2}\epsilon^{\mu\nu\rho\sigma}\mathrm{Tr}\left[F_{\mu\nu}F_{\rho\sigma}\right] = \frac{1}{16\pi^2}\epsilon^{\mu\nu\rho\sigma}\partial_\mu \mathrm{Tr}\left[A_\nu F_{\rho\sigma} + i\frac{2}{3}A_\nu A_\rho A_\sigma\right], \tag{3.27}$$

or with explicit $SU(2)$ group indices,

$$\frac{1}{64\pi^2}\epsilon^{\mu\nu\rho\sigma}F_{\mu\nu}^a F_{\rho\sigma}^a = \frac{1}{32\pi^2}\epsilon^{\mu\nu\rho\sigma}\partial_\mu\left(A_\nu^a F_{\rho\sigma}^a - \frac{1}{3}\epsilon^{abc}A_\nu^a A_\rho^b A_\sigma^c\right). \tag{3.28}$$

The Chern-Simons number is defined accordingly as

$$\begin{aligned} N_{CS} =& \frac{1}{16\pi^2}\int d^3x\epsilon^{ijk}\mathrm{Tr}\left[A_iF_{jk}+i\frac{2}{3}A_iA_jA_k\right] \\ =& \frac{1}{32\pi^2}\int d^3x\epsilon^{ijk}\left(A_i^aF_{jk}^a-\frac{1}{3}\epsilon^{abc}A_i^aA_j^bA_k^c\right). \end{aligned} \tag{3.29}$$

The vacuum states of pure $SU(2)$ gauge theory are degenerate in energy, but they can be discriminated by Chern-Simons numbers, as in Fig 3.1. To show this

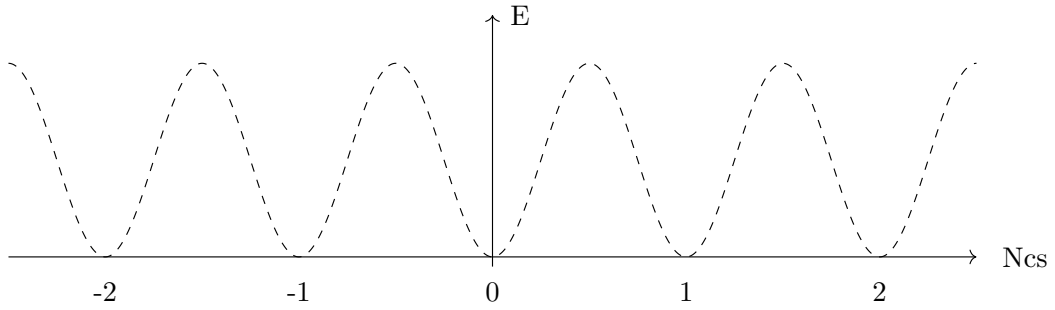


Figure 3.1. The degeneracy of the vacuum of the $SU(2)$ gauge field. The degeneracy remains when the Higgs field is included, but there will exist saddle points on the barrier between two vacuums. The Sphaleron accounts for such saddle points [24, 25]. With the existence of fermions, the degeneracy will vanish, and large $|N_{CS}|$ state will have large energy, as N_{CS} corresponds to the baryon numbers [28, 32].

elegantly, we will use the language of p-form, by which, for instance, a p-form g is related to a rank-p anti-symmetric tensor $g_{i_1i_2\ldots i_p}$ using the convention,

$$g=\frac{1}{p!}g_{i_1i_2\ldots i_p}dx^{i_1}\wedge dx^{i_2}\wedge\ldots dx^{i_p}, \tag{3.30}$$

specifically,

$$A=A_\mu dx^\mu,\quad F=\frac{1}{2}F_{\mu\nu}dx^\mu\wedge dx^\nu=dA-iA\wedge A. \tag{3.31}$$

In light of the p-form notation, the equations (3.27), (3.28) can be simply written as,

$$\frac{1}{8\pi^2}\mathrm{Tr}\left[F\wedge F\right]=\frac{1}{8\pi^2}\mathrm{Tr}\left[d\left(A\wedge F+\frac{i}{3}A\wedge A\wedge A\right)\right]. \tag{3.32}$$

To have a field configuration of zero energy, we choose the gauge field to be pure gauge, of the form, $A=-idGG^{-1}$ with $G(x)$ a $SU(2)$ matrix at each spacetime point, which in the end will provide $F=dA-iA\wedge A=0$ everywhere and therefore

lead to vanishing gauge energy $E = \int d^3x \left[\frac{1}{2}F^a_{0i}F^{a,0i} + \frac{1}{4}F^a_{ij}F^{a,ij}\right] = 0$. We further consider a static solution, that the gauge field is not time dependent, and moreover, we stick to the temporal gauge fixing, so $A_0 = 0$. One can then check the Chern-Simons number in this situation is a Cartan-Maurer integral invariant,

$$\begin{aligned} N_{CS} =& \frac{1}{8\pi^2}\int \mathrm{Tr}\left[A\wedge F + \frac{i}{3}A\wedge A\wedge A\right] \\ =& -\frac{1}{24\pi^2}\int \mathrm{Tr}\left[dGG^{-1}\wedge dGG^{-1}\wedge dGG^{-1}\right], \end{aligned} \tag{3.33}$$

and N_{CS} could be any integer. [2]

On the other hand, the vacuum state also requires the Higgs potential energy to be minimal and the kinetic energy to be zero. Especially, for minimizing the potential energy,

$$V(\phi) = \int d^3x \left[-\mu^2\phi^\dagger\phi + \lambda(\phi^\dagger\phi)^2\right], \tag{3.34}$$

the Higgs field can only be chosen under the restriction

$$\phi^\dagger\phi = \frac{\mu^2}{2\lambda} = \frac{v^2}{2}, \tag{3.35}$$

where the vacuum expectation value in reality is $v = 246$ GeV. To have vanishing kinetic energy, the equation $D_\mu\phi = 0$ should be met, in the language of p-forms, that is to say,

$$d\hat{\Phi} - iA\hat{\Phi} = 0, \quad \rightarrow \quad A = -id\hat{\Phi}\hat{\Phi}^{-1}, \tag{3.36}$$

where the $SU(2)$ matrix $\hat{\Phi}$ is

$$\hat{\Phi}(x) = \frac{1}{v}\begin{pmatrix} \phi_2^\star(x) & \phi_1(x) \\ -\phi_1^\star(x) & \phi_2(x) \end{pmatrix}. \tag{3.37}$$

[2] In a 4-dimensional Euclidean space, when the distance $r \to +\infty$, the gauge field there could also approach to pure gauge, so that $F = 0$ to guarantee a finite total energy. Similarly one would encounter the integer

$$\frac{1}{8\pi^2}\int_M \mathrm{Tr}\left[F\wedge F\right] = -\frac{1}{24\pi^2}\int_{\partial M} \mathrm{Tr}\left[dGG^{-1}\wedge dGG^{-1}\wedge dGG^{-1}\right],$$

as the element of homotopy group $\pi_3(S^3) = Z$.

The Higgs winding number is defined as

$$N_W = -\frac{1}{24\pi^2}\int \mathrm{Tr}\left[d\hat{\Phi}\hat{\Phi}^{-1}\wedge d\hat{\Phi}\hat{\Phi}^{-1}\wedge d\hat{\Phi}\hat{\Phi}^{-1}\right], \tag{3.38}$$

and according to the definition of the Chern-Simon number in (3.33), we can conclude for those vacuum states, $N_W = N_{CS}$.

As a result, there are three numbers that we can implement to indicate the state of the system. Especially, the created baryon (lepton) number would be the same as the change of the Chern-Simons number, from time 0 to t,

$$N_B(t) - N_B(0) = N_{CS}(t) - N_{CS}(0) = \int_0^t d\tau \int d^3x \frac{1}{32\pi^2}\epsilon^{\mu\nu\rho\sigma}\mathrm{Tr}\left[F_{\mu\nu}F_{\rho\sigma}\right], \tag{3.39}$$

with the Higgs winding number pointing to the nearest vacuum state.

3.1.3 Fermion mode functions and correlation functions

For free fermions, we choose the mode functions, labelled by $p = (p_1, p_2, p_3)$ and s, as

$$U_s(p;t,x) = e^{-i\omega t + ip.x}U_s(p), \qquad V_{-s}(-p;t,x) = e^{i\omega t + ip.x}V_{-s}(-p), \tag{3.40}$$

where the on-shell condition is $\omega = \sqrt{p^2+m^2}$ and dot products mean 3-vector products, i.e. $p.x = p_1x_1 + p_2x_2 + p_3x_3$. The mode function $U_s(p;t,x)$ eventually refers to a particle state of momentum p and spin $s/2$, and $V_{-s}(-p;t,x)$ an anti-particle state of momentum $-p$ and spin $-s/2$. The spinors $U_s(p)$ and $V_{-s}(-p)$ satisfy

$$(-i\gamma^0\omega + i\gamma.p + m)U_s(p) = 0, \qquad (i\gamma^0\omega + i\gamma.p + m)V_{-s}(-p) = 0, \tag{3.41}$$

and they can accordingly be chosen in the form of

$$U_s(p) = \frac{1}{\sqrt{2\omega}}\begin{pmatrix} -\sqrt{\omega-\sigma.p}\,\eta_s \\ \sqrt{\omega+\sigma.p}\,\eta_s \end{pmatrix}, \qquad V_{-s}(-p) = \frac{1}{\sqrt{2\omega}}\begin{pmatrix} \sqrt{\omega+\sigma.p}\,\eta_s \\ \sqrt{\omega-\sigma.p}\,\eta_s \end{pmatrix}, \tag{3.42}$$

with $\eta_s = \begin{pmatrix} 1 \\ 0 \end{pmatrix}, \begin{pmatrix} 0 \\ 1 \end{pmatrix}$ for s=1, -1 respectively. For the Dirac-conjugates $\bar{\psi} = \psi^\dagger i\gamma^0$, we get

$$\bar{U}_s(p) = \frac{1}{\sqrt{2\omega}} \left(-\eta_s^\dagger \sqrt{\omega_p + \sigma.p}, \quad \eta_s^\dagger \sqrt{\omega_p - \sigma.p} \right), \tag{3.43}$$

$$\bar{V}_{-s}(-p) = \frac{1}{\sqrt{2\omega}} \left(-\eta_s^\dagger \sqrt{\omega_p - \sigma.p}, \ -\eta_s^\dagger \sqrt{\omega_p + \sigma.p} \right), \tag{3.44}$$

and therefore in this convention, we have

$$\sum_s U_s(p)\bar{U}_s(p) = \frac{1}{2\omega} \left[i\gamma^0\omega - i\gamma.p + m \right] \tag{3.45}$$

$$\sum_s V_{-s}(-p)\bar{V}_{-s}(-p) = \frac{1}{2\omega} \left[i\gamma^0\omega + i\gamma.p - m \right], \tag{3.46}$$

given the fact that

$$\sum_s \eta_s \eta_s^\dagger = \mathbb{I}_{2\times 2}, \tag{3.47}$$

with $\mathbb{I}_{2\times 2}$ here standing for a 2×2 identity matrix.

We expand the field operator in the form of

$$\psi(t,x) = \sum_s \int \frac{d^3p}{(2\pi)^3} \left[b_s(p)U_s(p;t,x) + d_{-s}^\dagger(-p)V_{-s}(-p;t,x) \right],$$

with creation and annihilation operators satisfying anti-commutation relations

$$\{b_r^\dagger(p), b_s(p')\} = (2\pi)^3 \delta_{rs}\delta^3(p-p'), \tag{3.48}$$

$$\{d_{-r}^\dagger(-p), d_{-s}(-p')\} = (2\pi)^3 \delta_{rs}\delta^3(p-p').$$

One can check the expansion above eventually meets the canonical anti-commutation relation, which is

$$\{\psi_\alpha(t,x), \psi_\beta^\dagger(t,x')\} = \delta_{\alpha\beta}\delta^3(x-x'), \tag{3.49}$$

with α and β spinor indices.

In practice, we define the equal-time two-point function $D(t;x,y)$, with elements

$$D_{\alpha\beta}(t;x,x') = \langle \mathrm{T}\psi_\alpha(t,x)\bar{\psi}_\beta(t,x')\rangle = \frac{1}{2}\langle \psi_\alpha(t,x)\bar{\psi}_\beta(t,x') - \bar{\psi}_\beta(t,x')\psi_\alpha(t,x)\rangle. \tag{3.50}$$

When gauge fields are present, the complete correlation function to maintain the gauge invariance should have

$$D_{\alpha\beta}(t;x,x') = -\langle \mathrm{T}\bar{\psi}_\beta(t,x')U(t;x',x)\psi_\alpha(t,x)\rangle, \tag{3.51}$$

where the gauge link $U(t;x',x) = \exp(-i\int_{\mathcal{C}} A)$ with the line integral $\mathcal{C}$, extending from x' to x. With the two-point function, a Wigner function can then be constructed accordingly

$$W(t;p,x) = \int d^3z e^{-ip.z} D(t;x+\frac{z}{2},x-\frac{z}{2}). \tag{3.52}$$

For free fermions, the spatial averaged Wigner function is actually

$$\frac{1}{\mathrm{V}}\int d^3x W(t;p,x) = D(p;t) = \langle \mathrm{T}\psi(t,p)\bar{\psi}(t,p)\rangle, \tag{3.53}$$

where $\psi(t,p) = \int d^3x e^{-ip.x}\psi(t,x)$, and $D(p;t)$ then has a simple expansion,

$$D(p;t) = \frac{1}{2}\sum_s \left[U_s(p;t)\bar{U}_s(p;t)(1-2n_s(p;t)) - V_{-s}(-p;t)\bar{V}_{-s}(-p;t)(1-2\bar{n}_{-s}(-p;t))\right], \tag{3.54}$$

where similarly as in section 2.3, $n_s(p;t)$ is the number of the particle of momentum p and spin $s/2$ and $\bar{n}_{-s}(-p;t)$ the number of the anti-particle of momentum $-p$ and spin $-s/2$. By summing over the spin and making use of the relation (3.46), one can arrive at a gamma matrix expansion [45]

$$D(p;t) = [1-N(p;t)-\bar{N}(-p;t)]\frac{-ip.\gamma+m}{2\omega} + [\bar{N}(-p;t)-N(p;t)]\frac{i\gamma^0}{2} + ..., \tag{3.55}$$

with $N(p;t) = \sum_s n_s(p;t)/2$ and $\bar{N}(-p;t) = \sum_s \bar{n}_{-s}(-p;t)/2$. For fermions in more general situations, other gamma-matrix terms could also appear in the expansion, and would be of interest themselves, like γ^5 terms existing when there is an asymme-

try between particle numbers of different spins. But we will here focus only on the first two terms, and in addition, the second term actually vanishes if CP symmetry is a good symmetry, that $U_s^{\mathcal{C}P}(p) = sV_s(-p)$ and $n_s^{\mathcal{C}P}(p) = \bar{n}_s(-p)$.

If one measures

$$F_p = \mathrm{Tr}[D(p;t)], \qquad V_p = \mathrm{Tr}[i\frac{\gamma\cdot p}{p}D(p;t)], \tag{3.56}$$

one can obtain the averaged (anti-)particle number $N_{\mathrm{av}}(p;t) = (N(p;t)+\bar{N}(-p;t))/2$ and the practical energy $\omega = \sqrt{m^2+p^2}$ at the time t, of the form,

$$N_{\mathrm{av}}(p;t) = \frac{1}{2} - \mathrm{sign}\,(V_p)\,\frac{\sqrt{F_p^2+V_p^2}}{4}, \quad \omega(p;t) = \sqrt{\frac{4(1-2N_{\mathrm{av}})^2p^2}{V_p^2}}. \tag{3.57}$$

The determination of the energy is necessary, because masses of fermions in the theory depend on the Higgs field, which is time-varying during the evolution.

3.2 Ensemble fermions

As we see in Chapter 1, fully representing one quantum Dirac field requires a large number of variables, which is of the order of N^6, with N the number of sites in each spatial direction, and even worse, when there exist n species of fermions, the number of variables will be increased by a factor of n^2. To see what this number corresponds to in the mode functions, we write down the mode function expansion in a discrete form,

$$\psi(t,x) = \frac{1}{V}\sum_{q,s}\left[b_{q,s}U_{q,s}(t,x) + d^\dagger_{-q,-s}V_{-q,-s}(t,x)\right], \tag{3.58}$$

where the mode functions are orthonormal, in the sense,

$$\frac{1}{V}\sum_{p,s}\left[U_{p,s}(t,x)U^\dagger_{p,s}(t,y) + V_{-p,-s}(t,x)V^\dagger_{-p,-s}(t,y)\right] = \frac{1}{a^3}\mathbb{I}_{4\times4}\delta^3_{xy}, \tag{3.59}$$

$$a^3\sum_x U^\dagger_{p,s}(t,x)U_{q,s'}(t,x) = a^3\sum_x V^\dagger_{-p,-s}(t,x)V_{-q,-s'}(t,x) = V\delta^3_{pq}\delta_{ss'}, \tag{3.60}$$

and the creation and annihilation operators satisfy anti-commutation relations

$$\{b^\dagger_{p,r}, b_{p',s}\} = \delta_{rs} V \delta^3_{pp'}, \qquad \{d^\dagger_{-p,-r}, d_{-p',-s}\} = \delta_{rs} V \delta^3_{pp'}, \tag{3.61}$$

with a the lattice spacing and $V = a^3 N^3$ the spatial volume. As one can see, there are a total of $4N^3$ mode functions in 3+1 dimension, and each mode function has $8N^3$ real variables, because at every site there exists a spinor of 4 complex components. These mode functions are orthonormal as in (3.60), and accordingly there will be $16N^6$ real constraints. As a result, the number of degrees of freedom of one Dirac field is $32N^6 - 16N^6 = 16N^6$. [3] However, it is much easier in practice to keep those constraints in calculations and adopt $32N^6$ variables to represent the Dirac field. On the other hand, the same amount of variables can also be found in the two-point function $D(t; x, x')$, which is now of the form,

$$\begin{aligned} D(t; x, x') =& \frac{1}{2V} \sum_{q,s} \big[U_{q,s}(t, x) \bar{U}_{q,s}(t, x')(1 - 2n_{q,s}) \\ & - V_{-q,-s}(t, x) \bar{V}_{-q,-s}(t, x')(1 - 2\bar{n}_{-q,-s}) \big] , \end{aligned} \tag{3.62}$$

with $n_{q,s}$ and $\bar{n}_{-q,-s}$ being individually the initial particle and anti-particle number, because $D(t; x, x')$ is basically a $4N^3 \times 4N^3$ complex matrix. For our interest, the vacuum state would have,

$$D(t; x, x') = \frac{1}{2V} \sum_{q,s} \big[U_{q,s}(t, x) \bar{U}_{q,s}(t, x') - V_{-q,-s}(t, x) \bar{V}_{-q,-s}(t, x') \big] , \tag{3.63}$$

with which, one can check

$$\sum_{x'} D(t; x, x') i\gamma^0 D(t; x', x'') i\gamma^0 = \frac{1}{4a^6} \delta^3_{xx''} \mathbb{I}_{4\times 4}. \tag{3.64}$$

As the numbers show, the N^6-dependence will become a big challenge to numerical simulations. For instance when $N = 32$, it requires 256GB of computer memory space to represent such a fermionic field in $3 + 1$ real-time simulations; while when $N = 48$, the number becomes desperately 2.916TB.

[3] One can actually build a matrix with each column being a mode function rescaled by $1/\sqrt{N^3}$, and such a matrix will be a unitary matrix $U(4N^3)$ with the number of the generator being $16N^6$. Such construction leads to the super-matrix used in Chapter 1.

To alleviate the memory consumption challenge, a Monte Carlo method has been proposed by Borsanyi and Hindmarsh [61] and turned out to be efficient to deal with fermions interacting with classical bosonic fields in real-time simulations [61, 76, 78]. In this method, two fermionic fields, M(ale) and F(emale), are introduced,

$$\psi_M(t,x) = \frac{1}{\sqrt{2}V}\sum_{q,s}\left[\zeta_{q,s}U_{q,s}(t,x) + \eta_{-q,-s}V_{-q,-s}(t,x)\right], \tag{3.65}$$

$$\psi_F(t,x) = \frac{1}{\sqrt{2}V}\sum_{q,s}\left[\theta_{q,s}\zeta_{q,s}U_{q,s}(t,x) + \bar{\theta}_{q,s}\chi_{-q,-s}V_{-q,-s}(t,x)\right], \tag{3.66}$$

with complex random numbers ζ and χ following Gaussian distributions and having expectation values,

$$E\left[\zeta_{q,r}\zeta^{\star}_{q',s}\right] = V\delta_{rs}\delta_{qq'}|1-2n_{q,r}|, \quad E\left[\chi_{-q,-r}\chi^{\star}_{-q',-s}\right] = V\delta_{rs}\delta_{qq'}|1-2\bar{n}_{-q,-r}|. \tag{3.67}$$

The sign $\theta_{q,s}$ and $\bar{\theta}_{-q,-s}$ are chosen in such a way that,

$$\theta_{q,s} = \begin{cases} 1 & \text{if} \quad n_{q,s} < 1/2, \\ -1 & \text{if} \quad n_{q,s} > 1/2, \end{cases}, \quad \bar{\theta}_{-q,-s} = \begin{cases} -1 & \text{if} \quad \bar{n}_{-q,-s} < 1/2, \\ 1 & \text{if} \quad \bar{n}_{-q,-s} > 1/2, \end{cases}. \tag{3.68}$$

With the two-point function defined in this case as,

$$D(t;x,x') = \frac{1}{2}\left(\psi_M(t,x)\bar{\psi}_F(t,x') + \psi_F(t,x)\bar{\psi}_M(t,x')\right), \tag{3.69}$$

one can verify that the expectation of $D(t,x,x')$ is the same as the one in equation (3.62).

We will in practice implement N_q realizations of ψ_M and ψ_F, distinguished by the index j,

$$\psi^j_M(t,x) = \frac{1}{\sqrt{2}V}\sum_{q,s}\left[\zeta^j_{q,s}U_{q,s}(t,x) + \chi^j_{-q,-s}V_{-q,-s}(t,x)\right], \tag{3.70}$$

$$\psi^j_F(t,x) = \frac{1}{\sqrt{2}V}\sum_{q,s}\left[\theta^j_{q,s}\zeta_{q,s}U_{q,s}(t,x) + \bar{\theta}^j_{q,s}\chi_{-q,-s}V_{-q,-s}(t,x)\right], \tag{3.71}$$

and use the average

$$D(t;x,x') = \frac{1}{N_q}\sum_j \frac{1}{2}\left(\psi_M^j(t,x)\bar{\psi}_F^j(t,x') + \psi_F^j(t,x)\bar{\psi}_M^j(t,x')\right),$$

to represent (3.69) in the calculation. According to the law of large numbers, the error in the average is expected to be reduced as $\frac{1}{\sqrt{N_q}}$ when N_q becomes large.

Specifically, the low-cost fermions in the vacuum state are

$$\psi_M^j(t,x) = \frac{1}{\sqrt{2}V}\sum_p \left[\zeta_{p,s}^j U_{p,s}(t,x) + \eta_{-p,-s}^j V_{-p,-s}(t,x)\right], \tag{3.72}$$

$$\psi_F^j(t,x) = \frac{1}{\sqrt{2}V}\sum_p \left[\zeta_{p,s}^j U_{p,s}(t,x) - \eta_{-p,-s}^j V_{-p,-s}(t,x)\right], \tag{3.73}$$

with

$$\left\langle \zeta_{p,r}\zeta_{p',s}^\dagger \right\rangle_E = V\delta_{rs}\delta_{pp'}, \qquad \left\langle \eta_{p,r}\eta_{p',s}^\dagger \right\rangle_E = V\delta_{rs}\delta_{pp'}, \tag{3.74}$$

where the ensemble average is define in the form of $\langle ab\rangle_E = \frac{1}{N_q}\sum_j a^j b^j$. It is easy to show that the two-point function for ensemble fermions,

$$D(t;x,x') = \frac{1}{2}\left\langle \psi_M^j(t,x)\bar{\psi}_F^j(t,x') + \psi_F^j(t,x)\bar{\psi}_M^j(t,x') \right\rangle_E,$$

has the same expression as it did in the mode function expansion in (3.63). Uniquely for ensemble fermions, one can check for any Gender (Male or Female)

$$\frac{a^3}{2}\sum_x \left\langle \psi_G^{j\dagger}(t,x)\psi_G^j(t,x)\right\rangle = 1, \tag{3.75}$$

which has no analogue in the mode function approach. The relation (3.75) can be used in practice as a check of the correctness of simulations.

3.3 Lattice implementation

In order to move the continuum theory to a lattice, the spatial and temporal variables will be chosen in the discretized form. It would be straightforward to apply the change to the Higgs field and fermion fields. For fermion fields on the lattice, the Wilson terms should also be employed. For the gauge field, we in practice choose

the gauge link to main the gauge invariance of the action.

3.3.1 Action and equation of motion

The temporal and spatial gauge links are defined of the form

$$U_0(x) = \exp(-ia_t T^a A_0^a(x)), \qquad U_i(x) = \exp(-iaT^a A_i^a(x)), \tag{3.76}$$

with a_t and a being separately the temporal and spatial lattice spacing; and a plaquette is denoted as the product of four neighbouring gauge links,

$$U_{\mu\nu}(x) = U_\mu(x)U_\nu(x+\mu)U_\mu^\dagger(x+\nu)U_\nu^\dagger(x), \tag{3.77}$$

where indices μ and ν can be chosen among 0, 1, 2 and 3, and the symbol $(x+\mu)$ really refers to a site with μ-th coordinate increased by one, for instance, $(x+2)$ meaning (t, x_1, x_2+a, x_3) and $(x+0)$ standing for $(t+a_t, x_1, x_2, x_3)$. When the perturbation is valid, one finds, $U_{ij}(x) = U_i(x)U_j(x+i)U_i^\dagger(x+j)U_j^\dagger(x) \sim \exp\left(-ia^2T^aF_{ij}^a\right)$, therefore,

$$\begin{aligned} F_{ij}^a(x) =& \frac{1}{a^2}\mathrm{Tr}\left[i\sigma^a U_{ij}\right] + \mathcal{O}(a^2), \\ -\frac{1}{4g^2}\left(F_{ij}^a(x)\right)^2 =& -\frac{2}{(ga^2)^2}\left(1 - \frac{1}{2}\mathrm{Tr}\left[U_{ij}\right]\right) + \mathcal{O}(a^2), \\ \frac{1}{2g^2}\left(F_{0i}^a(x)\right)^2 =& \frac{4}{(gaa_t)^2}\left(1 - \frac{1}{2}\mathrm{Tr}\left[U_{0i}\right]\right) + \mathcal{O}(a^2). \end{aligned} \tag{3.78}$$

As we will stick to the gauge fixing $A_0 = 0$, for plaquettes with a temporal index, we define

$$E_i(x) = U_{0i}(x) = U_i(x+0)U_i^\dagger(x), \quad E_i^a(x) = \mathrm{Tr}\left[i\sigma^a U_i(x+0)U_i^\dagger(x)\right], \tag{3.79}$$

which will determine the evolution of the spatial gauge links, in the following way,

$$U_i(x+0) = E_i(x)U_i(x). \tag{3.80}$$

With the spatial lattice spacing a, we rewrite fermionic fields

$$\Psi(x) \to a^{3/2}\Psi(x), \quad \chi(x) \to a^{3/2}\chi(x), \quad \xi(x) \to a^{3/2}\xi(x), \tag{3.81}$$

thus making them dimensionless, and similarly rescale the Higgs field as

$$\Phi(x) \to \sqrt{\lambda} a \Phi(x). \tag{3.82}$$

We will also introduce the quantities

$$\beta_G^t = \frac{4}{g^2}\frac{a}{a_t}, \quad \beta_G^s = \frac{4}{g^2}\frac{a_t}{a}, \quad \beta_H^t = \frac{1}{\lambda}\frac{a}{a_t}, \quad \beta_H^s = \beta_R = \frac{1}{\lambda}\frac{a_t}{a}, \quad \beta_Y = \frac{a_t}{a}\frac{1}{\sqrt{\lambda}}. \tag{3.83}$$

On the other hand, the discretization of the covariant derivative on the lattice is not unique, and we define the forward and backward covariant difference individually as,

$$D_\mu \Psi(x) = U_\mu(x)\Psi(x+\mu) - \Psi(x), \qquad D'_\mu \Psi(x) = \Psi(x) - U_\mu^\dagger(x-\mu)\Psi(x-\mu),$$

and the symmetric covariant difference as their average

$$\tilde{D}_\mu \Psi(x) = \frac{1}{2}\left[D_\mu + D'_\mu\right]\Psi(x) = \frac{1}{2}\left[U_\mu(x)\Psi(x+\mu) - U_\mu^\dagger(x-\mu)\Psi(x-\mu)\right].$$

The lattice action is then given by

$$S = S_H + S_G + S_F + S_W + S_Y, \tag{3.84}$$

with components

$$\begin{aligned}
S_H &= \sum_{x,t} \frac{\beta_H^t}{2}\mathrm{Tr}\left[(D_0\Phi)^\dagger D_0\Phi\right] - \frac{\beta_H^s}{2}\mathrm{Tr}\left[(D_i\Phi)^\dagger D_i\Phi\right] - \beta_R\left(\frac{1}{2}\mathrm{Tr}\left[\Phi^\dagger\Phi\right] - \frac{(am_H)^2}{4}\right)^2, \\
S_G &= \sum_{x,t}\beta_G^t \sum_i \left(1 - \frac{1}{2}\mathrm{Tr}\left[U_{0i}(x)\right]\right) - \frac{\beta_G^s}{2}\sum_{ij}\left(1 - \frac{1}{2}\mathrm{Tr}\left[U_{ij}(x)\right]\right), \\
S_F &= \sum_{x,t} - \left[\bar{\Psi}\gamma^0\tilde{D}_0\Psi + \bar{\chi}\gamma^0\tilde{\partial}_0\chi + \bar{\xi}\gamma^0\tilde{\partial}_0\xi\right] - \frac{a_t}{a}\left[\bar{\Psi}\gamma^i\tilde{D}_i\Psi + \bar{\chi}\gamma^i\tilde{\partial}_i\chi + \bar{\xi}\gamma^i\tilde{\partial}_i\xi\right], \\
S_W &= \sum_{x,t}\frac{r_W a_t}{2a}\left[\bar{\Psi}D'_iD_i\Psi + \bar{\chi}\partial'_i\partial_i\chi + \bar{\xi}\partial'_i\partial_i\xi\right], \\
S_Y &= -\sum_{x,t}\beta_Y\left[\bar{\Psi}\Phi(\chi,\xi)^T + (\bar{\chi},\bar{\xi})\Phi^\dagger\Psi\right],
\end{aligned} \tag{3.85}$$

where S_W is the spatial Wilson term, with the Wilson parameter r_W.

The equations of motion are obtained from derivatives of the action with respect

to Φ^b, $\bar{\Psi}$, $(\bar{\chi},\bar{\xi})^T$ and A^a_μ individually,

$$\begin{aligned}
0 =& -\beta^t_H\partial'_0\partial_0\Phi + \beta^s_H D'_i D_i\Phi - 2\beta_R\left(\frac{1}{2}\mathrm{Tr}\,\Phi^\dagger\Phi - \frac{(am_H)^2}{4}\right)\Phi \\
& - \frac{1}{2}\beta_Y k^b\bar{\Psi}k^b(\chi,\xi)^T - \frac{1}{2}\beta_Y k^b(\bar{\chi},\bar{\xi})(k^b)^\dagger\Psi, \\
0 =& -\gamma^0\tilde{\partial}_0\Psi - \frac{a_t}{a}\gamma^i\tilde{D}_i\Psi + \frac{ra_t}{2a}D'_iD_i\Psi - \beta_Y\Phi(\chi,\xi)^T, \\
0 =& -\gamma^0\tilde{\partial}_0(\chi,\xi)^T - \frac{a_t}{a}\gamma^i\tilde{\partial}_i(\chi,\xi)^T + \frac{ra_t}{2a}\partial'_i\partial_i(\chi,\xi)^T - \beta_Y\Phi^\dagger\Psi, \\
0 =& \frac{1}{2}\beta^t_G\left[E^a_i(x) - E^a_i(x-0)\right] + \frac{1}{2}\beta^s_G\sum_j\left[\ {}^1U^a_{ij}(x) - \ {}^3U^a_{ij}(x-j)\right] \\
& - \frac{a_t}{2a}\left[\bar{\Psi}(x)\gamma^i i\sigma^a U_i(x)\Psi(x+i) + \bar{\Psi}(x+i)\gamma^i U^\dagger_i(x) i\sigma^a\Psi(x)\right] \\
& + \frac{ra_t}{2a}\left[\bar{\Psi}(x) i\sigma^a U_i(x)\Psi(x+i) - \bar{\Psi}(x+i)U^\dagger_i(x) i\sigma^a\Psi(x)\right] \\
& - \beta^s_H\mathrm{Tr}\left[\Phi^\dagger(x+i)U^\dagger_i(x) i\sigma^a\Phi(x)\right],
\end{aligned} \tag{3.86}$$

In practice, the derivative with respect to gauge fields is executed according to,

$$-\frac{1}{2}\left[i\sigma^a U_\rho(x)\frac{\delta S}{\delta U_\rho(x)} - \frac{\delta S}{\delta U^\dagger_\rho(x)}U^\dagger_\rho(x) i\sigma^a\right],$$

where we treat U_μ(x), $U^\dagger_\mu(x)$ as they are independent, and as a result

$$\mathrm{Tr}\left[i\sigma^a U_\rho(x)\frac{\delta U_{\mu\nu}(y)}{\delta U_\rho(x)} - \frac{\delta U_{\mu\nu}(y)}{\delta U^\dagger_\rho(x)}U^\dagger_\rho(x) i\sigma^a\right] =$$

$$\delta_{x,y}\delta_{\rho,\mu}\ {}^1U^a_{\rho\nu}(x) - \delta_{x,y+\nu}\delta_{\rho,\mu}\ {}^3U^a_{\rho\nu}(x-\nu) - \delta_{x,y}\delta_{\rho,\nu}\ {}^4U^a_{\mu\rho}(x) + \delta_{x,y+\mu}\delta_{\rho,\nu}\ {}^2U^a_{\mu\rho}(x-\mu),$$

where we have defined

$$\begin{aligned}
{}^1U^a_{\mu\nu}(x) =& \mathrm{Tr}\left[i\sigma^a U_\mu(x)U_\nu(x+\mu)U^\dagger_\mu(x+\nu)U^\dagger_\nu(x)\right], \\
{}^2U^a_{\mu\nu}(x) =& \mathrm{Tr}\left[U_\mu(x) i\sigma^a U_\nu(x+\mu)U^\dagger_\mu(x+\nu)U^\dagger_\nu(x)\right], \\
{}^3U^a_{\mu\nu}(x) =& \mathrm{Tr}\left[U_\mu(x)U_\nu(x+\mu)U^\dagger_\mu(x+\nu) i\sigma^a U^\dagger_\nu(x)\right], \\
{}^4U^a_{\mu\nu}(x) =& \mathrm{Tr}\left[U_\mu(x)U_\nu(x+\mu)U^\dagger_\mu(x+\nu)U^\dagger_\nu(x) i\sigma^a\right],
\end{aligned} \tag{3.87}$$

for which one can verify

$${}^1U^a_{\mu\nu}(x) = -\ {}^4U^{a\dagger}_{\nu\mu}(x), \qquad {}^2U^a_{\mu\nu}(x) = -\ {}^3U^{a\dagger}_{\nu\mu}(x). \tag{3.88}$$

The Gauss' law of the $SU(2)$ gauge theory can be obtained in the same way, by the derivative with respect to A_0^a,

$$\beta_G^t \sum_i \left(E_i^a(x) - {}^3U_{0i}^a(x-i)\right) = 2\beta_H^t \mathrm{Tr}\left[i\sigma^a \Phi(x)\Phi^\dagger(x+0)\right] - \left(\bar{\Psi}(x)\gamma^0 i\sigma^a \Psi(x+0) + \bar{\Psi}(x+0)\gamma^0 i\sigma^a \Psi(x)\right). \tag{3.89}$$

We will initialize $E_i(x)$ according to (3.89). The Gauss' law will be a constraint equation in a sense that if the equation (3.89) is satisfied in the beginning, it will remain to be true during the evolution. So in practice, we use the Gauss' law to indicate the precision of the simulation.

With the equations of motion listed above, one can check the total energy with following energy density components rescaled by $1/m_H^4$ will be conserved up to $\mathcal{O}\left(a_t^2/a^2\right)$

$$\begin{aligned}
e_H =& \frac{1}{c}\sum_x \frac{\beta_H^t}{2}\mathrm{Tr}\left[(D_0\Phi)^\dagger D_0\Phi\right] + \frac{\beta_H^s}{2}\mathrm{Tr}\left[(D_i\Phi)^\dagger D_i\Phi\right] + \beta_R\left(\frac{1}{2}\mathrm{Tr}\,\Phi^\dagger\Phi - \frac{(am_H)^2}{4}\right)^2,\\
e_G =& \frac{1}{c}\sum_x \beta_G^t \sum_i \left(1 - \frac{1}{2}\mathrm{Tr}\,U_{0i}\right) + \frac{\beta_G^s}{2}\sum_{ij}\left(1 - \frac{1}{2}\mathrm{Tr}\,U_{ij}\right),\\
e_\Psi =& \frac{1}{c}\sum_x Re\left[\frac{a_t}{a}\bar{\Psi}\gamma^i\tilde{D}_i\Psi - \frac{ra_t}{2a}\bar{\Psi}D_i'D_i\Psi + \beta_Y\bar{\Psi}\Phi(\chi,\xi)^T\right],\\
e_\chi =& \frac{1}{c}\sum_x Re\left[\frac{a_t}{a}\bar{\chi}\gamma^i\tilde{\partial}_i\chi - \frac{ra_t}{2a}\bar{\chi}\partial_i'\partial_i\chi + \beta_Y(\bar{\chi},0)\Phi^\dagger\Psi\right],\\
e_\xi =& \frac{1}{c}\sum_x Re\left[\frac{a_t}{a}\bar{\xi}\gamma^i\tilde{\partial}_i\xi - \frac{ra_t}{2a}\bar{\xi}\partial_i'\partial_i\xi + \beta_Y(0,\bar{\xi})\Phi^\dagger\Psi\right],
\end{aligned} \tag{3.90}$$

where Re means the real part of expressions and the factor $c = a_t V m_H^4$ with V the spatial volume and m_H the Higgs mass.

To depict the motion of the Higgs field in the potential, we define

$$\langle\phi^2\rangle = \frac{2}{\mathrm{V}}\int d^3x \frac{\phi^\dagger\phi}{v^2}, \tag{3.91}$$

which will be unit when the Higgs field is in the true vacuum.

With ensemble fermions, any fermion bilinear appearing in the expression of fermion backreaction or fermion energy will be in practice represented by the product

of Male and Female fields, for instance,

$$\bar{\Psi}\Phi(\chi,\xi)^T = -\frac{1}{2}\left\langle \mathrm{Tr}\left[\Phi(\chi_M,\xi_M)^T\bar{\Psi}_F + \Phi(\chi_F,\xi_F)^T\bar{\Psi}_M\right]\right\rangle_E . \tag{3.92}$$

3.3.2 Initial conditions

We will consider the instantaneous quench of the Higgs potential at zero temperature. After the quench, the modes with dispersion relation $\omega_k'^2 = k^2 - \mu^2 < 0$ will experience a spinodal instability, and increase exponentially. Before the quench, the Higgs potential is chosen as,

$$V(t<0) = +\mu^2\phi^\dagger\phi + \lambda(\phi^\dagger\phi)^2, \tag{3.93}$$

with the quadratic term flipped, comparing with the final potential in (3.5). In practice, we initialize these modes, following [40]

$$\langle\phi_k\phi_k^\dagger\rangle = \frac{1}{2\omega_k}, \qquad \langle\dot{\phi}_k\dot{\phi}_k^\dagger\rangle = \frac{\omega_k}{2}, \tag{3.94}$$

with $\omega = \sqrt{k^2+\mu^2}$. The initialization of other Higgs modes is set to be zero [51]. The gauge filed is initialized according to the Gauss' law (3.89), which is first implemented in the momentum space and then transferred to the configuration space.

Fermions are initialized as free ones, and satisfy the Wilson-Dirac equation, of the form,

$$\left[\frac{1}{a_t}\gamma^0\tilde{\partial}_0 + \frac{1}{a}\gamma^i\tilde{\partial}_i + m + \frac{r_W}{2a}\partial_i\partial_i'\right]\psi = 0, \tag{3.95}$$

where the forward and backward differences are defined as

$$\partial_\mu\psi(x) \equiv \psi(x+\mu) - \psi(x), \qquad \partial_\mu'\psi(x) \equiv \psi(x) - \psi(x-\mu),$$

and the symmetric difference is their average

$$\tilde{\partial}_\mu\psi(x) \equiv \frac{1}{2}\left[\partial_\mu + \partial_\mu'\right]\psi(x) = \frac{1}{2}\left[\psi(x+\mu) - \psi(x-\mu)\right].$$

In particular, the second-order difference in the equation is written as

$$\partial_i \partial_i' \psi(x) = \sum_i \psi(x+i) - 2\psi(x) + \psi(x-i). \tag{3.96}$$

For a cubic lattice with the number of sites in each direction being N, we choose integers s_i and q_i, ranging from 0 to $N-1$, and denote the length and mode number by

$$x_i = s_i a, \qquad p_i = \left(q_i + \frac{1}{2}\right)\frac{2\pi}{Na}, \tag{3.97}$$

as well as the physical momentum and energy

$$\tilde{p}_i = \frac{\sin(p_i a)}{a}, \quad |\tilde{p}| = \sqrt{\tilde{p}_1^2 + \tilde{p}_2^2 + \tilde{p}_3^2}, \quad \omega_p = \sqrt{|\tilde{p}|^2 + \left(m + r_W \sum_i \frac{1-\cos(p_i a)}{a}\right)^2}.$$

In the temporal direction, we denote $t = n a_t$ and $e^{-iEa_t} = \left(\sqrt{1-\omega_p^2 a_t^2} - i\omega_p a_t\right)$. We therefore write the mode functions as

$$U_{p,s}(t,x) = e^{-iEt+ip.x} U_{p,s}, \qquad V_{-p,-s}(t,x) = e^{iEt+ip.x} V_{-p,-s}, \tag{3.98}$$

with the spinors

$$U_{p,s} = \frac{1}{\sqrt{2\omega_p}} \begin{pmatrix} -\sqrt{\omega_p - \sigma.\tilde{p}}\ \ \eta_s \\ \sqrt{\omega_p + \sigma.\tilde{p}}\ \ \eta_s \end{pmatrix} \qquad V_{-p,-s} = \frac{1}{\sqrt{2\omega_p}} \begin{pmatrix} \sqrt{\omega_p + \sigma.\tilde{p}}\ \ \eta_s \\ \sqrt{\omega_p - \sigma.\tilde{p}}\ \ \eta_s \end{pmatrix}. \tag{3.99}$$

As a result, in the vacuum state, the ensemble fermions after the rescaling are constructed as

$$\psi_M^j(t,x) = \frac{a^{3/2}}{\sqrt{2}V} \sum_p \left[\zeta_{p,s}^j U_{p,s}(t,x) + \eta_{-p,-s}^j V_{-p,-s}(t,x)\right], \tag{3.100}$$

$$\psi_F^j(t,x) = \frac{a^{3/2}}{\sqrt{2}V} \sum_p \left[\zeta_{p,s}^j U_{p,s}(t,x) - \eta_{-p,-s}^j V_{-p,-s}(t,x)\right], \tag{3.101}$$

with the spatial volume $V = a^3 N^3$ and the complex random numbers following

Gaussian distributions and having the ensemble average

$$\left\langle \zeta_{p,r}\zeta^{\dagger}_{p',s}\right\rangle_E = V\delta_{rs}\delta_{pp'}, \qquad \left\langle \eta_{p,r}\eta^{\dagger}_{p',s}\right\rangle_E = V\delta_{rs}\delta_{pp'}. \tag{3.102}$$

In practice, as discussed in section 2.4.2, in order to remove the temporal doublers, we set initially both $\psi_G(0,x)$ and $\psi_G(a_t,x)$ according to (3.100) and (3.101).

One can verify that the equal-time two-point correlation function in this convention becomes

$$D(t;x,y) = \frac{a^3}{V}\sum_p e^{ip.(x-y)}\frac{-i\gamma.\tilde{p}+m_p}{2\omega_p}, \tag{3.103}$$

with $m_p = \sqrt{\omega_p^2 - |\tilde{p}|^2}$. In the limit $N\to\infty$, the sums can be replaced by integrals, of the form,

$$D(t;x,y) = \int_{-\pi}^{\pi}\frac{d^3k}{(2\pi)^3}e^{ip.(x-y)}\frac{-i\gamma.\tilde{p}+m_p}{2\omega_p}, \tag{3.104}$$

where $k_i = ap_i$ and according to (3.97), the range of k_i can be chosen as $[0,\ 2\pi]$ or $[-\pi,\ \pi]$.

3.3.3 Counterterms

In the simulation, we also introduce counterterms to compensate the initial fermion backreaction. In the beginning, the initialized fermions are able to influence the gauge field and Higgs field through the backreaction, eventually reducing the gauge coupling constant and distorting the Higgs potential. Therefore the practical bosonic action will be a combination of the fermion backreaction and the original action $S_H + S_G$ which we write down in the beginning, that in such a sense, the gauge coupling constant and the Higgs potential are renormalized. It is practically more convenient to adopt counterterms $S_C(A_\mu,\phi)$ to cancel the leading fermion backreaction, in the following way

$$e^{-iS_C+\dots} = \int [D\bar{\psi}][D\psi]e^{iS_F+iS_Y}, \tag{3.105}$$

and as a result, the effective bosonic action is really $S_H + S_G$ in the interaction theory.

In our approach, the full action S_C is chosen in the continuum theory in the shape of

$$S_C = -\int d^4x \left[\frac{(Z_3-1)}{4g^2}F^a_{\mu\nu}F^{a,\mu\nu} + (Z_\phi - 1)D_\mu\phi^\dagger D^\mu\phi + \delta V(\phi)\right], \tag{3.106}$$

or on the lattice,

$$\begin{aligned} S_C =& \sum_{x,t}(Z_3-1)\beta_G^t \sum_i \left(1 - \frac{1}{2}\mathrm{Tr}\left[U_{0i}(x)\right]\right) - (Z_3-1)\frac{\beta_G^s}{2}\sum_{ij}\left(1-\frac{1}{2}\mathrm{Tr}\left[U_{ij}(x)\right]\right) \\ &+ (Z_\phi - 1)\frac{\beta_H^t}{2}\mathrm{Tr}\left[(D_0\Phi)^\dagger D_0\Phi\right] - (Z_\phi-1)\frac{\beta_H^s}{2}\mathrm{Tr}\left[(D_i\Phi)^\dagger D_i\Phi\right] - \beta_R\delta V(\Phi). \end{aligned}$$

An equation of Z_3 can be obtained by a derivative of (3.105) with respect to the gauge field, of the form,

$$\begin{aligned} &\left(\frac{a}{a_t}\right)^2 \frac{4(Z_3-1)}{g^2}\left(E_i^a(x) - E_i^a(x-0) + \frac{4(Z_3-1)}{g^2}\sum_j \left[\ {}^1U_{ij}^a(x) - \ {}^3U_{ij}^a(x-j)\right]\right. \\ =& i\mathrm{Tr}[i\sigma^a U_i(x)G(x+i,x)\gamma^i] + i\mathrm{Tr}[U_i^\dagger(x)i\sigma^a G(x,x+i)\gamma^i] - ir_w\mathrm{Tr}[i\sigma^a U_i(x)G(x+i,x)] \\ &+ ir_w\mathrm{Tr}[U_i^\dagger(x)i\sigma^a G(x,x+i)]. \end{aligned} \tag{3.107}$$

where the Higgs field is set to zero in the expression for simplicity and the full fermion propagator is defined as,

$$G_{\alpha\beta}(x,y) = i\langle \mathrm{T}\psi_\alpha(x)\bar{\psi}_\beta(y)\rangle, \tag{3.108}$$

with 4-vector x and y. Similarly, a derivative of (3.105) with respect to the Higgs field, given $A_\mu = 0$, will provide

$$\begin{aligned} &-(Z_\phi-1)\beta_H^t\partial_0'\partial_0\Phi + (Z_\phi-1)\beta_H^s\partial_i'\partial_i\Phi - \frac{1}{2}\beta_R\delta V'(\Phi) \\ &= \frac{1}{2}\beta_Y k^b\bar{\Psi}k^b(\chi,\xi)^T + \frac{1}{2}\beta_Y k^b(\bar{\chi},\bar{\xi})(k^b)^\dagger\Psi, \end{aligned} \tag{3.109}$$

with $\delta V'$ indicating the derivative of δV with respect to Φ. Because fermions fields χ, ξ and Ψ are coupled through the Yukawa interaction, one needs to treat $(\Psi_u, \Psi_d, \chi, \xi)^T$ as a whole, and calculate its 4×4 Green function to solve equation (3.109). In practice, under the assumption that there exists only a ϕ_0 component of the Higgs field, this 4×4 Green function is then diagonalizable, by choosing the

mass eigenstates

$$\Omega_1 = \frac{\Psi_u + \chi}{\sqrt{2}}, \qquad \Omega_1' = \frac{\Psi_d + \xi}{\sqrt{2}},$$
$$\Omega_2 = \frac{\Psi_u - \chi}{\sqrt{2}}, \qquad \Omega_2' = \frac{\Psi_d - \xi}{\sqrt{2}}.$$

Moreover, Ω and Ω' states are actually degenerate. Thus one can simply denote $G_1(x,y)$ and $G_2(x,y)$ as the Green functions of $\Omega_1(\Omega_1')$ and $\Omega_2(\Omega_2')$, and then rewrite (3.109) as

$$\begin{aligned} &-(Z_\phi - 1)\beta_H^t \partial_0' \partial_0 \phi_0 + (Z_\phi - 1)\beta_H^s D_i' D_i \phi_0 - \frac{1}{2}\beta_R \delta V'(\phi_0) \\ &\quad = i\beta_Y \mathrm{Tr}[G_1(x,x) - G_2(x,x)]. \end{aligned} \tag{3.110}$$

During the simulations, the shape of δV that we choose is,

$$\delta V(\phi) = \frac{ct_1}{2}\phi^2 + \frac{ct_2}{4}\phi^4, \tag{3.111}$$

and to get ct_1 and ct_2, one can simply set ϕ constant in (3.110), which then becomes easy to solve to any order of ϕ. Dimensional analysis shows that ct_1 depends on the lattice spacing quadratically, and ct_2 logarithmically.

Similarly, both Z_3 and Z_ϕ are also expected to exhibit a logarithmic dependence of lattice spacing. To find them, we solve the equation (3.107) and (3.109) separately up to the first-order perturbation of A_μ and ϕ. With our choice of lattice parameters, we find $0.98 < Z_3 < 0.99$, and $Z_\phi \sim 1$. By recalling, $g = \sqrt{Z_3} g_B$, where g_B is the coupling constant when only the gauge field exists and g the coupling constant in the interacting theory, the calculation corresponds to the fact that the screening is one of results of fermion backreaction to the pure Yang-Mills theory.

3.3.4 Quantum field perturbation in real-time simulations

In order to solve the coefficients of counterterms, we need to establish perturbation theory for the fermion Green function in real-time simulations. Formally, the perturbation expansion can be carried out in a similar way as continuum quantum field theory with Minkowski signature. While in practice, the differences come when one tries to implement the integral, for the integral on the lattice has finite interval of

integration, compared with the infinite range in the continuum theory, where the regularization is often prescribed as a remedy to the divergent integration.

To maintain the similarity to the continuum theory, we write the free fermion propagator in real-time simulations as,

$$G_0(x,y) = \int \frac{d^4p}{(2\pi)^4} e^{ip.(x-y)} G_0(p), \qquad G_0(p) = \frac{1}{i\gamma^\mu \tilde{p}_\mu + m_p}, \tag{3.112}$$

with the 4-vector product in the Minkowski space, for instance, $p.x = -p_0 t_x + p_1 x_1 + p_2 x_2 + p_3 x_3$, and

$$p_0 \in (-\frac{\pi}{a_t},\ \frac{\pi}{a_t}], \qquad p_i \in (-\frac{\pi}{a},\ \frac{\pi}{a}], \tag{3.113}$$

$$\tilde{p}_0 = \frac{\sin(p_0 a_t)}{a_t}, \qquad \tilde{p}_i = \frac{\sin(p_i a)}{a}, \tag{3.114}$$

where in fact, we will choose $\tilde{p}_0$ as the temporal variable of integration, therefore, $d^4p = d\tilde{p}_0 d^3p$. In the expression, we recover the dimensionality of operators, so that the dimension of the fermion Green function is three, as it is in the continuum theory. Up to first-order in A_μ, the full propagator $G(x,y)$ can be expanded in the following way,

$$G(x,y) = G_0(x,y) + i \int \frac{d^4p}{(2\pi)^4} \frac{d^4p'}{(2\pi)^4} e^{ip'.x} e^{ip.(x-y)} G_0(p+p') A_\mu(p') \Gamma^\mu(p+p',p) G_0(p), \tag{3.115}$$

To get this expression, we interpret the gauge link as $[U_\mu(x)-1] = -iA_\mu(x)$, $[U_\mu^\dagger(x)-1] = iA_\mu(x)$ to first-order in A_μ, and write the interaction vertex induced on the lattice as,

$$\Gamma^\mu(p+p',p) = \frac{\gamma^\mu}{2}[e^{-i(p_\mu+p'_\mu)} + e^{ip_\mu}] + \frac{r_w}{2}[e^{-i(p_\mu+p'_\mu)} - e^{ip_\mu}], \tag{3.116}$$

where the second term on the right-handed side should be omitted when $\mu = 0$, as only spatial Wilson terms are introduced. The perturbation expansion above respects the gauge transformation, in the sense that the Ward identity is fulfilled

$$i\sum_\mu (1 - e^{ip'_\mu})\Gamma^\mu(p+p',p) = -iG_0^{-1}(p+p') + iG_0^{-1}(p). \tag{3.117}$$

In the same way, the perturbation of the fermion Green function up to first-order in the Higgs field (ϕ_0), can be written as

$$G_1(x,y) = G_0(x,y) - \lambda_{\text{yuk}} \int_{-\pi}^{\pi} \frac{d^4p'}{(2\pi)^4} e^{ip'.x} \phi_0(p') \int \frac{d^4p}{(2\pi)^4} e^{ip.(x-y)} G_0(p+p') G_0(p), \tag{3.118}$$

$$G_2(x,y) = G_0(x,y) + \lambda_{\text{yuk}} \int_{-\pi}^{\pi} \frac{d^4p'}{(2\pi)^4} e^{ip'.x} \phi_0(p') \int \frac{d^4p}{(2\pi)^4} e^{ip.(x-y)} G_0(p+p') G_0(p), \tag{3.119}$$

for $\Omega_1(\Omega_1')$ and $\Omega_2(\Omega_2')$ separately.

When calculating the integrals above with Minkowski signature, one will encounter poles in the fermion propagators. And different choices of open contour integration can lead to the definition of Feynman, advanced and retarded Green functions, and closed contour integrals will give the density function and statistical propagator. We will eventually introduce an $i\epsilon$ term in the denominator of the propagator, of the form, $i\gamma^\mu \tilde{p}_\mu + m_p + i\epsilon$, similarly as Feynman did in the continuous theory. Also, we rescale the temporal component p_0 into a dimensionless variable k_0

$$p_0 = \frac{1}{a_t} k_0, \qquad \tilde{p}_0 = \frac{1}{a_t} \sin k_0, \qquad \int \frac{d\tilde{p}_0}{2\pi} = \frac{1}{a_t} \int_{-\pi}^{\pi} \frac{dk_0}{2\pi} \cos k_0, \tag{3.120}$$

and similarly for spatial variables

$$p_i = \frac{1}{a} k_i, \qquad \tilde{p}_i = \frac{1}{a} \sin(k_i), \qquad \int \frac{dp_i}{2\pi} = \frac{1}{a} \int_{-\pi}^{\pi} \frac{dk_i}{2\pi}. \tag{3.121}$$

For instance, the Green function at equal-time then becomes

$$\begin{aligned} G_0(x,y)\Big|_{t_x=t_y} &= \int \frac{d^4p}{(2\pi)^4} e^{ip.(x-y)} \frac{1}{i\gamma^0 \tilde{p}_0 + i\gamma.\tilde{p} + m_p + i\epsilon} \\ &= \frac{a_t}{a^3} \int_{-\pi}^{\pi} \frac{d^3k}{(2\pi)^3} \int_{-\pi}^{\pi} \frac{dk_0}{2\pi} e^{ip.(x-y)} \frac{i\gamma.\tilde{p} - m_p}{\sin^2 k_0 - \omega_p^2 a_t^2 + i\epsilon} \cos k_0 \\ &= \frac{i}{a^3} \int_{-\pi}^{\pi} \frac{d^3k}{(2\pi)^3} e^{ip.(x-y)} \frac{-i\gamma.\tilde{p} + m_p}{2\omega_p}, \end{aligned} \tag{3.122}$$

where now the dot product stands for the spatial 3-vector product. From the second

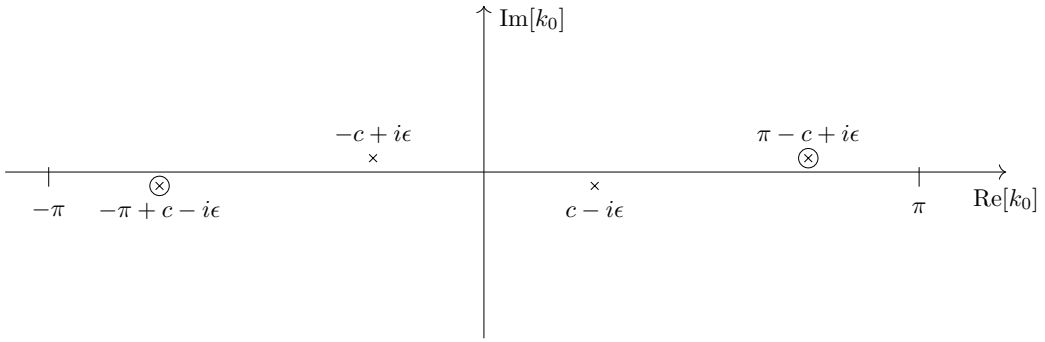


Figure 3.2. The integration ranging from -π to π. Because the integrand has a period with period 2π, points $-\pi$ and π are actually identical, so that the path of integration is really a closed line. The point $\pi - c + i\epsilon$ and $-\pi + c - i\epsilon$ refer to temporal doublers, which does not exist in practical simulations, therefore we drop the contribution from those two points in the contour integration.

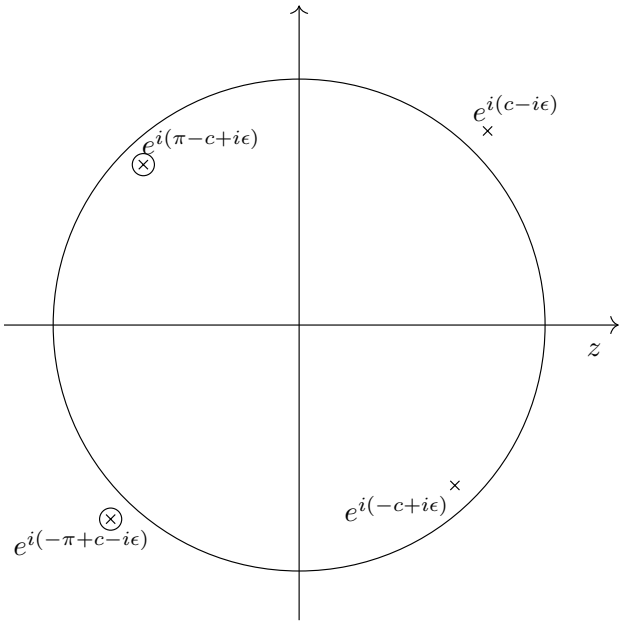


Figure 3.3. The circle $|z| = 1$ is the curve of integration. Similarly, we omit the point $e^{i(\pi-c+i\epsilon)}$ and $e^{i(-\pi+c-i\epsilon)}$, because they come from temporal doublers.

line to the third, the temporal integral is carried out in a manner

$$\int_{-\pi}^{\pi} \frac{dk_0}{2\pi} \frac{\cos k_0}{\sin^2 k_0 - \sin^2 c + i\epsilon} = -i\frac{1}{2\sin c}, \qquad \text{for} \quad c \in [0, \frac{\pi}{2}], \tag{3.123}$$

with the path of integration demonstrated in Fig 3.2. The result can be easily obtained via a substitution,

$$z = e^{ik_0}, \quad \sin k_0 = \frac{z - 1/z}{2i}, \quad [-\pi,\ \pi] \to |z| = 1, \tag{3.124}$$

and the new path of contour integration can be found in Fig 3.3. Notice in the integration, we ignore the contribution from temporal doublers, as in practical simulations those doublers will not be included.

The equal-time Green function in the form of (3.122) is consistent with the initial two-point function (3.104), which, if we restore its dimensions, is

$$D(t; x, y) = \frac{1}{a^3} \int_{-\pi}^{\pi} \frac{d^3k}{(2\pi)^3} e^{ip.(x-y)} \frac{-i\gamma.\tilde{p} + m_p}{2\omega_p}. \tag{3.125}$$

as their definitions in (3.50) and (3.108) dictates $iD(t; x, y) = G_0(x, y)|_{t_x = t_y = t}$.

3.4 Simulations and results

With ensemble fermions, we are going to simulate the cold electroweak transition, including the $SU(2)$ gauge field, Higgs field and one generation of fermions. The initial temperature is chosen as $T = 0$. For this reason, all fields are initialized as in the vacuum state, and hence the initial energy is merely in the form of Higgs potential energy. For most simulations, we will stick to the instantaneous quench transition, and therefore once simulations start, the Higgs field rolls down from the center of the potential. The IR modes of the Higgs field can experience a spinodal (tachyonic) instability, and increase exponentially. This will drive the system out of equilibrium. In the process, the Higgs potential energy will be transferred to its kinetic energy, as well as to the gauge field and fermions, to reheat the system. We are going to measure the fermion occupation number and accordingly extract the fermion temperature.

In addition, during the electroweak transition, the $B + L$ anomaly could also happen. If it occurs, we should observe the change in the baryon number as well

as in Chern-Simons number and Higgs winding number. But because we do not include any CP-violation source, the increase and decrease of the baryon number should be equally observed.

In the first place, it would important for us to test the validity of the ensemble fermions and to find out how many fermion realizations would be required in practice. To this end, we denote N_{qc} as the smallest N_q that can allow the dynamics and observables to converge. We will first decide N_{qc}.

3.4.1 Convergence of observables

Fig 3.4 illustrates a comparison of three different N_q: 1440, 2400, 9600. In the plots, the bosonic observables are separately the average Higgs squared $\langle\phi^2\rangle$, Chern-Simons number N_{CS}, Higgs winding number N_W and energy densities. During the comparison, other parameters are fixed, that $N = 32$, $\lambda_{\text{yuk}} = 0.03$ and $am_H = 0.42$. As we can conclude, the dynamics and the bosonic observables have already converged even with $N_q = 1440$. Here we take as a conservative choice, $N_{qc} = 2400$, and we find that this number is also safe for larger lattice, like $N = 48$. On the other hand, if we implement the mode function method, to get the same lattice size ($N = 32$) and fermion content, it would correspond to $N_q = 1{,}048{,}576$, that is 400 times larger than the ensemble fermion simulation.

But not all observable can converge quickly. In practice, (the only) one exception that we find is the fermion number which is defined as $N_f = (N_B + N_L)/2$. We demonstrate the convergence of the fermion number in Fig 3.5. A big N_q is always required in order to make the fermion number converge. But once the N_q is big enough, for instance, $N_q = 9600$ in the right-handed plot of Fig 3.5, the fermion number will follow closely the Chern-Simons number, as stated by the $B+L$ anomaly. This is due to the observable N_f being badly behaved, not the dynamics. Instead, other observables showed in the plot have already converged in Fig 3.5. In particular, we will conveniently use the Chern-Simon number N_{CS} to indicate the final baryon (lepton) number.

3.4.2 Fermion occupation number

We also study the difference caused by different Wilson parameters, with a comparison of energy densities illustrated in Fig 3.6. If assuming only the IR modes of

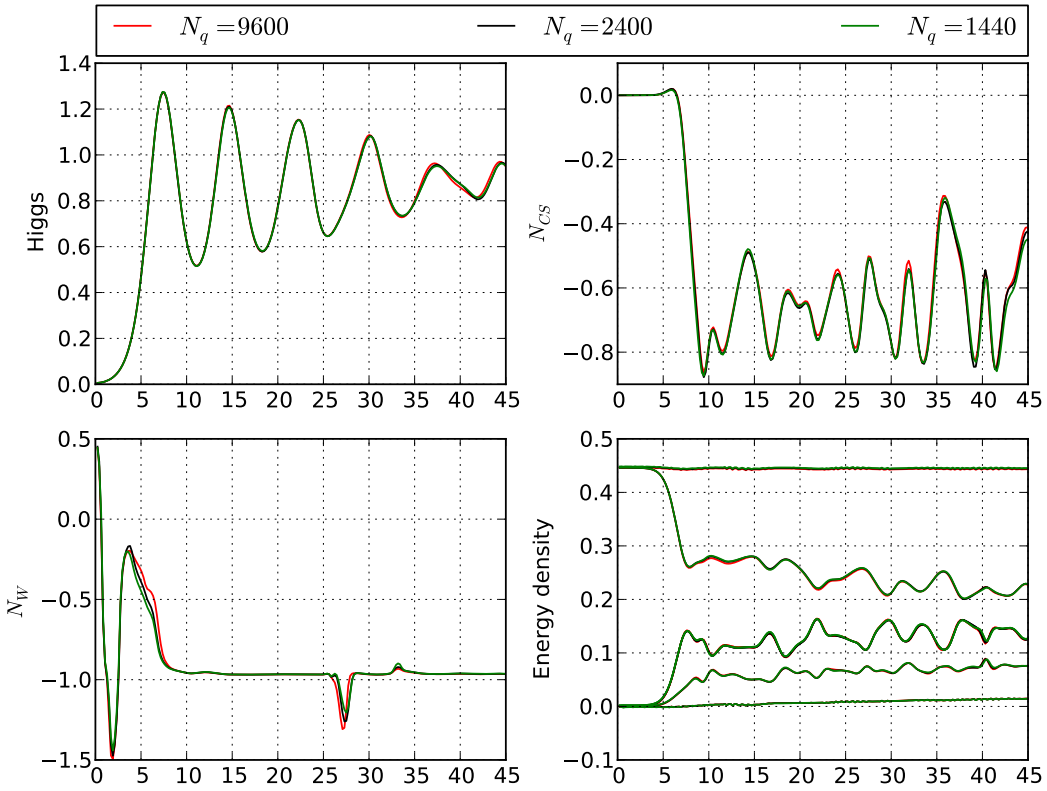


Figure 3.4. Convergence of Higgs ϕ^2, N_{CS}, N_W and energy densities with N_q. $N = 32$, $\lambda_{\rm yuk} = 0.03$ and $am_H = 0.42$. The x-axis is the time rescaled by m_H.

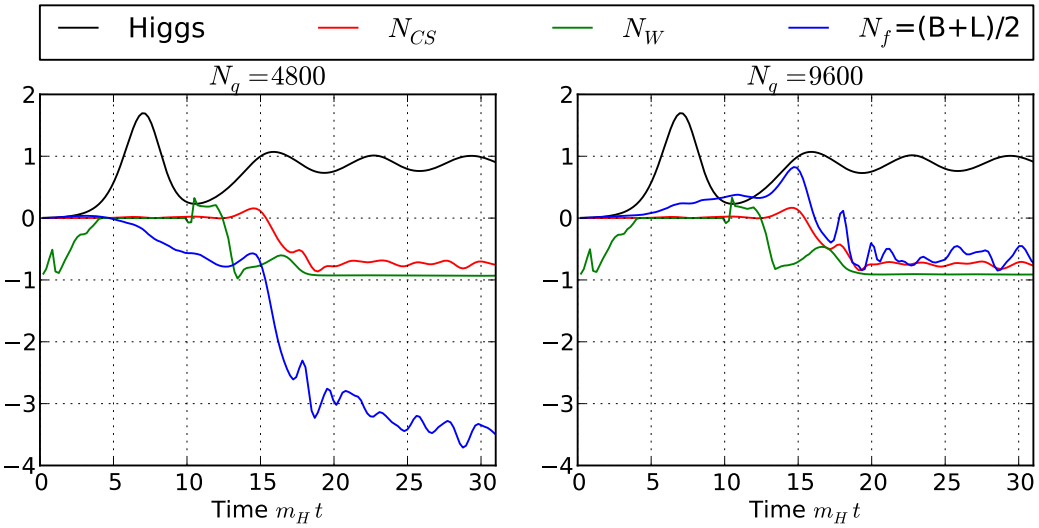


Figure 3.5. The convergence of the baryon (or fermion) number requires much larger N_q.

fermions are excited in the simulation, one would expect the fermion energy when $r_W = 0$ would be roughly 8 times larger than the energy when $r_W = 0.5$, as there are eight species of fermions, including 7 doublers, having light masses, while when $r_W = 0.5$, those 7 doublers become modes of heavy masses, and never excited during simulations.

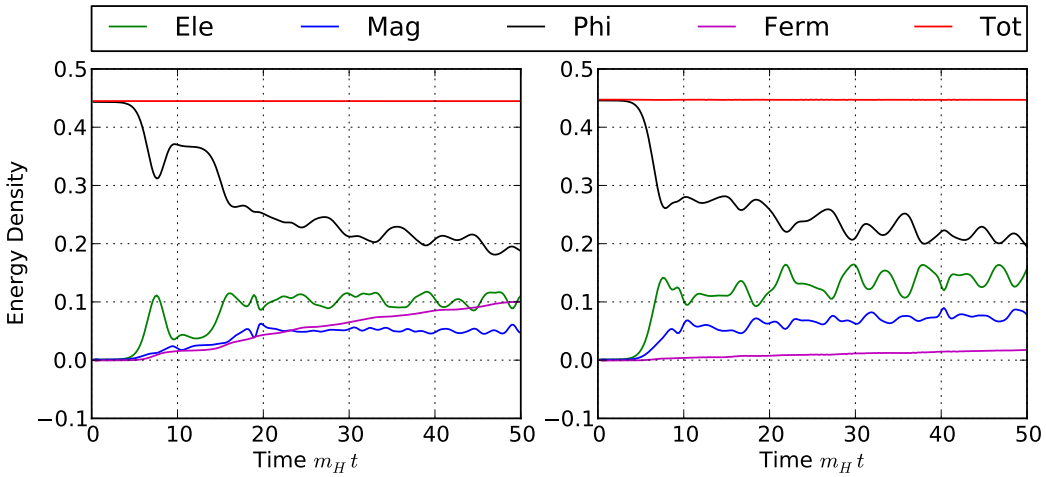


Figure 3.6. Different energy component in a tachyonic electroweak transition. The Wilson coefficient r_W is 0 in the left plot, and 0.5 in the right plot. The energy density is scaled by m_H^4. More energy is transferred to the fermion when the Wilson term is small. The final fermion energy of $r_W = 0$ is about 7 times larger than the finial fermion energy of $r_W = 0.5$.

As in section 3.1.3, we can calculate the fermion occupation number from the two-point correlation function. For gauge singlets, we define separately

$$D_\xi(t;x,y) = \langle 0|\mathrm{T}\xi(x,t)\bar{\xi}(y,t)|0\rangle, \quad D_\chi(t;x,y) = \langle 0|\mathrm{T}\chi(x,t)\bar{\chi}(y,t)|0\rangle. \tag{3.126}$$

For the $SU(2)$ doublet, a gauge-invariant correlation function should be written as

$$D_\Psi(t;x,y) = \langle 0|\mathrm{T}\Psi(x,t)\bar{\Psi}(y,t)U(t;y,x)|0\rangle, \tag{3.127}$$

where $U(t;y,x)$ is the gauge link connecting y and x at the time t. Including the gauge link in the correlation function of the doublet makes the calculation complicated, and theoretically there are ambiguities in choosing the link path in 3+1 dimension. Furthermore, because of the Yukawa interaction terms, the fermion $SU(2)$ doublet and singlets are not the eigenstates after the spontaneous symmetry breaking. Therefore, we will not in practice consider the gauge invariant two-point function, but instead we will chose unitary gauge fixing, where the mass eigenstates

can be found as:

$$\Omega_1 = \frac{1}{\sqrt{2}}(\Psi_u + \xi), \qquad \Omega_2 = \frac{1}{\sqrt{2}}(\Psi_d + \chi), \tag{3.128}$$

$$\Omega_1' = \frac{1}{\sqrt{2}}(\Psi_u - \xi), \qquad \Omega_2' = \frac{1}{\sqrt{2}}(\Psi_d - \chi), \tag{3.129}$$

with the up and down parts of the gauge doublet Ψ_u and Ψ_d.

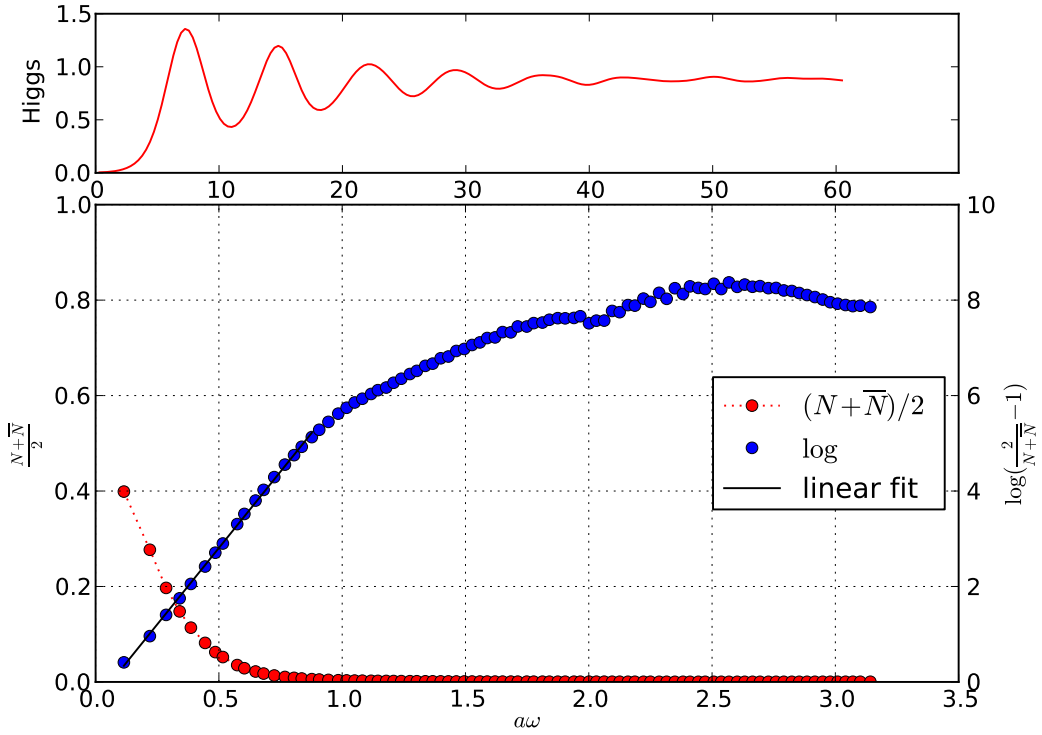


Figure 3.7. The fermion particle spectrum (bottom panel). The red line is the average particle number, the blue line the derived $\log(1/N_{\rm av} - 1)$, so that the slope is the inverse of the temperature. The black line is the linear fit of the lower energy range. For the linear fitting, we select the range $a\omega \in [0, 0.9]$. The upper plot shows the time evolution of the Higgs field observable and the time ($m_H t = 60.795$) at which the spectrum is computed. $N = 48$, $am_H = 0.63$ and $\lambda_{\rm yuk} = 0.03$.

Similar to (3.55), we assume the gamma-matrix expansion,

$$D(p;t) = [1 - N(p;t) - \bar{N}(-p;t)]\frac{-ip.\gamma + m(p;t)}{2\omega(p;t)} + ..., \tag{3.130}$$

where now the mass is also a function of time t, so is the energy. One can subsequently calculate

$$F = \mathrm{Tr}[D(p;t)], \qquad V = \mathrm{Tr}[i\frac{\gamma.p}{p}D(p;t)],, \tag{3.131}$$

and finally obtain the averaged occupation number and energy of the mode in the form of,

$$N_{\rm av}(p;t) = \frac{1}{2} - \text{sign}\,(V)\,\frac{\sqrt{F^2+V^2}}{4}, \quad \omega(p;t) = \sqrt{\frac{4(1-2N_{\rm av})^2p^2}{V^2}}, \tag{3.132}$$

given the on-shell condition $\omega(p;t) = \sqrt{p^2 + m^2(p;t)}$.

The averaged (anti-)particle number $N_{\rm av} = (N + \bar{N})/2$ against the practical energy $\omega = \sqrt{m^2 + p^2}$ at the later time of the evolution is plotted in Fig 3.7, where one can see the distribution in IR region follows precisely a Fermi-Dirac distribution. As a result, we can in practice measure the effective temperature T and chemical potential μ of fermions, by fitting the distribution to the form

$$\log\left(\frac{1}{N_{\rm av}} - 1\right) = \frac{\omega - \mu}{T}. \tag{3.133}$$

3.4.3 Fermion temperature

We compare the extracted temperature and chemical potential in Fig 3.8, with different types of correlation function, including the two-point function of mass eigenstate under the unitary gauge fixing, the two-point function of singlet $D_\xi(t;x,y)$, and the two-point function of the doublet $D_\Psi(t;x,y)$ but without the gauge link. In the beginning of the electroweak transition, the system is in an out-of-equilibrium state. We would not expect the existence of either well established Fermi-Dirac distribution or properly defined temperature or chemical potential. We can see in the plot the big changes during the time interval $[0,\ 10]$ existing in the observables extracted from D_ξ and D_ψ, While comparatively, the observables extracted from the unitary-gauge-fixing correlation function behave more smoothly, and therefore, we will stick to the choice afterwards.

We find in simulations that the fermion temperature and chemical potential converge fast with N_q, as shown in Fig 3.9. As one can conclude, not all fermionic observable converges as badly as the fermion number.

We also consider the impact of fermion masses on the finial temperature and chemical potential. The result is shown in Fig 3.10, with λ_{yuk} being 0.1, 0.03 and 0 individually, corresponding to fermion masses of $m_f = 17$, 5 and 0 GeV respectively. As a result, all masses of Standard Model fermions can be covered in the simulations,

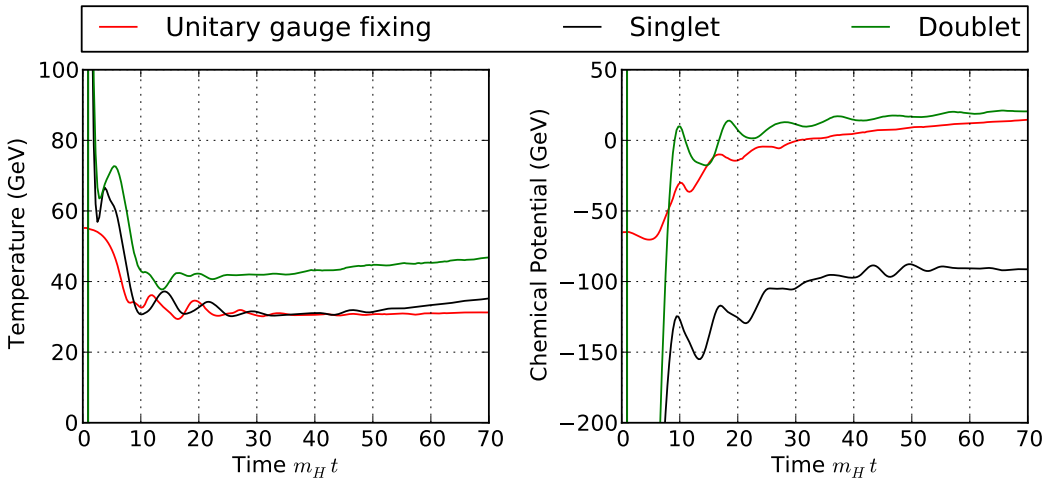


Figure 3.8. Three definitions of the temperature and chemical potential. The red line is extracted from the mass eigenstate (Ω_1) after the unitary gauge fixing. The singlet and doublet are extracted from the gauge singlet (ξ) and gauge doublet (Ψ_u) directly. $N = 48$, $N_q = 2400$, $\lambda_{\rm yuk}$=0.03 and $am_H = 0.63$.

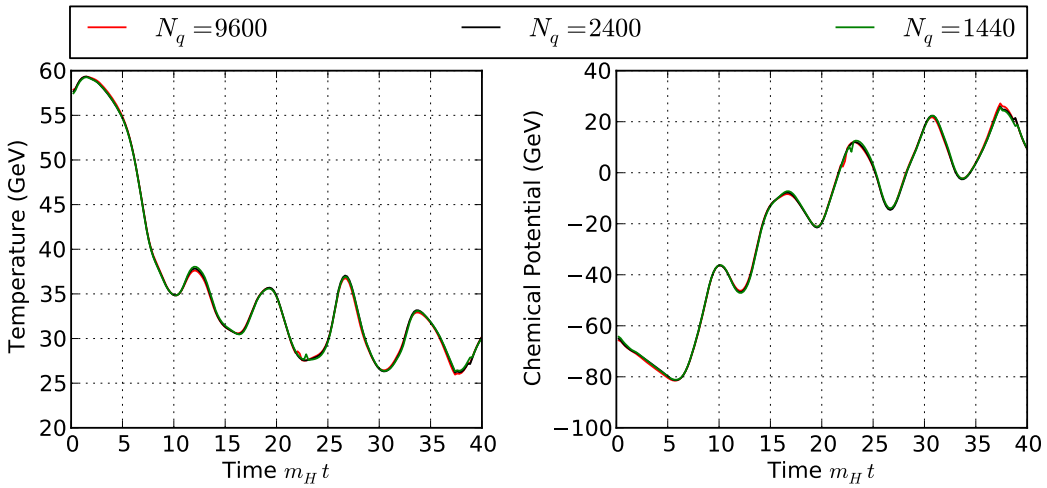


Figure 3.9. Convergence of the temperature and chemical potential with N_q. $N = 32$, $\lambda_{\rm yuk} = 0.03$ and $am_H = 0.42$.

except the top quark's, which would require $\lambda_{yuk} \sim 1$.

Up to now, we performed all simulations with an instantaneous quench transition. We further introduce a quench time τ_Q to parameterize the change of Higgs potential,

$$V(\phi) = \mu^2_{\rm eff}(t)\phi^\dagger\phi + \lambda(\phi^\dagger\phi)^2, \tag{3.134}$$

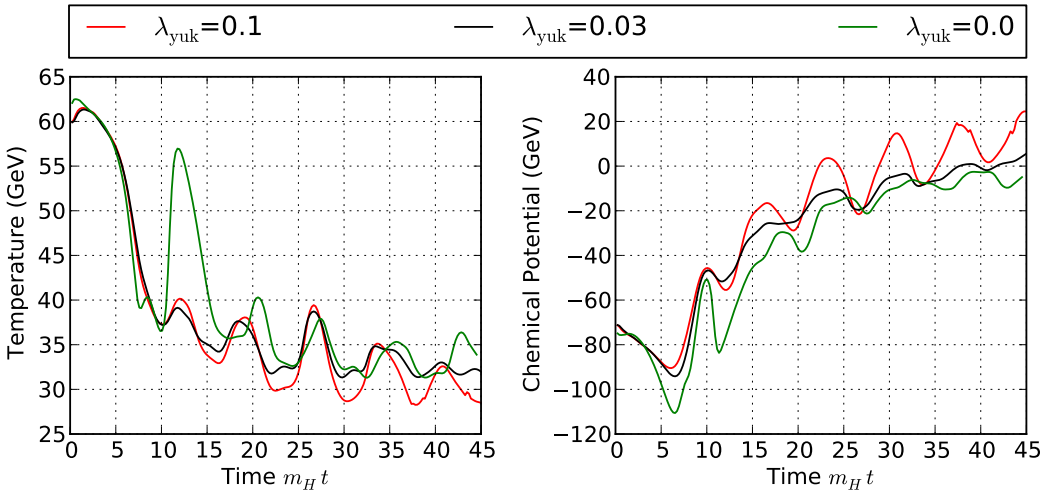


Figure 3.10. The effective temperature and chemical potential for different Yukawa couplings $\lambda_{\rm yuk} = 0.1$, 0.03 and 0, correspond to fermion masses of $m_f = 17$, 5 and 0 GeV respectively. $N_q = 2400$, $N = 32$, and $am_H = 0.42$.

with the coefficient of the quadratic term flipping its sign, in the shape of

$$\begin{aligned} \mu^2_{\rm eff}(t) =& \mu^2 \left(1 - \frac{2t}{\tau_Q}\right), \qquad t < \tau_Q, \\ =& -\mu^2, \qquad t > \tau_Q. \end{aligned} \tag{3.135}$$

We choose separately τ_Q =0, $15/m_H$ and $30/m_H$, and for each choice, we in addition average over 8 realizations of bosonic fields. In Fig 3.11 is statistical result of the temperature and chemical potential with $\tau_Q = 30/m_H$.

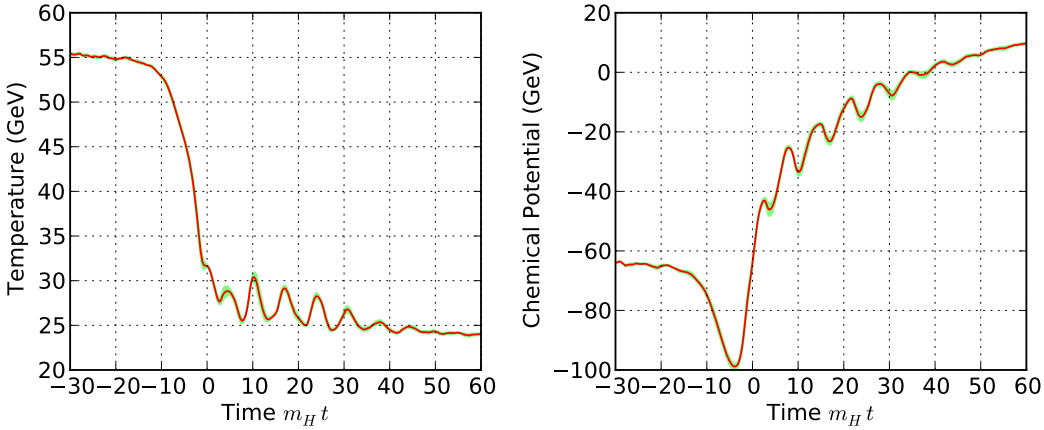


Figure 3.11. The effective temperature and chemical potential for a $\tau_Q = 30/m_H$ quench. Green bands denote statistical errors (1σ), over 8 bosonic realisations.

As the $B + L$ anomaly is created mainly during the first or second period of the

Higgs field oscillation, we measure individually the fermion temperatures at the first and second time the Higgs field rolling back to the minimum in the plot of $\langle\phi^2\rangle$, as well as at the late time. A comparison among different quench times is displayed in Fig 3.12, where a simple extrapolation to large quench time suggests that to reach the required 1 GeV by the Standard Model Cold Electroweak Baryogenesis [68], the quench time $\mu_Q \sim 150/m_H$, which would be too long to have a violent out-of-equilibrium phase transition, so that no efficient baryon-antibaryon asymmetry.

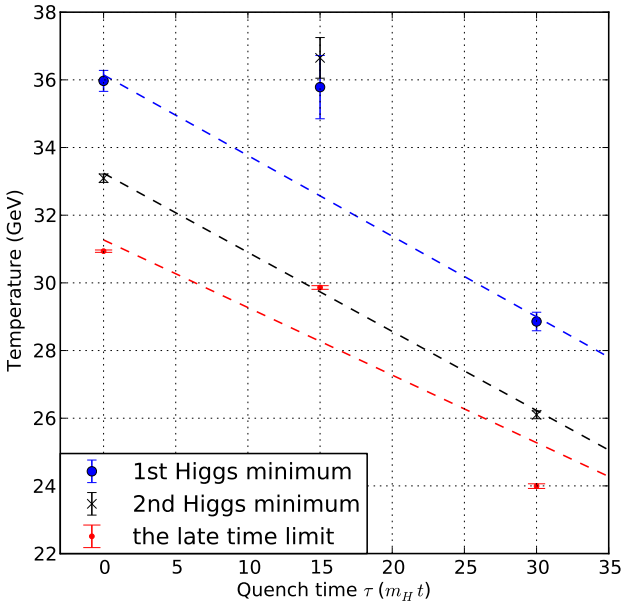


Figure 3.12. The first and second Higgs minimum correspond to the first and second time the Higgs field rolling back to the minimum of the average Higgs field squared. Each point is the statistical result of 8 runs, with the error bar stands for σ confidential interval. The statistical error for the late time limit is smaller than 0.2 GeV.

3.5 Conclusion

In summary, we have gradually developed real-time lattice simulations for the cold electroweak transition, including the $SU(2)$ gauge field, Higgs field and one generation of fermions. In practice, we implemented the ensemble fermions, and found the dynamics and most observables can converge with the order of 2000 realizations of fermion fields. To get similar results, the mode function method would consume 400 times larger storage space. We have also established a proper way to calculate the counterterms for real-time simulations and kept the renormalization on the lattice

under control.

The scenario that we have simulated corresponds to a preheating period in Cold Electroweak Baryogenesis, and the Higgs quench transition is triggered by its interaction with the inflaton [53, 56]. In the period, the energy is transferred from the inflaton to the Higgs field, and then to other Standard Model particles. And it is the last part that we have put into the simulation. A low temperature (of order of 1 GeV at most) is required in order to have the Standard Model baryogenesis. We have in practice measured the fermion temperature and found it never below 20 GeV. Thus, we can indirectly rule out the Standard Model CP-violation as the origin of the baryon asymmetry of the Universe. For this reason, we have to recruit new CP-violation from physics beyond the Standard Model to achieve a viable baryogenesis.

In simulations, we have observed that the $B + L$ anomaly could be accurately produced, with the Chern-Simons number, baryon(lepton) number and the Higgs winding number pointing consistently at the same state. In addition, the out-of-equilibrium can also be achieved during the electroweak transition, as a result of the spinodal instability in Higgs IR modes. To satisfy Sakharovs three necessary conditions, we further need to include CP-violation.

Chapter 4

Baryogenesis in the Two-Higgs Doublet Model

The chapter is dedicated to introducing CP-violation to real-time simulations and subsequently to measure the baryon asymmetry via a statistical analysis. We learned from the last chapter that the $B+L$ anomaly could be accurately reproduced in real-time simulations, and we go further in this chapter to include new terms which can ultimately violate CP-symmetry. As a result, Sakharov's three necessary conditions for a successful baryogenesis, namely, (1) baryon number non-conservation; (2) C and CP-violation; (3) out-of-equilibrium state, could be met simultaneously in our first-principle simulations. We will not introduce here three generations of fermions to replicate the CKM matrix, as it might provide too small CP-violation to explain the observed baryon asymmetry of the Universe. In the reduced Standard Model (3.5) with one generation of fermions, there is no CP-violation, albeit separate C and P symmetry are violated maximally by the fermion action. We will consider a minimal extension of the Standard Model, by introducing another Higgs doublet, and eventually obtain CP-violation as a result of including extra C-violating terms in the two-Higgs potential.

4.1 Continuum action

As a consequence of the extra Higgs doublet, four scalars, two neutral and two charged Higgs bosons, will be added to the particle spectrum of the Standard Model (for more experimental constraints on these extra scalars, see [67, 80]). Based on the

reduced Standard Model introduced in (3.5), and with modifications on the Higgs action and Yukawa interaction to incorporate the Two-Higgs Doublet model, we write the continuum action in the form of

$$\begin{aligned} S = -\int d^4x \Big[& \frac{1}{4g^2} F^a_{\mu\nu} F^{a,\mu\nu} + (D_\mu \phi_1)^\dagger (D^\mu \phi_1) + (D_\mu \phi_2)^\dagger (D^\mu \phi_2) \\ & + \bar{q}_L \gamma^\mu D_\mu q_L + \bar{u}_R \gamma^\mu \partial_\mu u_R + \bar{d}_R \gamma^\mu \partial_\mu d_R \\ & + \bar{l}_L \gamma^\mu D_\mu l_L + \bar{\nu}_R \gamma^\mu \partial_\mu \nu_R + \bar{e}_R \gamma^\mu \partial_\mu e_R \\ & + V(\phi_1, \phi_2) + Y(q, l, \phi_1, \phi_2) \Big], \end{aligned} \tag{4.1}$$

where the Higgs potential $V(\phi_1, \phi_2)$ and Yukawa interaction $Y(q, l, \phi_1, \phi_2)$ will be specified in following sections.

We continue to adopt the convention for Higgs fields

$$\Phi_1(x) = \left(\tilde{\phi}_1(x), \phi_1(x)\right), \quad \Phi_2(x) = \left(\tilde{\phi}_2(x), \phi_2(x)\right), \tag{4.2}$$

with $\tilde{\phi}_i = i\sigma\phi_i^\star$, and for the redefined fermionic fields,

$$\begin{aligned} \Psi_L =& q_L, & \Psi_R =& -i\sigma^2\gamma^2 l_L^\star, \\ \chi_L =& -\gamma^2 e_R^\star, & \chi_R =& u_R, \\ \xi_L =& \gamma^2 \nu_R^\star, & \xi_R =& d_R. \end{aligned} \tag{4.3}$$

As they were in the last chapter, the definition of baryon current and lepton current are the same, of the form,

$$\begin{aligned} j_b^\mu &= i\left[\bar{q}_L \gamma^\mu q_L + \bar{u}_R \gamma^\mu u_R + \bar{d}_R \gamma^\mu d_R\right] = i\bar{q}\gamma^\mu q, \\ j_l^\mu &= i\left[\bar{l}_L \gamma^\mu l_L + \bar{\nu}_R \gamma^\mu \nu_R + \bar{e}_R \gamma^\mu e_R\right] = i\bar{l}\gamma^\mu l, \end{aligned} \tag{4.4}$$

which correspond to the chiral current of the redefined fields, through the relation,

$$j_5^\mu = i\left[\bar{\Psi}\gamma^\mu\gamma^5\Psi - \bar{\chi}\gamma^\mu\gamma^5\chi - \bar{\xi}\gamma^\mu\gamma^5\xi\right] = j_b^\mu + j_l^\mu. \tag{4.5}$$

The $B + L$ anomaly is still present in the theory, therefore

$$N_B(t) - N_B(0) = N_L(t) - N_L(0) = N_{CS}(t) - N_{CS}(0) = \int_0^t d\tau \int d^3x \frac{1}{32\pi^2} \epsilon^{\mu\nu\rho\sigma} \mathrm{Tr}\left[F_{\mu\nu} F_{\rho\sigma}\right], \quad (4.6)$$

where $N_B = \int d^3x j_b^0$ is the total baryon number, $N_L = \int d^3x j_l^0$ the total lepton number and N_{CS} the Chern-Simons number. We now have two winding numbers, defined separately by each Higgs field,

$$N_W^1 = -\frac{1}{24\pi^2} \int \mathrm{Tr}\left[d\hat{\Phi}_1 \hat{\Phi}_1^{-1} \wedge d\hat{\Phi}_1 \hat{\Phi}_1^{-1} \wedge d\hat{\Phi}_1 \hat{\Phi}_1^{-1}\right],$$
$$N_W^2 = -\frac{1}{24\pi^2} \int \mathrm{Tr}\left[d\hat{\Phi}_2 \hat{\Phi}_2^{-1} \wedge d\hat{\Phi}_2 \hat{\Phi}_2^{-1} \wedge d\hat{\Phi}_2 \hat{\Phi}_2^{-1}\right]. \quad (4.7)$$

In the vacuum state, these topological numbers are forced to the same value, precisely, $N_W^1 = N_W^2 = N_{CS}$.

4.1.1 Higgs potential and Yukawa interaction

Higgs potential

The standard two-Higgs scalar potential [80] can be written as

$$\begin{aligned} V(\phi_1, \phi_2) = &-\frac{\mu_{11}^2}{2}(\phi_1^\dagger \phi_1) - \frac{\mu_{22}^2}{2}(\phi_2^\dagger \phi_2) - \frac{\mu_{12}^2}{2}(\phi_1^\dagger \phi_2) - \frac{\mu_{12}^{2,\star}}{2}(\phi_2^\dagger \phi_1) \\ &+ \frac{\lambda_1}{2}(\phi_1^\dagger \phi_1)^2 + \frac{\lambda_2}{2}(\phi_2^\dagger \phi_2)^2 + \lambda_3(\phi_1^\dagger \phi_1)(\phi_2^\dagger \phi_2) + \lambda_4(\phi_2^\dagger \phi_1)(\phi_1^\dagger \phi_2) \\ &+ \frac{\lambda_5}{2}(\phi_1^\dagger \phi_2)^2 + \frac{\lambda_5^\star}{2}(\phi_2^\dagger \phi_1)^2, \end{aligned} \quad (4.8)$$

where we choose to put the coupling parameters $\lambda_{6,7}$ to zero for simplicity. The parameters μ_{12}^2 and λ_5 are allowed to be complex, and a simultaneous phase shift

$$\phi_1 \to e^{i\alpha}\phi_1, \quad \phi_2 \to e^{i\gamma}\phi_2, \quad \mu_{12}^2 \to e^{i(\alpha-\gamma)}\phi_2, \quad \lambda_5 \to e^{i2(\alpha-\gamma)}\lambda_5, \quad (4.9)$$

will leave action (not including the Yukawa interaction) invariant. The parameters μ_{12}^2 and λ_5 are also crucial in determining the Higgs vacuum expectation values. To show this, we denote the vacuum state, $\langle\phi_1\rangle = v_1$ and $\langle\phi_2\rangle = v_2$, where v_1 and v_2 are complex constants. The vanish of kinetic energy calls for $D_\mu v_1 = D_\mu v_2 = 0$, and therefore equations of motions become constraint equations. For instance, the

derivative of the potential with respect to $\phi_1^\dagger$ leads to

$$Av_1 + Bv_2 = 0, \tag{4.10}$$

with coefficients

$$A = -\frac{\mu_{11}^2}{2} + \lambda_1|v_1|^2 + \lambda_3|v_2|^2, \qquad B = -\frac{\mu_{12}^2}{2} + \lambda_4(v_2^\dagger v_1) + \lambda_5(v_1^\dagger v_2). \tag{4.11}$$

By multiplying the equation (4.10) with $v_1^\dagger$ and $v_2^\dagger$ separately, we have

$$A|v_1|^2 = Bv_1^\dagger v_2, \qquad Av_2^\dagger v_1 = B|v_2|^2, \tag{4.12}$$

which yields

$$|v_2^\dagger v_1| = |v_1||v_2|. \tag{4.13}$$

For this reason, we employ an angle θ and parameterize in the vacuum state the product

$$v_2^\dagger v_1 = |v_1||v_2|e^{i\theta}. \tag{4.14}$$

On the other hand, a mere complex conjugate provides

$$A|v_1|^2 = Bv_1^\dagger v_2 = B^\star v_2^\dagger v_1, \tag{4.15}$$

as both A and $|v_1|^2$ are real, and with a substitution of the expression of B, we eventually arrive at

$$\mathrm{Im}(\mu_{12}^2 e^{-i\theta}) = 2|v_1||v_2|\mathrm{Im}(\lambda_5 e^{-2i\theta}). \tag{4.16}$$

Accordingly, if $\mathrm{Im}(\mu_{12}^2) = 2|v_1||v_2|\mathrm{Im}(\lambda_5)$, both Higgs vevs v_1 and v_2 can be chosen real. Otherwise, there must exist the relative angle θ between them. We will stick to the maximal angle

$$\theta = \frac{\pi}{2}. \tag{4.17}$$

We also choose the magnitudes of vacuum expectation values as constants, in such a way,

$$|v_1| = 110 \text{ GeV}, \qquad |v_2| = 220 \text{ GeV}, \tag{4.18}$$

and specifically the vevs are related to the observed Higgs vacuum expectation value through the relation,

$$|v_1|^2 + |v_2|^2 = (246 \text{ GeV})^2, \tag{4.19}$$

in order to achieve the right masses for W and Z bosons. For the neutral Higgs bosons, we in practice choose the masses,

$$m_1 = 125 \text{ GeV}, \quad m_2 = 300 \text{ GeV}, \quad m_3 = 350 \text{ GeV}, \tag{4.20}$$

and for charged modes,

$$m_\pm = 400 \text{ GeV}. \tag{4.21}$$

These choices satisfy constraints from experiments [59, 71, 72, 75].

We aim to choose the potential under which sphaleron transition can occur easily. To this purpose, we scan the parameter space $(\mu, \alpha_1, \alpha_2)$, where $\mu^2 = \text{Re}(\mu_{12}^2)$ and $\alpha_{1,2}$ are mixing angles of the three neutral Higgs modes. The black dots on the left-handed plot refer to the parameter choice of (α_1, α_2) that has the center of the potential as a local maximum. For each possible parameter choice, we run 10 simulations without involving fermions, and then calculate average $|N_{CS}|$.

Fig 4.1 displays one of such scans with $\mu = 200$ GeV. The right-handed picture is the contour plot of the average $|N_{CS}|$, in which we eventually choose the most fertile site, $(\alpha_1, \alpha_2) = (0.314, -1.49)$. Accordingly, the coefficients in the potential are settled on to

$$\mu_{11}^2 = (233 \text{ GeV})^2, \qquad \mu_{22}^2 = (311 \text{ GeV})^2, \qquad \mu_{12}^2 = (78.6 \text{ GeV})^2 + i(200 \text{ GeV})^2, \tag{4.22}$$

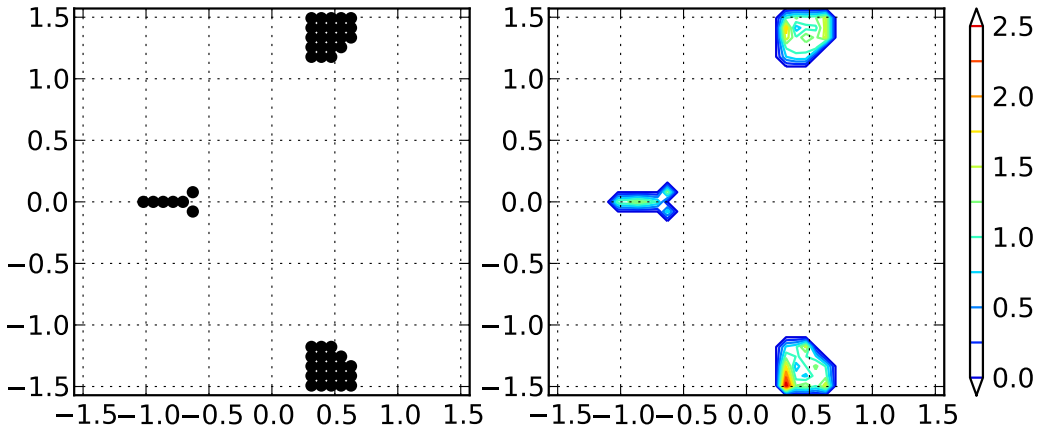


Figure 4.1. $\mu = 200$ GeV. The x-axis is α_1, y-axis α_2. We scan the parameter space (α_1, α_2) with a resolution of 40×40. On the left-handed plot, each black dot refers to a parameter choice that could provide the original point of the two-Higgs potential being a local maximum. With each possible parameter choice, we perform 10 simulations to calculate the sphaleron transition rate. The right-handed plot is the contour plot of the sphaleron rate, with the color bar indicating the average $|N_{CS}|$. The left-handed plot has a reflection symmetry along $\alpha_2 = 0$. But such symmetry has not been preserved on the right-handed plot.

and

$$\lambda_1 = 5.2, \qquad \lambda_2 = 2.0, \qquad \lambda_3 = 5.1, \qquad \lambda_4 = -4.2, \qquad \lambda_5 = -0.56 + i0.26. \tag{4.23}$$

The C-symmetry will be violated, due to the complex μ_{12}^2 and λ_5 in the Higgs potential, which now have non-zero phase arguments,

$$\mathrm{Arg}(\mu_{12}^2) = 0.45\pi, \qquad \mathrm{Arg}(\lambda_5) = -0.14\pi, \tag{4.24}$$

and there is no chance to make both parameters real by a phase shift of Higgs fields. In Fig 4.2, we show the contour plot of the potential in the $|v_1|$, $|v_2|$ plane. The center of the potential has energy density

$$V_0 = V(\phi_1 = \phi_2 = 0) - V(v_1, v_2) = (174 \text{ GeV})^4. \tag{4.25}$$

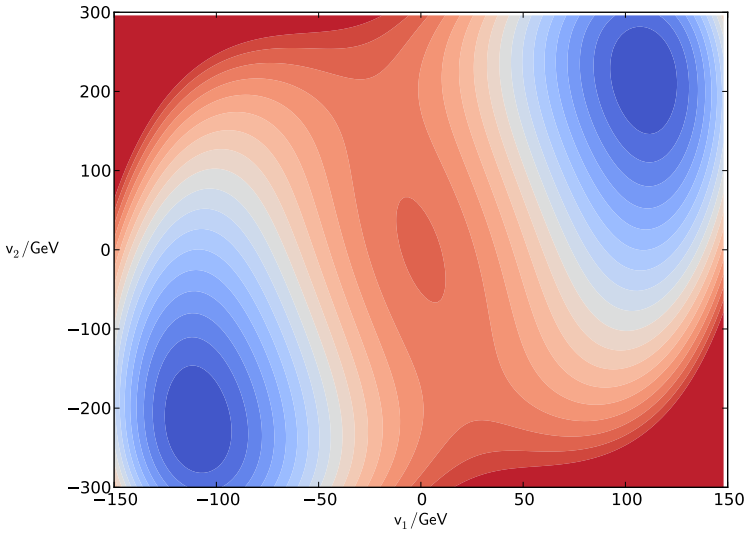


Figure 4.2. The Higgs potential as a function of the unitary gauge Higgs field components $|v_1|$, $|v_2|$. The two degenerate minima are at $(v_1, v_2) = (\pm 110, \pm 220)$ GeV.

With the Higgs matrix $\Phi_i(x) = \left(\tilde{\phi}_i(x), \phi_i(x)\right)$, it is easy to show,

$$\begin{aligned}\phi_1^\dagger \phi_2 &= \frac{1}{2}\mathrm{Tr}\left[\Phi_1^\dagger \Phi_2\right] + i\frac{1}{2}\mathrm{Tr}\left[\Phi_1^\dagger \Phi_2 i\sigma_3\right], \\ \phi_2^\dagger \phi_1 &= \frac{1}{2}\mathrm{Tr}\left[\Phi_1^\dagger \Phi_2\right] - i\frac{1}{2}\mathrm{Tr}\left[\Phi_1^\dagger \Phi_2 i\sigma_3\right],\end{aligned} \tag{4.26}$$

as well as

$$\Phi_i = -i\sigma^2 \Phi_i^\star i\sigma^2, \tag{4.27}$$

given $\tilde{\phi}_i = i\sigma^2 \phi_i^\star$. In such a way, we rewrite the potential, in the form of,

$$\begin{aligned}V(\Phi_1, \Phi_2) = &-\frac{\mu_{11}^2}{4}\mathrm{Tr}\left[\Phi_1^\dagger \Phi_1\right] - \frac{\mu_{22}^2}{4}\mathrm{Tr}\left[\Phi_2^\dagger \Phi_2\right] - \frac{\mu_{12RE}^2}{2}\mathrm{Tr}\left[\Phi_1^\dagger \Phi_2\right] \\ &+ \frac{\mu_{12IM}^2}{2}\mathrm{Tr}\left[\Phi_1^\dagger \Phi_2 i\sigma^3\right] \\ &+ \frac{\lambda_1}{8}\left(\mathrm{Tr}\left[\Phi_1^\dagger \Phi_1\right]\right)^2 + \frac{\lambda_2}{8}\left(\mathrm{Tr}\left[\Phi_2^\dagger \Phi_2\right]\right)^2 \\ &+ \frac{\lambda_3}{4}\mathrm{Tr}\left[\Phi_2^\dagger \Phi_2\right]\mathrm{Tr}\left[\Phi_1^\dagger \Phi_1\right] \\ &+ \frac{\lambda_4}{4}\left(\mathrm{Tr}\left[\Phi_1^\dagger \Phi_2\right]\right)^2 + \frac{\lambda_4}{4}\left(\mathrm{Tr}\left[\Phi_1^\dagger \Phi_2 i\sigma^3\right]\right)^2 \\ &+ \frac{\lambda_{5RE}}{4}\left(\mathrm{Tr}\left[\Phi_1^\dagger \Phi_2\right]\right)^2 - \frac{\lambda_{5RE}}{4}\left(\mathrm{Tr}\left[\Phi_1^\dagger \Phi_2 i\sigma^3\right]\right)^2 \\ &- \frac{\lambda_{5IM}}{2}\mathrm{Tr}\left[\Phi_1^\dagger \Phi_2 i\sigma^3\right]\mathrm{Tr}\left[\Phi_1^\dagger \Phi_2\right],\end{aligned} \tag{4.28}$$

where we denote the real and imaginary part of μ_{12}^2 as μ_{12RE}^2, μ_{12IM}^2, and apply the same convention to λ_5. As a result, the Higgs action becomes,

$$S_H = -\int d^4x \,[\, \frac{1}{2}\mathrm{Tr}\left[\Phi_1^\dagger \overleftarrow{D}_\mu^\dagger D^\mu \Phi_1\right] + \frac{1}{2}\mathrm{Tr}\left[\Phi_2^\dagger \overleftarrow{D}_\mu^\dagger D^\mu \Phi_2\right] + V(\Phi_1, \Phi_2). \tag{4.29}$$

Notice that under charge conjugation $\phi^{\mathcal{C}} = \phi^\star$, therefore $\Phi^{\mathcal{C}} = \Phi^\star$, terms with coefficients μ_{12IM}^2, λ_{5IM} will change their signs, and in such a way, the Higgs action yields C-violation.

The normal $SU(2)$ gauge transformation that leaves S_H invariant is performed on Higgs fields in the form of a left multiplication, i.e. $\Phi_i \to U\Phi_i$. Moreover, the action is also invariant under the transformation of a right multiplication, $\Phi_i \to \Phi_i i\sigma^2$, if μ_{12IM}^2 and λ_{5IM} change their signs at the same time. [1] As a result, one can always design a joint transformation, of the form, $\Phi_i \to \Phi_i^\star i\sigma^2$, under which the Higgs action will be invariant. We denote the new transformation as C', which on the other hand acts on fermion fields and the gauge field just like the normal C-conjugation would do. It will be a potential problem if the whole theory is $C'P$ invariant, because the Chern-Simons number is actually $C'P$ odd, and therefore, statistically, there could only exist zero N_{CS}. We in practice avoid this disaster by choosing a proper Yukawa interaction to break the $C'P$ symmetry via inhibiting $\Phi_i \to \Phi_i i\sigma^2$ transformation.

Yukawa interaction

In general, all quarks and leptons can interact with both Higgs fields, with the entire Yukawa interaction written as

$$\begin{aligned} Y(q, l, \phi_1, \phi_2) = \; & G_1^d \bar{q}_L \phi_1 d_R + G_2^d \bar{q}_L \phi_2 d_R + G_1^e \bar{l}_L \phi_1 e_R + G_2^e \bar{l}_L \phi_2 e_R \\ & + G_1^u \bar{q}_L \tilde{\phi}_1 u_R + G_2^u \bar{q}_L \tilde{\phi}_2 u_R + G_1^\nu \bar{l}_L \tilde{\phi}_1 \nu_R + G_2^\nu \bar{l}_L \tilde{\phi}_2 \nu_R \\ & + G_1^{d\dagger} \bar{d}_R \phi_1^\dagger q_L + G_2^{d\dagger} \bar{d}_R \phi_2^\dagger q_L + G_1^{e\dagger} \bar{e}_R \phi_1^\dagger l_L + G_2^{e\dagger} \bar{e}_R \phi_2^\dagger l_L \\ & + G_1^{u\dagger} \bar{u}_R \tilde{\phi}_1^\dagger q_L + G_2^{u\dagger} \bar{u}_R \tilde{\phi}_2^\dagger q_L + G_1^{\nu\dagger} \bar{\nu}_R \tilde{\phi}_1^\dagger l_L + G_2^{\nu\dagger} \bar{\nu}_R \tilde{\phi}_2^\dagger l_L. \end{aligned} \tag{4.30}$$

[1] Besides $i\sigma^2$, any 2×2 unitary matrix that anti-commutates with σ^3 could function in the same way.

With the redefined fields, the complete Yukawa interaction becomes

$$\begin{aligned} Y(\Psi,\chi,\xi,\Phi_1,\Phi_2) = \; & G_1^u\bar{\Psi}\Phi_1 P_U P_R(\chi,\xi)^T + G_1^{u\dagger}(\bar{\chi},\bar{\xi})P_U\Phi_1^\dagger P_R\Psi \\ & + G_2^u\bar{\Psi}\Phi_2 P_U P_L(\chi,\xi)^T + G_2^{u\dagger}(\bar{\chi},\bar{\xi})P_U\Phi_2^\dagger P_R\Psi \\ & + G_1^d\bar{\Psi}\Phi_1 P_D P_L(\chi,\xi)^T + G_1^{d\dagger}(\bar{\chi},\bar{\xi})P_D\Phi_1^\dagger P_R\Psi \\ & + G_2^d\bar{\Psi}\Phi_2 P_D P_L(\chi,\xi)^T + G_2^{d\dagger}(\bar{\chi},\bar{\xi})P_D\Phi_2^\dagger P_R\Psi \\ & + G_1^e\bar{\Psi}\Phi_1 P_U P_R(\chi,\xi)^T + G_1^{e\dagger}(\bar{\chi},\bar{\xi})P_U\Phi_1^\dagger P_L\Psi \\ & + G_2^e\bar{\Psi}\Phi_2 P_U P_R(\chi,\xi)^T + G_2^{e\dagger}(\bar{\chi},\bar{\xi})P_U\Phi_2^\dagger P_L\Psi \\ & + G_1^\nu\bar{\Psi}\Phi_1 P_D P_R(\chi,\xi)^T + G_1^{\nu\dagger}(\bar{\chi},\bar{\xi})P_D\Phi_1^\dagger P_L\Psi \\ & + G_2^\nu\bar{\Psi}\Phi_2 P_D P_R(\chi,\xi)^T + G_2^{\nu\dagger}(\bar{\chi},\bar{\xi})P_D\Phi_2^\dagger P_L\Psi, \end{aligned} \tag{4.31}$$

in terms of a number of projectors

$$P_U = \frac{1+\sigma^3}{2}, \quad P_D = \frac{1-\sigma^3}{2}, \quad P_L = \frac{1+\gamma^5}{2}, \quad P_R = \frac{1-\gamma^5}{2}. \tag{4.32}$$

We have to avoid terms, like $\bar{\Psi}\Phi_i(\chi,\xi)^T$, which will be invariant under $\Phi_i \to \Phi_i i\sigma^2$ and $(\chi,\xi)^T \to -i\sigma^2(\chi,\xi)^T$, otherwise the whole action will be $C'P$ symmetric, as the rotation on singlets does not change their kinetic terms.

For the sake of simplicity, we will in practice choose the Yukawa interaction as

$$\begin{aligned} Y(q,l,\phi_1,\phi_2) = \; & y_{\rm uk}(\bar{q}_L\phi_2 d_R + \bar{l}_L\phi_2 e_R + \bar{q}_L\tilde{\phi}_1 u_R + \bar{l}_L\tilde{\phi}_1\nu_R \\ & + \bar{d}_R\phi_2^\dagger q_L + \bar{e}_R\phi_2^\dagger l_L + \bar{u}_R\tilde{\phi}_1^\dagger q_L + \bar{\nu}_R\tilde{\phi}_1^\dagger l_L), \end{aligned} \tag{4.33}$$

or with the redefined fields,

$$\begin{aligned} Y(\Psi,\chi,\xi,\Phi_1,\Phi_2) = & y_{uk}\Big(\bar{\Psi}\Phi_1 P_U P_R(\chi,\xi)^T + (\bar{\chi},\bar{\xi})P_U\Phi_1^\dagger P_L\Psi \\ & + \bar{\Psi}\Phi_2 P_D P_R(\chi,\xi)^T + (\bar{\chi},\bar{\xi})P_D\Phi_2^\dagger P_L\Psi \\ & + \bar{\Psi}\Phi_2 P_U P_L(\chi,\xi)^T + (\bar{\chi},\bar{\xi})P_U\Phi_2^\dagger P_R\Psi \\ & + \bar{\Psi}\Phi_1 P_D P_L(\chi,\xi)^T + (\bar{\chi},\bar{\xi})P_D\Phi_1^\dagger P_R\Psi\Big), \end{aligned} \tag{4.34}$$

where we have selected parameters,

$$y_{\rm uk} = G_2^d = G_2^e = G_1^u = G_1^\nu, \qquad G_1^d = G_1^e = G_2^u = G_2^\nu = 0. \tag{4.35}$$

Moreover, it will be also easier to calculate the counterterms from this simple Yukawa interaction. Notice that if the projectors P_U and P_D are absent, the interaction is invariant under transformation,

$$\Phi_i \to \Phi_i i\sigma^2, \qquad (\chi, \xi)^T \to -i\sigma^2(\chi, \xi)^T, \tag{4.36}$$

and in addition, the latter does not impact the kinetic terms of singlets. For this reason, we specify the existence of P_U and P_D in our selected Yukawa interaction, in order to break $C'P$-symmetry by inhibiting the transformation $\Phi_i \to \Phi_i i\sigma^2$.

We in practice take

$$y_{\rm uk} = 0.1, \tag{4.37}$$

which corresponds the fermion masses of $11/\sqrt{2} \sim 8$ GeV and $22/\sqrt{2} \sim 16$ GeV, depending on which Higgs field they are coupled to. The masses are easily larger than all masses of quark and leptons in the Standard Model, except of top quark.

4.1.2 CP-symmetric initial conditions

We will consider an instantaneous quench of the Higgs potential at zero temperature. So, instead of the potential (4.8) which we will use to evolve the Higgs fields during the simulation, we generate the initial conditions for Higgs fields, according to the potential, of the form

$$V(t<0) = \frac{\mu_{11}^2}{2}(\phi_1^\dagger\phi_1) + \frac{\mu_{22}^2}{2}(\phi_2^\dagger\phi_2) + \frac{\mu_{12}^2}{2}(\phi_1^\dagger\phi_2) + \frac{\mu_{12}^{2,\star}}{2}(\phi_2^\dagger\phi_1). \tag{4.38}$$

Because of the existence of μ_{12}^2, one has to diagonalise the mass matrix in (4.38) and transfer the Higgs fields into mass eigenstates. The initial states have ($\langle\phi_1\rangle = \langle\phi_2\rangle = 0$), and the fluctuations around the vacuum are determined by

$$\langle\phi_{\mathbf{k}}^i(\phi_{\mathbf{k}}^j)^\dagger\rangle = \frac{1}{2\omega_{\mathbf{k}}}\delta_{ij}, \qquad \langle\dot{\phi}_{\mathbf{k}}^i(\dot{\phi}_{\mathbf{k}}^j)^\dagger\rangle = \frac{\omega_{\mathbf{k}}}{2}\delta_{ij}, \tag{4.39}$$

where $\dot{\phi}_{\mathbf{k}}^i$ and $\phi_{\mathbf{k}}^i$ are the momentum space variables for each real component of the mass eigenstates of the Higgs fields (8 in total), and $\omega_{\mathbf{k}}^2 = M^2 + k^2$, with M^2 the eigenvalues of the mass matrix. After initializing the fluctuations, one then needs

to rotate configurations back to the ϕ_1, ϕ_2 basis.

For each randomly generated configuration ϕ^i, $\dot{\phi}^i$, we also generate an entire ensemble of $N_f = 4000$ fermion configurations. The initialization of fermion fields is the same as in section 3.3.2. The gauge field is initialized in the form of $A_\mu = 0$, and the $SU(2)$ electric field E_i is determined through Gauss' law, sourced by the $SU(2)$ charges of the randomly generated Higgs fields and fermion fields.

We also wish to maintain the CP symmetry in the initial samplings. To this end, for each realization of field configurations $(q, l, A_\mu, \phi_{1,2})$, we generate its CP-conjugate realization, with fields,

$$\begin{aligned}
q_L^{\mathcal{C}P}(t,x) &= i\gamma^0\gamma^2\ q_L^\star(t,-x), & l_L^{\mathcal{C}P}(t,x) &= i\gamma^0\gamma^2\ l_L^\star(t,-x),\\
u_R^{\mathcal{C}P}(t,x) &= i\gamma^0\gamma^2\ u_R^\star(t,-x), & d_R^{\mathcal{C}P}(t,x) &= i\gamma^0\gamma^2\ d_R^\star(t,-x),\\
\nu_R^{\mathcal{C}P}(t,x) &= i\gamma^0\gamma^2\ \nu_R^\star(t,-x), & e_R^{\mathcal{C}P}(t,x) &= i\gamma^0\gamma^2\ e_R^\star(t,-x),
\end{aligned} \tag{4.40}$$

and

$$A^{\mathcal{C}P}(t,x) = A^T(t,-x), \qquad \phi_1^{\mathcal{C}P}(t,x) = \phi_1^\star(t,-x), \qquad \phi_2^{\mathcal{C}P}(t,x) = \phi_2^\star(t,-x). \tag{4.41}$$

We force the initial samplings to be CP-symmetric, in order to quickly reduce the statistical error. In such a way, when the C-violation is turned off in the Higgs potential, an average between a normal and its CP-conjugate realization will yield N_{CS} and $N_W^{1,2}$ of precisely zero. We have checked numerically that this is indeed the case, which also means that there is no spurious CP-violation from counter terms or discretization.

4.2 Lattice implementation

The action on the lattice can be written as:

$$
\begin{aligned}
S_G =& \sum_{x,t} \beta_G^t \sum_i \left(1 - \frac{1}{2}\mathrm{Tr}\, U_{0i,x}\right) - \frac{\beta_G^s}{2} \sum_{ij} \left(1 - \frac{1}{2}\mathrm{Tr}\, U_{ij,x}\right), \\
S_H =& \sum_{x,t} \sum_n \left(\frac{\beta_H^t}{2} \mathrm{Tr}\left[(D_0\Phi_n)^\dagger D_0 \Phi_n\right] - \frac{\beta_H^s}{2}\mathrm{Tr}\left[(D_i\Phi_n)^\dagger D_i \Phi_n\right]\right) \\
& - \beta_R V(\Phi_1, \Phi_2) + \beta_Y C(\Phi_1, \Phi_2), \\
S_F =& \sum_{x,t} - \left[\bar\Psi\gamma^0 \tilde D_0 \Psi + \bar\chi\gamma^0\tilde\partial_0\chi + \bar\xi\gamma^0\tilde\partial_0\xi\right] - \frac{a_t}{a}\left[\bar\Psi\gamma^i\tilde D_i\Psi + \bar\chi\gamma^i\tilde\partial_i\chi + \bar\xi\gamma^i\tilde\partial_i\xi\right] \\
& + \frac{r a_t}{2a}\left[\bar\Psi D_i' D_i \Psi + \bar\chi\partial_i'\partial_i\chi + \bar\xi\partial_i'\partial_i\xi\right] - \beta_Y Y(\Psi, \chi, \xi, \Phi_1, \Phi_2),
\end{aligned} \tag{4.42}
$$

where, as they were in (3.81) and (3.82), the fields are rescaled to be dimensionless by the lattice spacing a

$$
\Psi(x) \to a^{3/2}\Psi(x), \quad \chi(x) \to a^{3/2}\chi(x), \quad \xi(x) \to a^{3/2}\xi(x), \quad \Phi(x) \to a\Phi(x), \tag{4.43}
$$

and the lattice parameters are defined in the form of

$$
\beta_G^t = \frac{4}{g^2}\frac{a}{a_t}, \quad \beta_G^s = \frac{4}{g^2}\frac{a_t}{a}, \quad \beta_H^t = \frac{a}{a_t}, \quad \beta_H^s = \frac{a_t}{a}, \quad \beta_R = \frac{a_t}{a}, \quad \beta_Y = \frac{a_t}{a}. \tag{4.44}
$$

The two-Higgs scalar potential on the lattice turns into

$$
\begin{aligned}
V(\Phi_1, \Phi_2) =& - \frac{a^2\mu_{11}^2}{4}\mathrm{Tr}\left[\Phi_1^\dagger\Phi_1\right] - \frac{a^2\mu_{22}^2}{4}\mathrm{Tr}\left[\Phi_2^\dagger\Phi_2\right] - \frac{a^2\mu_{12RE}^2}{2}\mathrm{Tr}\left[\Phi_1^\dagger\Phi_2\right] \\
& + \frac{a^2\mu_{12IM}^2}{2}\mathrm{Tr}\left[\Phi_1^\dagger\Phi_2 i\sigma^3\right] \\
& + \frac{\lambda_1}{8}\left(\mathrm{Tr}\left[\Phi_1^\dagger\Phi_1\right]\right)^2 + \frac{\lambda_2}{8}\left(\mathrm{Tr}\left[\Phi_2^\dagger\Phi_2\right]\right)^2 \\
& + \frac{\lambda_3}{4}\mathrm{Tr}\left[\Phi_2^\dagger\Phi_2\right]\mathrm{Tr}\left[\Phi_1^\dagger\Phi_1\right] \\
& + \frac{\lambda_4}{4}\left(\mathrm{Tr}\left[\Phi_1^\dagger\Phi_2\right]\right)^2 + \frac{\lambda_4}{4}\left(\mathrm{Tr}\left[\Phi_1^\dagger\Phi_2 i\sigma^3\right]\right)^2 \\
& + \frac{\lambda_{5RE}}{4}\left(\mathrm{Tr}\left[\Phi_1^\dagger\Phi_2\right]\right)^2 - \frac{\lambda_{5RE}}{4}\left(\mathrm{Tr}\left[\Phi_1^\dagger\Phi_2 i\sigma^3\right]\right)^2 \\
& - \frac{\lambda_{5IM}}{2}\mathrm{Tr}\left[\Phi_1^\dagger\Phi_2 i\sigma^3\right]\mathrm{Tr}\left[\Phi_1^\dagger\Phi_2\right],
\end{aligned} \tag{4.45}
$$

and the Yukawa interaction we choose is

$$\begin{aligned} Y(\Psi,\chi,\xi,\Phi_1,\Phi_2) =& y_{uk}\Big(\bar{\Psi}\Phi_1 P_U P_R(\chi,\xi)^T + (\bar{\chi},\bar{\xi})P_U\Phi_1^\dagger P_L\Psi \\ &+ \bar{\Psi}\Phi_2 P_D P_R(\chi,\xi)^T + (\bar{\chi},\bar{\xi})P_D\Phi_2^\dagger P_L\Psi \\ &+ \bar{\Psi}\Phi_2 P_U P_L(\chi,\xi)^T + (\bar{\chi},\bar{\xi})P_U\Phi_2^\dagger P_R\Psi \\ &+ \bar{\Psi}\Phi_1 P_D P_L(\chi,\xi)^T + (\bar{\chi},\bar{\xi})P_D\Phi_1^\dagger P_R\Psi\Big), \end{aligned} \tag{4.46}$$

which is exactly the same as its continuum expression in (4.34), for the rescaling does not change its countenance.

From the complete lattice action, we derive the equations of motion by straightforward variation. For the fermions, we find the following linear equations in the bosonic field background:

$$\begin{aligned} 0 =& -\gamma^0\tilde{\partial}_0\Psi - \frac{a_t}{a}\gamma^i\tilde{D}_i\Psi + \frac{ra_t}{2a}D_i'D_i\Psi - y_{uk}\beta_Y\left[\Phi_1 P_U + \Phi_2 P_D\right]P_R(\chi,\xi)^T \\ &- y_{uk}\beta_Y\left[\Phi_2 P_U + \Phi_1 P_D\right]P_L(\chi,\xi)^T, \\ 0 =& -\gamma^0\tilde{\partial}_0(\chi,\xi)^T - \frac{a_t}{a}\gamma^i\tilde{\partial}_i(\chi,\xi)^T + \frac{ra_t}{2a}\partial_i'\partial_i(\chi,\xi)^T - y_{uk}\beta_Y\left[P_U\Phi_1^\dagger + P_D\Phi_2^\dagger\right]P_L\Psi \\ &- y_{uk}\beta_Y\left[P_U\Phi_2^\dagger + P_D\Phi_1^\dagger\right]P_R\Psi. \end{aligned} \tag{4.47}$$

For the gauge field

$$\begin{aligned} 0 =& \frac{1}{2}\beta_G^t\left(E_n^a(y) - E_n^a(y-0)\right) - \frac{1}{2}\beta_G^s\sum_m D_m^{ab'}\mathrm{Tr}\left[i\sigma^b U_{y,m}U_{y+m,n}U_{y+n,m}^\dagger U_{y,n}^\dagger\right] \\ &- \beta_H^s\mathrm{Tr}\left[i\sigma^a\Phi_{1,y}(U_{y,n}\Phi_{1,y+n})^\dagger\right] - \beta_H^s\mathrm{Tr}\left[i\sigma^a\Phi_{2,y}(U_{y,n}\Phi_{2,y+n})^\dagger\right] \\ &- \frac{a_t}{2a}\left[\bar{\Psi}_y\gamma^n i\sigma^a U_{y,n}\Psi_{y+n} + \bar{\Psi}_{y+n}\gamma^n U_{y,n}^\dagger i\sigma^a\Psi_y\right], \\ &+ \frac{ra_t}{2a}\left[\bar{\Psi}_y i\sigma^a U_{y,n}\Psi_{y+n} - \bar{\Psi}_{y+n}U_{y,n}^\dagger i\sigma^a\Psi_y\right]. \end{aligned} \tag{4.48}$$

And for the two Higgs fields

$$
\begin{aligned}
0 =& -\beta_H^t \partial_0' \partial_0 \Phi_1 + \beta_H^s \partial_i' \partial_i \Phi_1 \\
&+ \frac{\beta_R}{2}\left(a^2\mu_{11}^2 - \lambda_1 \mathrm{Tr}\left[\Phi_1^\dagger \Phi_1\right] - \lambda_3 \mathrm{Tr}\left[\Phi_2^\dagger \Phi_2\right]\right)\Phi_1 \\
&+ \frac{\beta_R}{2}\left(a^2\mu_{12re}^2 - (\lambda_4+\lambda_{5re)} \mathrm{Tr}\left[\Phi_1^\dagger \Phi_2\right] + \lambda_{5im} \mathrm{Tr}\left[\Phi_1^\dagger \Phi_2 i\sigma^3\right]\right)\Phi_2 \\
&+ \frac{\beta_R}{2}\left(-a^2\mu_{12im}^2 + (-\lambda_4+\lambda_{5re)} \mathrm{Tr}\left[\Phi_1^\dagger \Phi_2 i\sigma^3\right] + \lambda_{5im} \mathrm{Tr}\left[\Phi_1^\dagger \Phi_2\right]\right)\Phi_2 i\sigma^3 \\
&- \frac{y_{uk}\beta_Y}{2} k^b \left[\bar{\Psi} k^b P_U P_R (\chi,\xi)^T + (\bar{\chi},\bar{\xi}) P_U k^{a\dagger} P_L \Psi\right] \\
&- \frac{y_{uk}\beta_Y}{2} k^b \left[\bar{\Psi} k^b P_D P_L (\chi,\xi)^T + (\bar{\chi},\bar{\xi}) P_D k^{a\dagger} P_R \Psi\right] \\
&+ \beta_Y a^2 c t_{11} \Phi_1 + \beta_Y a^2 c t_{12} \Phi_2, \\
0 =& -\beta_H^t \partial_0' \partial_0 \Phi_2 + \beta_H^s \partial_i' \partial_i \Phi_2 \\
&+ \frac{\beta_R}{2}\left(a^2\mu_{22}^2 - \lambda_2 \mathrm{Tr}\left[\Phi_2^\dagger \Phi_2\right] - \lambda_3 \mathrm{Tr}\left[\Phi_1^\dagger \Phi_1\right]\right)\Phi_2 \\
&+ \frac{\beta_R}{2}\left(a^2\mu_{12re}^2 - (\lambda_4+\lambda_{5re)} \mathrm{Tr}\left[\Phi_1^\dagger \Phi_2\right] + \lambda_{5im} \mathrm{Tr}\left[\Phi_1^\dagger \Phi_2 i\sigma^3\right]\right)\Phi_1 \\
&+ \frac{\beta_R}{2}\left(a^2\mu_{12im}^2 + (\lambda_4-\lambda_{5re)} \mathrm{Tr}\left[\Phi_1^\dagger \Phi_2 i\sigma^3\right] - \lambda_{5im} \mathrm{Tr}\left[\Phi_1^\dagger \Phi_2\right]\right)\Phi_1 i\sigma^3 \\
&- \frac{y_{uk}\beta_Y}{2} k^b \left[\bar{\Psi} k^b P_D P_R (\chi,\xi)^T + (\bar{\chi},\bar{\xi}) P_D k^{a\dagger} P_L \Psi\right] \\
&- \frac{y_{uk}\beta_Y}{2} k^b \left[\bar{\Psi} k^b P_U P_L (\chi,\xi)^T + (\bar{\chi},\bar{\xi}) P_U k^{a\dagger} P_R \Psi\right] \\
&+ \beta_Y a^2 c t_{11} \Phi_2 + \beta_Y a^2 c t_{12} \Phi_1,
\end{aligned}
\tag{4.49}
$$

with $k^b = (\mathbb{I}, i\sigma^1, i\sigma^2, i\sigma^3)$. All fermion bilinears in simulations will be replaced by ensemble averages, as shown in (3.92).

For the redefined fields, CP-transformation induced from (4.40) and (4.41) can be written as

$$
\begin{aligned}
\chi^{\mathcal{C}P}(t,x) =& -\gamma^5 i\gamma^0\gamma^2 \chi^\star(t,-x), \\
\xi^{\mathcal{C}P}(t,x) =& -\gamma^5 i\gamma^0\gamma^2 \xi^\star(t,-x), \\
\Psi^{\mathcal{C}P}(t,x) =& \gamma^5 i\gamma^0\gamma^2 \Psi^\star(t,-x), \\
U_i^{\mathcal{C}P}(t,x) =& U_i^T(t,-x-i), \\
\Phi^{\mathcal{C}P}(t,x) =& \Phi^\star(t,-x).
\end{aligned}
\tag{4.50}
$$

To prove the CP-symmetry in the fermion action, one needs to exchange the position of two fermionic fields, and as a result, obtain a minus sign, for fermionic

fields are essentially Grassmann numbers. While with normal numbers in numerical simulations, we have to in practice compensate the minus sign by hand, when dealing with the CP-conjugate of fermion two-point functions, for instance, in the fermionic backreaction to the gauge field. The transformation also requires the Wilson parameter r_W in CP-conjugate simulations being opposite to its value in normal simulations.

The evolution with the equation of motion (4.47, 4.48, 4.49) will conserve the total energy, with components of energy density in the form of

$$\begin{aligned}
e_G =& \frac{1}{Va_t}\sum_x \beta_G^t \sum_i \left(1-\frac{1}{2}\mathrm{Tr}\, U_{0i,x}\right) + \frac{\beta_G^s}{2}\sum_{ij}\left(1-\frac{1}{2}\mathrm{Tr}\, U_{ij,x}\right),\\
e_H =& \frac{1}{Va_t}\sum_x \sum_n \left(\frac{\beta_H^t}{2}\mathrm{Tr}\left[(D_0\Phi_n)^\dagger D_0\Phi_n\right] + \frac{\beta_H^s}{2}\mathrm{Tr}\left[(D_i\Phi_n)^\dagger D_i\Phi_n\right]\right) + \beta_R V(\Phi_1,\Phi_2),\\
e_F =& \frac{1}{Va_t}\sum_x \frac{a_t}{a}\left[\bar\Psi\gamma^i\tilde D_i\Psi + \bar\chi\gamma^i\tilde\partial_i\chi + \bar\xi\gamma^i\tilde\partial_i\xi\right] - \frac{ra_t}{2a}\left[\bar\Psi D_i' D_i\Psi + \bar\chi\partial_i'\partial_i\chi + \bar\xi\partial_i'\partial_i\xi\right]\\
&+ \beta_Y Y(\Psi,\chi,\xi,\Phi_1,\Phi_2) - \beta_Y C(\Phi_1,\Phi_2).
\end{aligned} \tag{4.51}$$

We also consider the renormalization and include counterterms for possible quadratic divergences in the continuous theory, which are on the lattice, not infinities, but most likely, large numbers. The counterterms with coefficients ct_{11} and ct_{12} are introduced, of the form

$$C(\Phi_1,\Phi_2) = \frac{a^2 ct_{11}}{2}\left(\mathrm{Tr}\left[\Phi_1^\dagger\Phi_1\right] + \mathrm{Tr}\left[\Phi_2^\dagger\Phi_2\right]\right) + \frac{a^2 ct_{12}}{2}\left(\mathrm{Tr}\left[\Phi_1^\dagger\Phi_2\right] + \mathrm{Tr}\left[\Phi_2^\dagger\Phi_1\right]\right), \tag{4.52}$$

and simple dimensional analysis indicates these two coefficients might be quadratically divergent in the continuous theory, or have $1/a^2$ dependence in the lattice regularization. We calculate them in the following way.

4.2.1 Counterterms and renormalization

In light of the technique we have developed in section 3.3.4 to calculate

$$e^{-iS_C+\cdots} = \int [D\bar\psi][D\psi] e^{iS_F+iS_Y},$$

we can explicitly carry out the path integral above when the Higgs fields are constant, and the result is

$$\begin{aligned} & i\int \frac{d^4p}{(2\pi)^4} \ln \mathrm{Det} \left[\begin{array}{cc} i\gamma^\mu \tilde{p}_\mu + m_D & y_{uk}K \\ -y_{uk}\gamma^0 K^\dagger \gamma^0 & i\gamma^\mu \tilde{p}_\mu + m_S \end{array} \right]_{16\times 16} \\ =& \frac{ct_{11}}{2}\left(\mathrm{Tr}\left[\Phi_1^\dagger \Phi_1\right] + \mathrm{Tr}\left[\Phi_2^\dagger \Phi_2\right]\right) + \frac{ct_{12}}{2}\left(\mathrm{Tr}\left[\Phi_1^\dagger \Phi_2\right] + \mathrm{Tr}\left[\Phi_2^\dagger \Phi_1\right]\right) + ..., \end{aligned} \tag{4.53}$$

where m_D and m_S are respectively the masses of the doublets and singlets, and the 2×2 matrix K stands for

$$K = \Phi_1 P_U \otimes P_R + \Phi_2 P_D \otimes P_R + \Phi_2 P_U \otimes P_L + \Phi_1 P_D \otimes P_L. \tag{4.54}$$

We follow the convention in section 3.3.4 and denote

$$p_0 \in (-\frac{\pi}{a_t},\ \frac{\pi}{a_t}], \qquad p_i \in (-\frac{\pi}{a},\ \frac{\pi}{a}], \tag{4.55}$$

$$\tilde{p}_0 = \frac{\sin(p_0 a_t)}{a_t}, \qquad \tilde{p}_i = \frac{\sin(p_i a)}{a}, \tag{4.56}$$

as well as $d^4p = d\tilde{p}_0 d^3p$. We have also recovered the dimensionality of fields, so one would find the calculation in this section to be similar to the result in the continuum theory.

Notice in the backreaction of fermion fields, there is a symmetry between Φ_1 and Φ_2, owing to the fact that K is invariant under the exchange of Φ_1 and Φ_2, and up and down simultaneously, while the latter exchange does not affect the determinant of the matrix. Therefore, the simplicity of the counterterms (4.52) should be attributed to the symmetry in the Yukawa interaction (4.46).

To obtain the expression for ct_{11} and ct_{12}, we consider two cases:
(a) $\Phi_2 = \Phi_1 = \frac{\phi}{y_{uk}} I$,

$$i\int \frac{d^4p}{(2\pi)^4} \ln \mathrm{Det} \left[\begin{array}{cc} i\gamma^\mu \tilde{p}_\mu + m_D & \phi \\ \phi & i\gamma^\mu \tilde{p}_\mu + m_S \end{array} \right]_{16\times 16} = 2\frac{ct_{11}}{y_{uk}^2}\phi^2 + 2\frac{ct_{12}}{y_{uk}^2}\phi^2 + ... \tag{4.57}$$

The series on the right-handed side contains a constant term of zero order of ϕ which is the result of the free fermions, as one can see by simply setting $\phi = 0$ on

the left-handed side. Thus, instead of implementing the equation above, we consider its derivative where the constant term is removed,

$$i\int\frac{d^4p}{(2\pi)^4}\frac{d}{d\phi}\ln\mathrm{Det}\left[\begin{array}{cc} i\gamma^\mu\tilde{p}_\mu+m_D & \phi \\ \phi & i\gamma^\mu\tilde{p}_\mu+m_S \end{array}\right]_{16\times16}=4\frac{ct_{11}}{y_{uk}^2}\phi+4\frac{ct_{12}}{y_{uk}^2}\phi+.... \tag{4.58}$$

The determinant in the expression can be calculated in the following way,

$$\begin{aligned}&\mathrm{Det}\left[\begin{array}{cc} i\gamma^\mu\tilde{p}_\mu+m_D & \phi \\ \phi & i\gamma^\mu\tilde{p}_\mu+m_S \end{array}\right]_{16\times16}=\mathrm{Det}\left[\tilde{p}_0+H\right]\\ =&(\tilde{p}_0^2-\omega_{1a}^2+i\epsilon)^4(\tilde{p}_0^2-\omega_{2a}^2+i\epsilon)^4,\end{aligned} \tag{4.59}$$

where H refers to the Hamiltonian

$$H=\left[\begin{array}{cc} i\gamma^0i\gamma\tilde{p}+i\gamma^0m_D & i\gamma^0\phi \\ i\gamma^0\phi & i\gamma^0i\gamma\tilde{p}+i\gamma^0m_S \end{array}\right]_{16\times16}, \tag{4.60}$$

and its eigenenergies ω_{1a} and ω_{2a} satisfy [2]

$$\begin{aligned}\omega_{1a}^2&=\tilde{p}^2+\phi^2+\frac{(m_D^2+m_S^2)+\sqrt{(m_D^2-m_S^2)^2+4\phi^2(m_D+m_S)^2}}{2},\\ \omega_{1a}^2&=\tilde{p}^2+\phi^2+\frac{(m_D^2+m_S^2)-\sqrt{(m_D^2-m_S^2)^2+4\phi^2(m_D+m_S)^2}}{2}.\end{aligned} \tag{4.61}$$

As a result, we arrive at the equation

$$\begin{aligned}&\frac{ct_{11}}{y_{uk}^2}\phi+\frac{ct_{12}}{y_{uk}^2}\phi+...\\ =&\int\frac{d^3p}{(2\pi)^3}i\int\frac{d\tilde{p}_0}{2\pi}\left[\frac{-\frac{d\omega_{1a}}{d\phi}}{\tilde{p}_0-\omega_{1a}+i\epsilon}+\frac{\frac{d\omega_{1a}}{d\phi}}{\tilde{p}_0+\omega_{1a}-i\epsilon}+\frac{-\frac{d\omega_{2a}}{d\phi}}{\tilde{p}_0-\omega_{2a}+i\epsilon}+\frac{\frac{d\omega_{2a}}{d\phi}}{\tilde{p}_0+\omega_{2a}-i\epsilon}\right]\\ =&-\int\frac{d^3p}{(2\pi)^3}\left[\frac{d\omega_{1a}}{d\phi}+\frac{d\omega_{2a}}{d\phi}\right],\end{aligned} \tag{4.62}$$

where the contour integral on the second line is executed in the same way as in (3.123), and we also assume here no temporal doublers contributing.

[2] It would be easier to achieve the eigenenergies from H^2 than from H.

(b) $-\Phi_2 = \Phi_1 = \frac{\phi}{y_{uk}} I$,

$$i\int \frac{d^4p}{(2\pi)^4} \ln \mathrm{Det} \begin{bmatrix} i\gamma^\mu \tilde{p}_\mu + m_D & \phi\sigma^3 \otimes \gamma^5 \\ -\phi\sigma^3 \otimes \gamma^5 & i\gamma^\mu \tilde{p}_\mu + m_S \end{bmatrix}_{16\times 16} = 2\frac{ct_{11}}{y_{uk}^2}\phi^2 - 2\frac{ct_{12}}{y_{uk}^2}\phi^2 + ... \tag{4.63}$$

The calculation here would be similar to it in the first case, and one can eventually achieve an equation, of the form

$$\frac{ct_{11}}{y_{uk}^2}\phi - \frac{ct_{12}}{y_{uk}^2}\phi + ... = -\int \frac{d^3p}{(2\pi)^3}\left[\frac{d\omega_{1b}}{d\phi} + \frac{d\omega_{2b}}{d\phi}\right], \tag{4.64}$$

with now the eigenenergies

$$\begin{aligned} \omega_{1b}^2 &= \tilde{p}^2 + \phi^2 + \frac{(m_D^2 + m_S^2) + \sqrt{(m_D - m_S)^2[(m_D + m_S)^2 + 4\phi^2]}}{2}, \\ \omega_{2b}^2 &= \tilde{p}^2 + \phi^2 + \frac{(m_D^2 + m_S^2) - \sqrt{(m_D - m_S)^2[(m_D + m_S)^2 + 4\phi^2]}}{2}. \end{aligned} \tag{4.65}$$

The equation (4.62) and (4.64) must be valid to any order of Higgs fields, For our purpose, we only need the leading terms, which read

$$\begin{aligned} -\int \frac{d^3p}{(2\pi)^3}\phi\left[\frac{1}{\omega_1} + \frac{1}{\omega_2} - \frac{(m_D + m_S)^2}{\omega_1\omega_2(\omega_1 + \omega_2)}\right] &= \frac{ct_{11}}{y_{uk}^2}\phi + \frac{ct_{11}}{y_{uk}^2}\phi, \\ -\int \frac{d^3p}{(2\pi)^3}\phi\left[\frac{1}{\omega_1} + \frac{1}{\omega_2} - \frac{(m_D - m_S)^2}{\omega_1\omega_2(\omega_1 + \omega_2)}\right] &= \frac{ct_{11}}{y_{uk}^2}\phi - \frac{ct_{11}}{y_{uk}^2}\phi. \end{aligned} \tag{4.66}$$

Accordingly, the coefficients are determined by

$$\begin{aligned} ct_{11} &= -y_{uk}^2 \int \frac{d^3p}{(2\pi)^3}\left[\frac{1}{\omega_1} + \frac{1}{\omega_2} - \frac{m_D^2 + m_S^2}{\omega_1\omega_2(\omega_1 + \omega_2)}\right], \\ ct_{12} &= y_{uk}^2 \int \frac{d^3p}{(2\pi)^3}\left[\frac{2m_D m_S}{\omega_1\omega_2(\omega_1 + \omega_2)}\right], \end{aligned} \tag{4.67}$$

where

$$\begin{aligned} \omega_1^2 &= \tilde{p}^2 + m_D^2, \\ \omega_2^2 &= \tilde{p}^2 + m_S^2. \end{aligned} \tag{4.68}$$

Considering the continuum theory, one may immediately notice that ct_{11} is quadratically divergent, as expected; while the divergence of ct_{12} is logarithmic,

or null for massless fermions.

On the lattice, they are really calculated by

$$\begin{aligned} a^2 ct_{11} =& -y_{uk}^2 \int_{-\pi}^{\pi} \frac{d^3k}{(2\pi)^3} \left[\frac{1}{a\omega_1} + \frac{1}{a\omega_2} - \frac{am_D^2 + am_S^2}{a\omega_1 a\omega_2 (a\omega_1 + a\omega_2)} \right], \\ a^2 ct_{12} =& \ y_{uk}^2 \int_{-\pi}^{\pi} \frac{d^3k}{(2\pi)^3} \left[\frac{2am_D am_S}{a\omega_1 a\omega_2 (a\omega_1 + a\omega_2)} \right], \end{aligned} \tag{4.69}$$

where the rescaled energies are

$$\begin{aligned} a\omega_1^2 =& \sin^2(k_1) + \sin^2(k_2) + \sin^2(k_3) + am_D^2, \\ a\omega_2^2 =& \sin^2(k_1) + \sin^2(k_2) + \sin^2(k_3) + am_S^2, \end{aligned} \tag{4.70}$$

and the masses

$$\begin{aligned} am_D =& r_D(3 - \cos^2(k_1) - \cos^2(k_2) - \cos^2(k_3)), \\ am_S =& r_S(3 - \cos^2(k_1) - \cos^2(k_2) - \cos^2(k_3)). \end{aligned} \tag{4.71}$$

with Wilson parameters r_D and r_S for doublets and singlets separately. Then it is easy to carry out the finite integral (4.69) numerically.

4.3 Simulations and results

We perform the simulations on a cubic lattice of physical volume $(Na)^3$ with the number of sites $N = 32$ in each direction and a lattice spacing $a = 1.2/v$ where v=246 GeV is the Higgs vacuum expectation value. We implement the ensemble fermion method in simulations and eventually choose the number of realizations N_q=4000, with which we have tested and found the dynamics and all observables (except N_f) safely converge. The simulations are in practice carried out by MPI-parallelized runs, and each job normally takes 80 processors and about 8 hours. Therefore the total cpu-hours used for 400 pairs of normal and CP-conjugate configuration is approximately 500,000 hours.

In Fig 4.3, we demonstrate the observables that are measured every 10 steps in a single simulation, including the average Higgs fields, the Higgs winding numbers, the Chern-Simons number and the fermion number. In fact, $\langle \phi_{1,2}^2 \rangle$ have been rescaled separately for two Higgs fields by their vacuum expectations, and therefore these

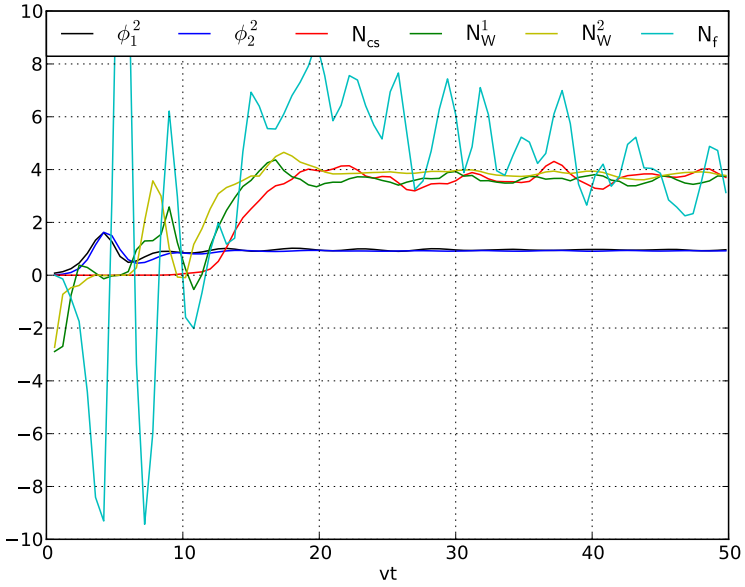


Figure 4.3. Basic observables for a single bosonic realisation; $\phi^2_{1,2}$, $N_W^{1,2}$, $N_{\rm cs}$ and a not very well converged N_f.

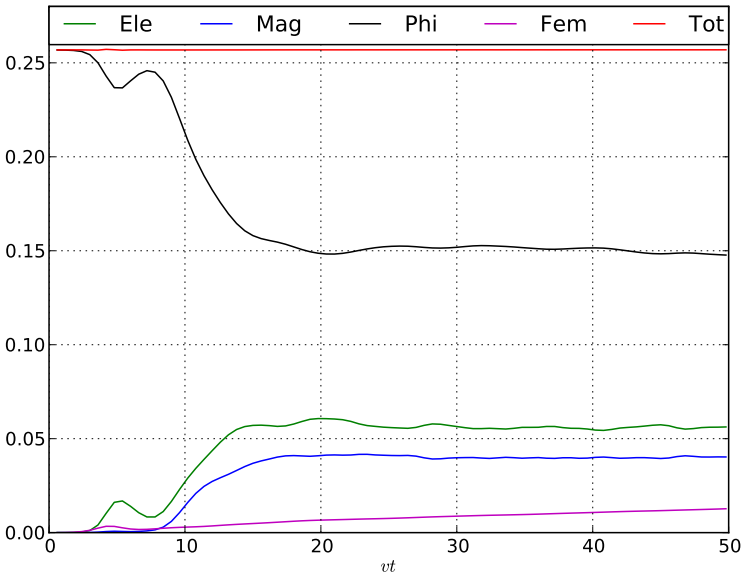


Figure 4.4. The energy densities from the same simulation as in Fig 4.3

two numbers are unity when the Higgs fields are in the finial vacuum state. One can read from the average Higgs fields that after the start of the simulation, the two Higgs fields roll down from the center of the potential, and after the first two big oscillations which happen before $t \simeq 10/v$, the average Higgs fields eventually settle down with smaller oscillations around the minimum of the potential. During the first two oscillations, the energy is mainly stored in the Higgs fields, accompanied with energy transferring between kinetic energies and potential energies. This is the observation that we can deduce from energy densities in Fig 4.4. After the second oscillation, the energy transfers quickly from Higgs fields to the gauge field. At the same time, the topological structures start to be generated and in this example, the Chern-Simons number changes from 0 to 4, following the two Higgs winding numbers. Those observables do not settle until $t \simeq 20/v$, and afterwards the energy in bosonic fields also remains stable. In comparison, the fermion fields gain energy gradually but persistently.

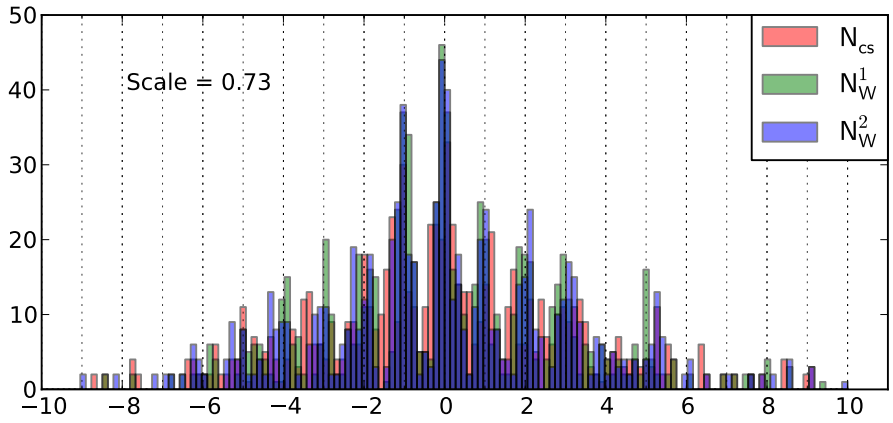


Figure 4.5. Histograms of final values of $N_{\rm cs}$ and $N_W^{1,2}$. The distribution peaks around integers, when normalised by a multiplicative lattice correction factor of 0.73.

The winding numbers, the degree of a continuous mapping in the continuum theory, are more likely an integer when the Higgs fields settle down. While in reality, they suffer from the finite lattice resolution which would reduce the number to somewhat below the integer, so does the Chern-Simons number. (An example with a fine lattice resolution can be found in Fig 3.4, 3.5.) Fortunately, such impact can be easily estimated through a statistical study and effectively compensated by a rescaling. In Fig 4.5, we list in a histogram all collected final winding numbers and Chern-Simons numbers, after all numbers have been in fact rescaled by $1/0.73$

to compensate the lattice corrections. As a result, the peaks can be observed well around integers.

4.3.1 Events and averages

Now we move on to study the CP-violation. For this purpose, we first pair two simulations, one with normal initialization and the other its CP-conjugate. Over the pair, the average Chern-Simons number and winding numbers will be exactly zero if the C-violation is off in the Higgs potential. With the C-violation on, the CP asymmetry in these topological numbers is usually tiny. In Fig 4.6, we show the outputs from such a pair of negligible CP asymmetry, where for comparison, we have flipped the sign of the observables in the CP-conjugate simulation.

But there is the possibility that noticeable CP-violation could occur in pairs of simulations. Fig 4.7 demonstrates one such successful example. We see similar evolution of observables (up to an overall sign) in the beginning, but around $t \simeq 20/v$, a deviation starts to appear. Eventually, the asymmetry settles down after $t \simeq 30/v$ and a net winding number of $N_W = +1$ can be read for the event, after we count the flipped sign for the observables from CP-conjugate simulations and the rescaling factor of $1/0.73$ due to the lattice corrections. There is also the possibility that pairs attain net $N_W = -1$.

In Fig 4.8, we display the final values of N_W^2 with all 400 normal configurations (black) and their CP-conjugate (white), rescaled with the correction factor $1/0.73$. As it shows, the two outputs in a pair most likely overlap each other, so that the black square is practically hidden. But we can indeed observe a few exceptions. In summary, among 400 pairs we have accumulated, there are a total of 16 events where a simulation and its CP pair have different topological numbers (up to an overall sign), and they correspond to flips, 6 times net +1 and 10 times net -1.

The statistical results over time, with the mean (red line) and one standard deviation (green band), are shown in fig 4.9, on observables, (in the clockwise direction), $\langle\phi_1^2\rangle$, $\langle\phi_2^2\rangle$, N_{CS}, N_f, N_W^2 and N_W^1. The average Higgs fields are well behaved statistically, and described by damped oscillations around the minimum of the potential. Both $\langle\phi^2\rangle$ will be unity, if the Higgs fields sit exactly at the minimum point. While the oscillations in practice reduce the average Higgs fields to somewhat smaller than unity, because around the minimum, the potential is broader where Higgs fields stay

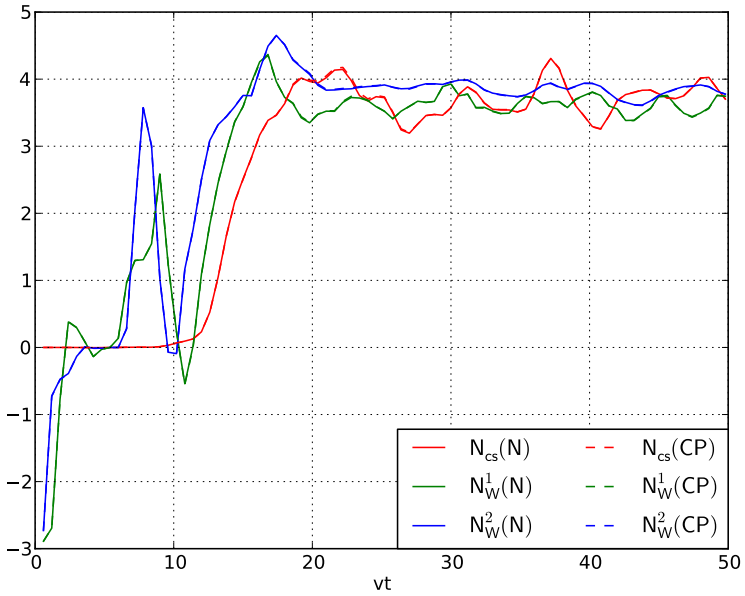


Figure 4.6. A configuration and its CP conjugate, where no net asymmetry is produced. The sign of the observables for the CP conjugate has been flipped.

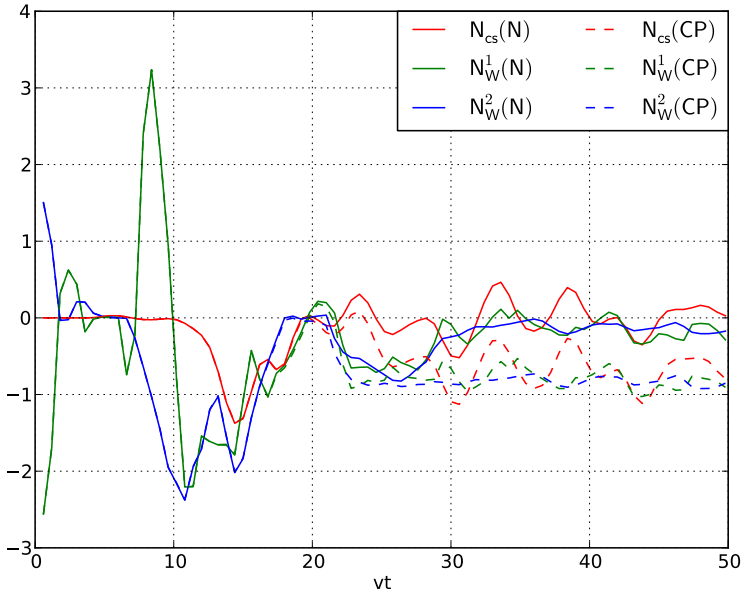


Figure 4.7. A configuration and its CP conjugate, where a flip occurs and an asymmetry is produced.

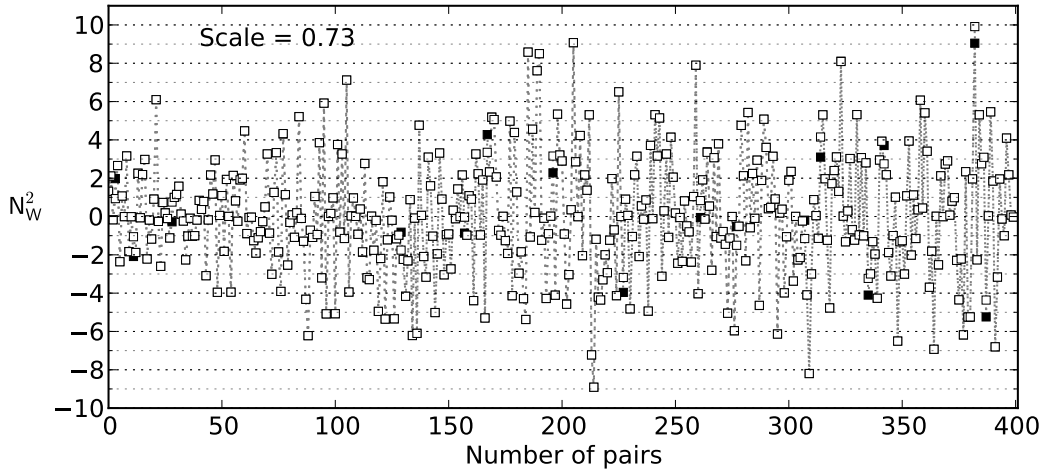


Figure 4.8. Final values of N_W^2 for configurations (black) and their CP-conjugate (white).

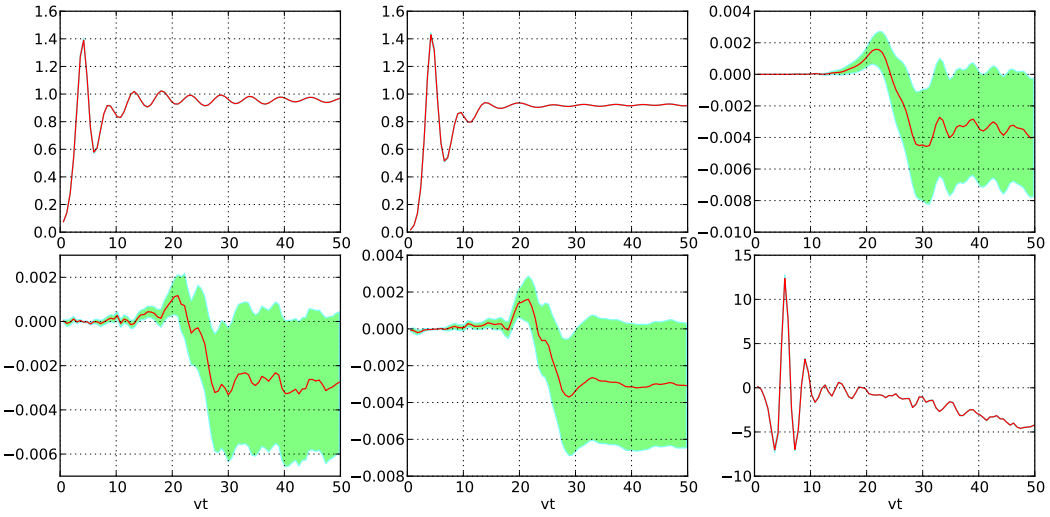


Figure 4.9. Clockwise: $\langle\phi_1^2\rangle$, $\langle\phi_2^2\rangle$, N_{CS}, N_f, N_W^2 and N_W^1, when averaged over the entire bosonic ensemble. The mean values are represented by red lines. The one standard deviations are displayed in green bands.

close to the center and steeper where $\langle|\phi|\rangle$ are bigger than the vacuum expectation values. Comparatively, the statistical uncertainty is larger in the Chern-Simon number and Higgs winding numbers and we can see $N_{CS} = N_W = 0$ is on the edge of one standard deviation. The fermion number is badly behaved, but probably suggests the same sign of CP asymmetry as Chern-Simons number and winding numbers indicates.

4.3.2 Asymmetry

Our simulations provide a baryon asymmetry of

$$n_B = \frac{1}{V}\frac{N_+ - N_-}{2N_{\rm tot}}, \tag{4.72}$$

where the practical physical volume is $V = (Na)^3$, with $N = 32$ and $a = 1.2/v$. The energy density available in the beginning of simulations is approximately the initial potential energy density, $\rho_0 = (174\ \text{GeV})^4$. On the other hand, by assuming the energy should be distributed over all active degrees of freedom, we can write

$$\rho = g^* \frac{\pi^2}{30} T^4. \tag{4.73}$$

The effective number g^* is 28 for the reduced Standard Model that we are using, specifically

$$g^* = 3 \times 3 + 5 + \frac{7}{8} \times 4 \times 4 = 28, \tag{4.74}$$

with three gauge bosons ($(W^{\pm}$, $Z)$ of spin 1, three neutral Higgs bosons and two charged ones, as well as four Dirac fermions. We assign $g^* = 7/8$ to each fermionic degree of freedom, as for relativistic fermions, we calculate the energy density in the form of

$$\rho = \int \frac{d^3p}{(2\pi)^3} \frac{p}{e^{p/T} + 1} = \frac{7}{8}\frac{\pi^2}{30} T^4, \tag{4.75}$$

while for bosons,

$$\rho = \int \frac{d^3p}{(2\pi)^3} \frac{p}{e^{p/T} - 1} = \frac{\pi^2}{30} T^4. \tag{4.76}$$

We can also write down the entropy density as

$$s = g^* \frac{2\pi^3}{45} T^3 = 1.01 \times (g^*)^{1/4} \rho_0^{3/4}, \tag{4.77}$$

and (n_B/s) is constant during the evolution afterwards. One can relate the present entropy density with the photon density via $s = 7.04 n_r$, by noticing

$$n_r = 2 \int \frac{d^3p}{(2\pi)^3} \frac{1}{e^{p/T} - 1} = \frac{2\zeta(3)}{\pi^2} T^3, \tag{4.78}$$

where $\zeta(n)$ is the zeta function, and to achieve the right number 7.04, one also needs to consider the effective number of neutrino species.

As a result, we get

$$\frac{n_B}{n_\gamma} = 6.97 \, \frac{1}{(av)^3 N^3} \frac{N_+ - N_-}{2N_{\rm tot}} (g^*)^{-1/4} \left(\frac{v}{\rho_0^{1/4}} \right)^3 . \tag{4.79}$$

Using $g^* = 28$, $v = 246$ GeV, $\rho_0^{1/4} \simeq 174$ GeV, $N = 32$ and $av = 1.2$, we find

$$\eta = 8.3 \times 10^{-5} \times \frac{N_+ - N_-}{2N_{\rm tot}} \left(1 \pm \sqrt{\frac{N_+ + N_-}{(N_+ - N_-)^2}} \right), \tag{4.80}$$

where the one standard deviation error applies for $N_{\rm tot} \gg 1$, and the statistical error will be large if there are many flips cancelled out $(N_+ + N_-) > (N_+ - N_-)^2$ The observed asymmetry of 6.0×10^{-10} corresponds to one uncancelled flip in 10^5 configurations.

In all 400 pairs of realizations that we have accumulated, we found $N_+ = 6$ flips with +1 difference in N_W; and $N_- = 10$ with -1. Therefore, we obtain the baryon-to-photon ratio of

$$\eta \simeq -3.5 \times 10^{-7} \times (1.0 \pm 1.0) \, . \tag{4.81}$$

The numerical signal is at the boundary of what is numerically discernible with the available computer resources, but we tentatively find an asymmetry of $|\eta| \leq 3.5 \times 10^{-7}$.

4.4 Conclusion

In this chapter, we have measured a baryon asymmetry, by including simultaneously the $B + L$ anomaly, C- and CP-violation, as well as an out-of-equilibrium state, in real-time lattice simulations. As a result, we have calculated the baryon-to-photon

ratio and obtained $\eta \simeq -3.5 \times 10^{-7} \times (1.0 \pm 1.0)$. Because of the big statistical error, the present simulations can not exclude zero explicitly. But the remedy is straightforward, one can always improve the result with larger statistics, which means more simulations.

We in practice introduce the CP-violation to the reduced Standard Model, through breaking the C-symmetry in the two-Higgs potential. It is always our wish to know which parameter choice in the model could provide the maximal CP-violation. Given the parameters allowed by experiments, we realize it is still difficult to answer how big the CP-violation could be, unless we simulate the scenario explicitly.

Despite not knowing which parameter choice could yield maximal CP-violation, we indeed discover there are some choices which will definitely lead to no asymmetry, even though the C-symmetry violated explicitly in the Higgs potential. This corresponds to the accidental symmetry $C'P$ that we found in section 4.1.1. On the other hand, it is easy to show that such accidental symmetry will be automatically forbidden when the hyper $U(1)$ gauge field exits in the simulation.

Chapter 5

Summary and Outlook

The main goal of the thesis was to establish real-time simulations for Cold Electroweak Baryogenesis, with one-generation of fermions explicitly included. As a result, all Sakharov's three conditions can be fulfilled in our first-principles numerical simulations and a baryon asymmetry can be measured from large-scale computer simulations.

We first presented the chiral anomaly by solving the Dirac equation for fermions in parallel electric and magnetic fields. The anomaly is related only to the lowest-energy Landau levels. For massless fermions, the chiral anomaly can be seen as a result of the production of particles of one chirality, and no production of particles of the other chirality. If fermions are massive, the method can lead to the chiral anomaly in the general form,

$$\partial_\mu \langle \mathrm{T}\bar{\psi} i\gamma^\mu \gamma^5 \psi \rangle = 2im\langle \mathrm{T}\bar{\psi}\gamma^5\psi\rangle - \frac{e^2}{2\pi^2} E\cdot B, \tag{5.1}$$

or

$$\partial_\mu \langle \mathrm{T}\bar{\psi} i\gamma^\mu \gamma^5 \psi \rangle = 2im\langle \mathrm{T}\bar{\psi}\gamma^5\psi\rangle + \frac{e^2}{16\pi^2} \epsilon^{\mu\nu\rho\sigma} F_{\mu\nu}F_{\rho\sigma}. \tag{5.2}$$

Notice the proper regularization is necessary to obtain the expression above. As a matter of fact, it is the regularization that accounts for the E in the last term of (5.1), instead of the particle production whose rate $e^{-\frac{m^2+p_\perp^2}{eE}\pi}$ would be non-perturbative of E. More importantly, the regularization in the continuum theory can not be applied to the lattice theory, where the range of momentums is finite, in comparison with the infinite momentum range in the continuum theory. On the lattice, the

chiral anomaly is obtained by Wilson fermions, which yield the chiral anomaly in a sequence [20],

$$\partial_\mu \langle \mathrm{T}\bar{\psi} i\gamma^\mu \gamma^5 \psi \rangle = -2i\frac{ar_W}{2}\langle \mathrm{T}\bar{\psi}\gamma^5 D^i D_i \psi\rangle = \frac{e^2}{16\pi^2}\epsilon^{\mu\nu\rho\sigma}F_{\mu\nu}F_{\rho\sigma}, \tag{5.3}$$

where D_i is the spatial gauge covariant derivative and the expression (5.3) does not depend on the value of r_W, as long as it is not zero. We in practice only introduced spatial Wilson terms to remove spatial doublers. For the temporal doubling problem, we discovered that by choosing the initial values for fermion properly, the temporal doublers will not be excited in the practical simulations. To cooperate with real-time simulations and such initialization, a proper renormalization scheme has been constructed and the coefficients of counterterms can be determined accordingly.

On the other hand, we extended the calculation of the chiral anomaly to the general anomaly cancellation, and found that with the fermion content of the Standard Model, the $B - L$ symmetry is anomaly free, but the $B + L$ symmetry must be violated as a quantum anomaly. Therefore, the baryon number non-conservation can be explained by the $B + L$ anomaly. Another necessary condition for the baryogenesis, the out-of-equilibrium, can be achieved as a result of the spinodal (tachyonic) instability in Higgs IR modes during a cold electroweak transition.

With ensemble fermions, we carried out real-time simulations of the cold electroweak transition, based on the reduced Standard Model [70], which included the $SU(2)$ gauge field, the Higgs field and one generation of fermions. We tested the validity of the method of ensemble fermions and found the dynamics and most observables could converge with the number of fermion realizations, $N_q = 2400$, which was numerically tractable. In particular, the $B + L$ anomaly could be measured accurately with large N_q and the spinodal instability in practice leaded to a large energy transfer in the beginning of the transition. We applied the method to measure the fermion occupation number, and observed that at the later time of the evolution, a thermal equilibrium could emerge to fermion IR modes. According to the Fermi-Dirac distribution, the fermion temperature during the transition was calculated, which was found never below 20 GeV. The result could indirectly rule out the Standard Model CP-violation as the source of the baryon asymmetry of the Universe, because the viable Standard Model baryogenesis requires the transition

temperature of order 1 GeV at most.

Therefore, we moved on to recruit another Higgs doublet, so that new CP-violation could be introduced as a result of extra C-violating terms included in the two-Higgs potential. We selected the scalar potential by requiring a high sphaleron-transition rate. We also chose carefully the Yukawa interaction in order to avoid some accidental symmetry that could ruin the baryon asymmetry. With all Sakharov's three necessary conditions fulfilled, we eventually performed such first-principles simulations with 400 pairs of initial configurations, and finally obtained the baryon-to-photon ratio,

$$\eta \simeq -4.2 \times 10^{-7} \times (1.0 \pm 1.0)\,. \tag{5.4}$$

As the next project, we intend to reduce the statistic error in (5.4), by implementing more simulations. Also as an interesting plan, simulations can be extended to involve three generations of fermions, such that the baryon anomaly caused by the CKM and PMNS matrices can be studied. This approach will be non-perturbative, in a sense that all orders of fermion backreaction will be included. Possibly, this might not be easily achieved by the ensemble fermions, as a very large number of fermion realizations will be required to enable the top quark physics converge. But theoretically, there is no problem to implement the simulation with the mode function method.

At present, we have only involved the $SU(2)$ gauge theory, which is essential in the $B + L$ anomaly, because of the existence of the non-trivial topological number, the Chern-Simons number,

$$N_{CS} = \frac{1}{16\pi^2} \int d^3x \epsilon^{ijk} \mathrm{Tr} \left[A_i F_{jk} + i \frac{2}{3} A_i A_j A_k \right],$$

while in comparison the Chern-Simon number for the $U(1)$ gauge field is zero. By including the complete electroweak $SU(2) \times U(1)$, we can further measure from simulations the cosmic magnetic fields as a result of the electroweak transition [64]. Also we see in Chapter 4 that the $U(1)$ gauge theory could remove the unwanted accidental symmetry. In order to have anomaly-free $SU(2) \times U(1)$ without the $SU(3)$ color index, the weak hypercharge for quarks must be modified. The possibility is discussed in Appendix A.

Appendix A

Anomaly free $SU(2) \times U(1)$

Assume the hypercharge for $(u_L,\ d_L)$, $u_R^{\mathcal{C}}$, $d_R^{\mathcal{C}}$, $(\nu_L,\ e_L)$ and $e_R^{\mathcal{C}}$ are a, b, c, d and e respectively. By requiring that the $SU(2) \times U(1)$ gauge theory and $B-L$ symmetry are anomaly free, we need to carry out the anomaly cancellation in following way, (similar as we did in Chapter 2)

$SU(2) - SU(2) - U(1)$:

$$a + d = 0, \tag{A.1}$$

$U(1) - U(1) - U_{B-L}(1)$:

$$2a^2 - b^2 - c^2 - 2d^2 + e^2 = 0. \tag{A.2}$$

$U(1) - U(1) - U(1)$:

$$2a^3 + b^3 + c^3 + 2d^3 + e^3 = 0, \tag{A.3}$$

The solution can be easily found as

$$a = -d, \quad b = -e, \quad c = 0; \tag{A.4}$$

$$a = -d, \quad c = -e, \quad b = 0. \tag{A.5}$$

Apparently, the Standard Model hypercharge ($a = -\frac{1}{6},\ b = \frac{2}{3},\ c = -\frac{1}{3},\ d = \frac{1}{2},\ e = -1$), can not be the solution. In addition, if we want to have the same $B+L$ anomaly

as it is in the Standard Model,

$$\partial_\mu j_b^\mu = \partial_\mu j_l^\mu = \frac{1}{64\pi^2}\epsilon^{\mu\nu\rho\sigma}F_{\mu\nu}^a F_{\rho\sigma}^a - \frac{1}{64\pi^2}\epsilon^{\mu\nu\rho\sigma}B_{\mu\nu}B_{\rho\sigma}, \tag{A.6}$$

the following equation should be satisfied,

$$2d^2 - e^2 = -\frac{1}{2}. \tag{A.7}$$

In practice, we can keep the same weak hypercharge for leptons, that is ($d = \frac{1}{2},\ e = -1$), and therefore the electromagnetic charge should be calculated in the same way as it is in the Standard Model, i.e. $Q = T_3 - Y$. Another requirement is that the electromagnetic charge of quarks will be opposite to the charge of anti-quarks,

$$\text{up quark}: \quad \frac{1}{2} - a = -(0 - b), \qquad \text{down quark}: \quad -\frac{1}{2} - a = -(0 - c). \tag{A.8}$$

Finally, the solution can only be:

$$a = -\frac{1}{2}, \quad b = +1, \quad c = 0, \quad d = +\frac{1}{2}, \quad e = -1. \tag{A.9}$$

As we can see in Table A.1, without color $SU(3)$, the quark charges are no longer fractional.

	electromagnetic charge $Q = T_3 - Y$	weak isospin T_3	weak hypercharge Y
$\begin{pmatrix} u \\ d \end{pmatrix}_L$	$+1$ 0	$+1/2$ $-1/2$	$-1/2$
$u_R^{\mathcal{C}}$	-1	0	$+1$
$d_R^{\mathcal{C}}$	0	0	0
$\begin{pmatrix} \nu \\ e \end{pmatrix}_L$	0 -1	$+1/2$ $-1/2$	$+1/2$
$\nu_R^{\mathcal{C}}$	0	0	0
$e_R^{\mathcal{C}}$	$+1$	0	-1

Table A.1. For $SU(2) \times U(1)$, the electromagnetic charge Q, weak isospin T_3 and weak hypercharge Y of the first-generation fermions, with a relation $Q = T_3 - Y$.

Bibliography

[1] P. A. M. Dirac, "The Quantum theory of electron," Proc. Roy. Soc. Lond. A **117** (1928) 610.

[2] P. A. M. Dirac, "Quantized Singularities in the Electromagnetic Field," Proc. Roy. Soc. Lond. A **133** (1931) 60.

[3] F. Sauter, "On the behavior of an electron in a homogeneous electrical eld according to the relativistic Theory of Dirac," Z. Phys. **69** (1931) 742.

[4] W. Heisenberg and H. Euler, "Consequences of Dirac's theory of positrons," Z. Phys. **98** (1936) 714 [physics/0605038].

[5] J. S. Schwinger, "On gauge invariance and vacuum polarization," Phys. Rev. **82** (1951) 664.

[6] B. Pontecorvo, "Inverse beta processes and nonconservation of lepton charge," Sov. Phys. JETP **7** (1958) 172 [Zh. Eksp. Teor. Fiz. **34** (1957) 247].

[7] Z. Maki, M. Nakagawa and S. Sakata, "Remarks on the unified model of elementary particles," Prog. Theor. Phys. **28** (1962) 870.

[8] S. Weinberg, "A Model of Leptons," Phys. Rev. Lett. **19** (1967) 1264.

[9] A. D. Sakharov, "Violation of CP Invariance, c Asymmetry, and Baryon Asymmetry of the Universe," Pisma Zh. Eksp. Teor. Fiz. **5** (1967) 32 [JETP Lett. **5** (1967) 24] [Sov. Phys. Usp. **34** (1991) 392] [Usp. Fiz. Nauk **161** (1991) 61].

[10] S. L. Adler, "Axial vector vertex in spinor electrodynamics," Phys. Rev. **177** (1969) 2426.

[11] J. S. Bell and R. Jackiw, "A PCAC puzzle: $\Pi^0 \to$ gamma gamma in the sigma model," Nuovo Cim. A **60** (1969) 47.

[12] M. Kobayashi and T. Maskawa, "CP Violation in the Renormalizable Theory of Weak Interaction," Prog. Theor. Phys. **49** (1973) 652.

[13] T. D. Lee, "A Theory of Spontaneous T Violation," Phys. Rev. D **8** (1973) 1226.

[14] K. G. Wilson, "Confinement of Quarks," Phys. Rev. D **10** (1974) 2445.

[15] J. B. Kogut and L. Susskind, "Hamiltonian Formulation of Wilson's Lattice Gauge Theories," Phys. Rev. D **11** (1975) 395.

[16] K. G. Wilson, "Quarks and Strings on a Lattice," CLNS-321.

[17] G. 't Hooft, "Symmetry Breaking Through Bell-Jackiw Anomalies," Phys. Rev. Lett. **37** (1976) 8.

[18] L. Susskind, "Lattice Fermions," Phys. Rev. D **16** (1977) 3031.

[19] L. D. Landau and E. M. Lifschitz, "Quantum Mechanics: Non-relativistic Theory. Course of Theoretical Physics. Vol. 3," London, UK: Pergamon Press. (1977) 677 p

[20] L. H. Karsten and J. Smit, "Lattice Fermions: Species Doubling, Chiral Invariance, and the Triangle Anomaly," Nucl. Phys. B **183** (1981) 103.

[21] P. H. Ginsparg and K. G. Wilson, "A Remnant of Chiral Symmetry on the Lattice," Phys. Rev. D **25** (1982) 2649.

[22] W. Kerler, "Axial Vector Anomaly in Lattice Gauge Theory," Phys. Rev. D **23** (1981) 2384.

[23] J. Ambjorn, J. Greensite and C. Peterson, "The Axial Anomaly and the Lattice Dirac Sea," Nucl. Phys. B **221** (1983) 381.

[24] N. S. Manton, "Topology in the Weinberg-Salam Theory," Phys. Rev. D **28** (1983) 2019.

[25] F. R. Klinkhamer and N. S. Manton, "A Saddle Point Solution in the Weinberg-Salam Theory," Phys. Rev. D **30** (1984) 2212.

[26] Y. Nagahama, "Higher Derivative Regularization And Chiral Anomaly," Prog. Theor. Phys. **75** (1986) 427.

[27] O. W. Greenberg, "Example of Infinite Statistics," Phys. Rev. Lett. **64** (1990) 705.

[28] L. D. McLerran, E. Mottola and M. E. Shaposhnikov, "Sphalerons and Axion Dynamics in High Temperature QCD," Phys. Rev. D **43** (1991) 2027.

[29] V. G. Bagrov and D. M. Gitman, "Exact solutions of relativistic wave equations," Dordrecht, Netherlands: Kluwer (1990) 323 p. (Mathematics and its applications. Soviet series, 39)

[30] N. Turok and J. Zadrozny, "Dynamical generation of baryons at the electroweak transition," Phys. Rev. Lett. **65** (1990) 2331.

[31] N. Turok and J. Zadrozny, "Electroweak baryogenesis in the two doublet model," Nucl. Phys. B **358** (1991) 471.

[32] A. G. Cohen, D. B. Kaplan and A. E. Nelson, "Progress in electroweak baryogenesis," Ann. Rev. Nucl. Part. Sci. **43** (1993) 27 [hep-ph/9302210].

[33] J. W. Goodison and D. J. Toms, "No Generalized statics from dynamics in cured space-time," Phys. Rev. Lett. **71** (1993) 3240 [hep-th/9311057].

[34] L. Kofman, A. D. Linde and A. A. Starobinsky, "Reheating after inflation," Phys. Rev. Lett. **73** (1994) 3195 [hep-th/9405187].

[35] W. Bock, J. E. Hetrick and J. Smit, "Fermion production despite fermion number conservation," Nucl. Phys. B **437** (1995) 585 [hep-lat/9406015].

[36] S. Weinberg, "The Quantum theory of fields. Vol. 1: Foundations,"

[37] M. E. Peskin and D. V. Schroeder, "An Introduction to quantum field theory," Reading, USA: Addison-Wesley (1995) 842 p.

[38] K. Kajantie, M. Laine, K. Rummukainen and M. E. Shaposhnikov, "Is there a hot electroweak phase transition at m(H) larger or equal to m(W)?," Phys. Rev. Lett. **77** (1996) 2887 [hep-ph/9605288].

[39] K. Kajantie, M. Laine, K. Rummukainen and M. E. Shaposhnikov, "A Nonperturbative analysis of the finite T phase transition in SU(2) x U(1) electroweak theory," Nucl. Phys. B **493** (1997) 413 [hep-lat/9612006].

[40] S. Y. Khlebnikov and I. I. Tkachev, "Classical decay of inflaton," Phys. Rev. Lett. **77** (1996) 219 [hep-ph/9603378].

[41] S. Weinberg, "The quantum theory of fields. Vol. 2: Modern applications," Cambridge, UK: Univ. Pr. (1996) 489 p.

[42] L. Kofman, A. D. Linde and A. A. Starobinsky, "Towards the theory of reheating after inflation," Phys. Rev. D **56** (1997) 3258 [hep-ph/9704452].

[43] P. B. Greene and L. Kofman, "Preheating of fermions," Phys. Lett. B **448** (1999) 6 [hep-ph/9807339].

[44] G. Aarts and J. Smit, "Real time dynamics with fermions on a lattice," Nucl. Phys. B **555** (1999) 355 [hep-ph/9812413].

[45] G. Aarts and J. Smit, "Particle production and effective thermalization in inhomogeneous mean field theory," Phys. Rev. D **61** (2000) 025002 [hep-ph/9906538].

[46] L. M. Krauss and M. Trodden, "Baryogenesis below the electroweak scale," Phys. Rev. Lett. **83** (1999) 1502 [hep-ph/9902420].

[47] J. Garcia-Bellido, D. Y. Grigoriev, A. Kusenko and M. E. Shaposhnikov, "Nonequilibrium electroweak baryogenesis from preheating after inflation," Phys. Rev. D **60** (1999) 123504 [hep-ph/9902449].

[48] P. B. Greene and L. Kofman, "On the theory of fermionic preheating," Phys. Rev. D **62** (2000) 123516 [hep-ph/0003018].

[49] A. Rajantie and E. J. Copeland, "Phase transitions from preheating in gauge theories," Phys. Rev. Lett. **85** (2000) 916 [hep-ph/0003025].

[50] A. Rajantie, P. M. Saffin and E. J. Copeland, "Electroweak preheating on a lattice," Phys. Rev. D **63** (2001) 123512 [hep-ph/0012097].

[51] G. D. Moore, JHEP **0111** (2001) 021 [hep-ph/0109206].

[52] G. Aarts and J. Berges, "Classical aspects of quantum fields far from equilibrium," Phys. Rev. Lett. **88** (2002) 041603 [hep-ph/0107129].

[53] E. J. Copeland, D. Lyth, A. Rajantie and M. Trodden, "Hybrid inflation and baryogenesis at the TeV scale," Phys. Rev. D **64** (2001) 043506 [hep-ph/0103231].

[54] J. Smit, "Introduction to quantum fields on a lattice: A robust mate," Cambridge Lect. Notes Phys. **15** (2002) 1.

[55] D. V. Vassilevich, "Heat kernel expansion: User's manual," Phys. Rept. **388** (2003) 279 [hep-th/0306138].

[56] A. Tranberg and J. Smit, "Baryon asymmetry from electroweak tachyonic preheating," JHEP **0311** (2003) 016 [hep-ph/0310342].

[57] G. V. Dunne, "Heisenberg-Euler effective Lagrangians: Basics and extensions," In *Shifman, M. (ed.) et al.: From fields to strings, vol. 1* 445-522 [hep-th/0406216].

[58] M. van der Meulen, D. Sexty, J. Smit and A. Tranberg, "Chern-Simons and winding number in a tachyonic electroweak transition," JHEP **0602** (2006) 029 [hep-ph/0511080].

[59] A. W. El Kaffas, W. Khater, O. M. Ogreid and P. Osland, "Consistency of the two Higgs doublet model and CP violation in top production at the LHC," Nucl. Phys. B **775** (2007) 45 [hep-ph/0605142].

[60] A. Tranberg, J. Smit and M. Hindmarsh, "Simulations of cold electroweak baryogenesis: Finite time quenches," JHEP **0701** (2007) 034 [hep-ph/0610096].

[61] S. Borsanyi and M. Hindmarsh, "Low-cost fermions in classical field simulations," Phys. Rev. D **79** (2009) 065010 [arXiv:0809.4711 [hep-ph]].

[62] T. D. Cohen and D. A. McGady, "The Schwinger mechanism revisited," Phys. Rev. D **78** (2008) 036008 [arXiv:0807.1117 [hep-ph]].

[63] N. Tanji, "Dynamical view of pair creation in uniform electric and magnetic fields," Annals Phys. **324** (2009) 1691 [arXiv:0810.4429 [hep-ph]].

[64] C. J. Copi, F. Ferrer, T. Vachaspati and A. Achucarro, "Helical Magnetic Fields from Sphaleron Decay and Baryogenesis," Phys. Rev. Lett. **101** (2008) 171302 [arXiv:0801.3653 [astro-ph]].

[65] R. Allahverdi, R. Brandenberger, F. Y. Cyr-Racine and A. Mazumdar, "Reheating in Inflationary Cosmology: Theory and Applications," Ann. Rev. Nucl. Part. Sci. **60** (2010) 27 [arXiv:1001.2600 [hep-th]].

[66] F. Hebenstreit, R. Alkofer and H. Gies, "Schwinger pair production in space and time-dependent electric fields: Relating the Wigner formalism to quantum kinetic theory," Phys. Rev. D **82** (2010) 105026 [arXiv:1007.1099 [hep-ph]].

[67] G. C. Branco, P. M. Ferreira, L. Lavoura, M. N. Rebelo, M. Sher and J. P. Silva, "Theory and phenomenology of two-Higgs-doublet models," Phys. Rept. **516** (2012) 1 [arXiv:1106.0034 [hep-ph]].

[68] T. Brauner, O. Taanila, A. Tranberg and A. Vuorinen, "Temperature Dependence of Standard Model CP Violation," Phys. Rev. Lett. **108** (2012) 041601 [arXiv:1110.6818 [hep-ph]].

[69] P. M. Saffin and A. Tranberg, "Real-time Fermions for Baryogenesis Simulations," JHEP **1107** (2011) 066 [arXiv:1105.5546 [hep-ph]].

[70] P. M. Saffin and A. Tranberg, "Dynamical simulations of electroweak baryogenesis with fermions," JHEP **1202** (2012) 102 [arXiv:1111.7136 [hep-ph]].

[71] A. Tranberg and B. Wu, "Cold Electroweak Baryogenesis in the Two Higgs-Doublet Model," JHEP **1207** (2012) 087 [arXiv:1203.5012 [hep-ph]].

[72] A. Tranberg and B. Wu, "On using Cold Baryogenesis to constrain the Two-Higgs Doublet Model," JHEP **1301** (2013) 046 [arXiv:1210.1779 [hep-ph]].

[73] G. Hinshaw *et al.* [WMAP Collaboration], "Nine-Year Wilkinson Microwave Anisotropy Probe (WMAP) Observations: Cosmological Parameter Results," Astrophys. J. Suppl. **208** (2013) 19 [arXiv:1212.5226 [astro-ph.CO]].

[74] G. V. Dunne, "The Heisenberg-Euler Effective Action: 75 years on," Int. J. Mod. Phys. A **27** (2012) 1260004 [Int. J. Mod. Phys. Conf. Ser. **14** (2012) 42] [arXiv:1202.1557 [hep-th]].

[75] P. H. Damgaard, D. O'Connell, T. C. Petersen and A. Tranberg, "Constraints on New Physics from Baryogenesis and Large Hadron Collider Data," Phys. Rev. Lett. **111** (2013) 22, 221804 [arXiv:1305.4362 [hep-ph]].

[76] Z. G. Mou, P. M. Saffin and A. Tranberg, "Ensemble fermions for electroweak dynamics and the fermion preheating temperature," JHEP **1311** (2013) 097 [arXiv:1307.7924 [hep-ph]].

[77] F. Hebenstreit, J. Berges and D. Gelfand, "Simulating fermion production in 1+1 dimensional QED," Phys. Rev. D **87** (2013) 10, 105006 [arXiv:1302.5537 [hep-ph]].

[78] J. Berges, D. Gelfand and D. Sexty, "Amplified Fermion Production from Overpopulated Bose Fields," Phys. Rev. D **89** (2014) 2, 025001 [arXiv:1308.2180 [hep-ph]].

[79] V. Kasper, F. Hebenstreit and J. Berges, "Fermion production from real-time lattice gauge theory in the classical-statistical regime," Phys. Rev. D **90** (2014) 2, 025016 [arXiv:1403.4849 [hep-ph]].

[80] K. A. Olive *et al.* [Particle Data Group Collaboration], "Review of Particle Physics," Chin. Phys. C **38** (2014) 090001.

[81] P. A. R. Ade *et al.* [Planck Collaboration], "Planck 2015 results. XIII. Cosmological parameters," arXiv:1502.01589 [astro-ph.CO].

[82] G. Aad *et al.* [ATLAS and CMS Collaborations], "Combined Measurement of the Higgs Boson Mass in pp Collisions at $\sqrt{s} = 7$ and 8 TeV with the ATLAS and CMS Experiments," Phys. Rev. Lett. **114** (2015) 191803 [arXiv:1503.07589 [hep-ex]].

[83] Z. G. Mou, P. M. Saffin and A. Tranberg, "Cold Baryogenesis from first principles in the Two-Higgs Doublet model with Fermions," JHEP **1506** (2015) 163 [arXiv:1505.02692 [hep-ph]].